Technical Progress Report 87-7

October 1988

COMPARISON OF MEASURED AND MODELED RADIATION, HEAT AND WATER VAPOR FLUXES: FIFE PILOT STUDY

A Final Technical Report During Period
From April 1, 1985 - December 31, 1987
to
National Aeronautics and Space Administration
Goddard Space Flight Center
Under Grant No. NAG 5-561

by

Blaine L. Blad, Shashi B. Verma, Kenneth G. Hubbard
Patrick Starks and Cynthia Hays
Center for Agricultural Meteorology and Climatology
and
John M. Norman and Elizabeth Walter-Shea
Department of Agronomy

University of Nebraska
Lincoln, Nebraska 68583

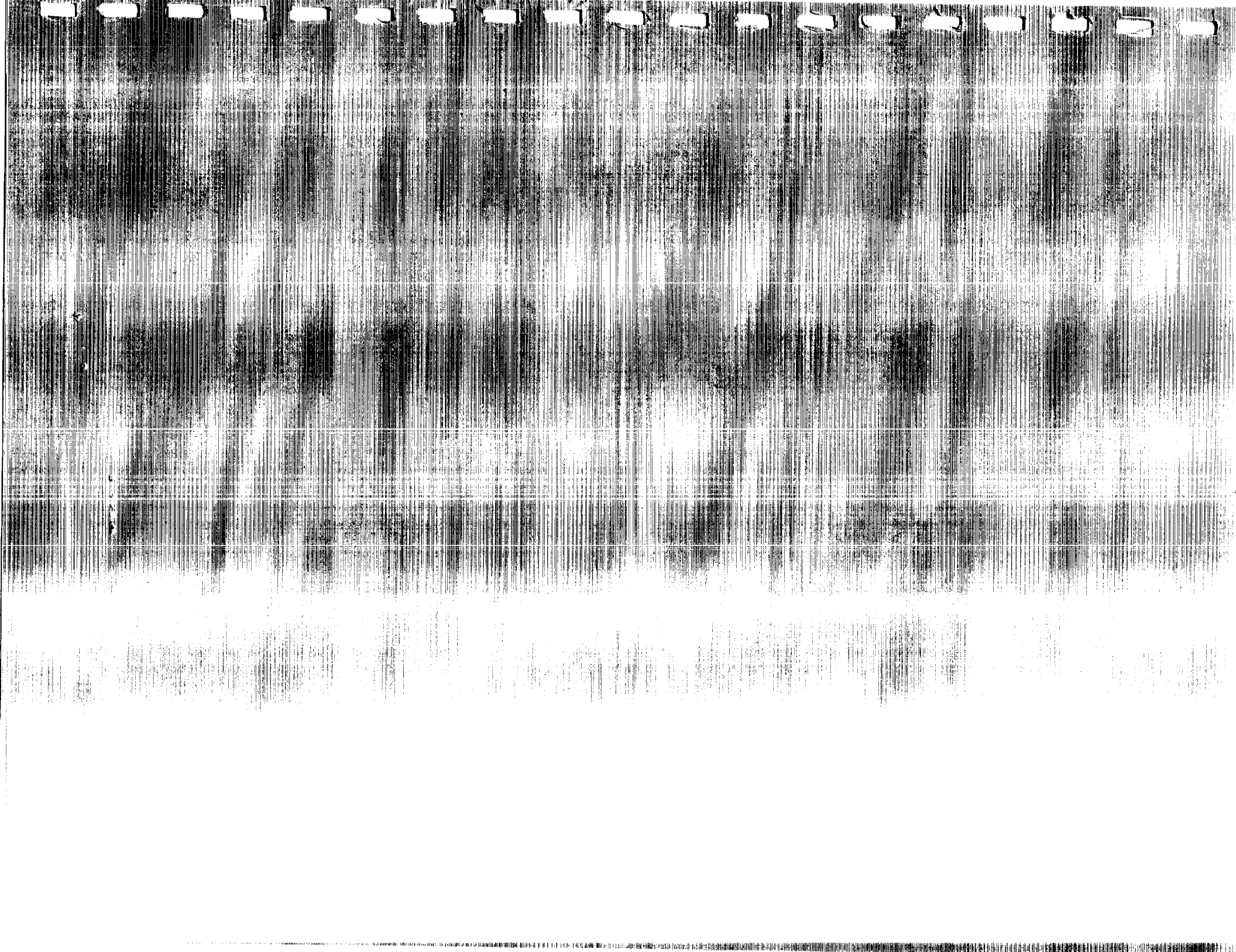

COMPARISON OF MEASURED AND MODELED RADIATION, HEAT AND WATER VAPOR FLUXES: FIFE PILOT STUDY

A Final Technical Report During Period

From April 1, 1985 - December 31, 1987

to

National Aeronautics and Space Administration
Goddard Space Flight Center
Under Grant No. NAG 5-561

by

Blaine L. Blad, Shashi B. Verma, Kenneth G. Hubbard
Patrick Starks and Cynthia Hays
Center for Agricultural Meteorology and Climatology

and

John M. Norman and Elizabeth Walter-Shea
Department of Agronomy

Institute of Agriculture and Natural Resources
University of Nebraska, Lincoln, Nebraska

CAMaC Progress Report 87-7

ABSTRACT

This report describes findings of research conducted at the University of Nebraska Agricultural Research and Development Center in 1985 and during a pilot study at the FIFE site in 1986.

The primary objectives of the 1985 study were (1) to test the feasibility of using radio frequency receivers to collect data from automated weather stations and (2) to evaluate the use of the data collected by the automated weather stations for modeling the fluxes of latent heat, sensible heat and radiation over wheat. The model Cupid was used to calculate these fluxes which were compared with fluxes of these entities measured using micrometeorological techniques.

The objectives of the 1986 study were (1) to measure and model reflected and emitted radiation streams at a few locations within the FIFE site and (2) to compare modeled and measured latent heat and sensible heat fluxes from the prairie vegetation.

During the 1985 study we found that it was feasible to use radio frequency transmitters and receivers to collect data from automated weather stations. We found that modeled estimates of latent heat (LE), sensible heat (H) and net radiation (Rn) agreed well with the fluxes measured over wheat, especially during the time when the wheat crop was growing vigorously. The agreement between measured fluxes and modeled estimates diminished later in the season as wheat anthesis ended and the wheat began to senesce.

Reflectances and transmittances from leaves of some of the more abundant grass and forb species were made using a specially designed radiometer. This instrument was equipped with filters to measure values in the same waveband intervals as those found on the Barnes Modular Multiband Radiometer (MMR). All grass and forb leaves exhibited peak reflectance and transmittance values

in the visible region in MMR band 2. Peak reflectance in the near infrared region occurred in MMR band 4 for grasses, but for forb leaves peak reflectance occurred in MMR bands 4 or 5. The magnitudes of reflectances and transmittances were similar for measurements made on either the adaxial (top) or the abaxial (bottom) surfaces of grass leaves, but such was not the case for forb leaves. These results suggest that it should be possible to characterize the leaf reflectance and transmittance by making measurements on either the adaxial or abaxial surface of grass leaves, but transmittance and reflectance measurements must be made on both sides of forb leaves.

Reflectances from the prairie vegetation canopies were measured in the MMR wavebands at two sites, one on the Konza (a sloping site) and the second off the Konza (a level site). Reflectances were made at seven angles in the principal plane of the sun. The angles were -50, -30, -20, nadir, 20, 30 and 50. Negative values signify backscattered radiation and positive values forward scattering. There were several similarities in the reflectance patterns made at different locations, but also some differences. At both sites, the minimum reflectances tended to occur at 20 or 30°. On the Konza site the maximum reflectance occurred consistently for MMR band 4, but at the off-Konza site, it occurred for band 4 or 5, depending on the specific sampling location. Forward scattered reflectances were generally 2-5 percent lower in absolute terms than backscatter reflectances. The effect of changing zenith angle on reflectances was inconclusive over the range of solar zeniths we experienced. Changes in canopy or leaf characteristics during the measurement periods may have masked any solar zenith effects.

Global albedo values were calculated from bidirectional reflectances in the MMR wavebands using weighting coefficients determined from solar radiation data by Moon (1940) and hemispherical reflectances calculated by the model of

Walthall (1985). Calculated values ranged from about 20-25%. These values are reasonable, but albedo measurements using total hemispherical albedometers should be made concurrently with the bidirectional reflectance measurements for comparison purposes.

Measurements of fluxes of LE, H and soil heat (S) were made on eleven days over wheat in 1985 and two days over the grasslands in 1986 using Bowen ratio energy balance and eddy correlation techniques. The partitioning of net radiation into sensible heat was dependent on soil moisture, atmospheric conditions and the stage of vegetative development. The measured values of these fluxes were used to compare with fluxes estimated with the model Cupid.

The performance of the Cupid model for estimating LE, Rn and H fluxes in 1986 from prairie vegetation was poorer than that for the more homogeneous wheat canopy in 1985 even at comparable LAI values. Modifications to Cupid are needed to account for the nonhomogeneous, randomly-spaced clumps of prairie vegetation as well as a need to incorporate the influence of leaf litter on the fluxes of LE, H and S.

INTRODUCTION

The main objective of the International Land Surface Climatology Project (ISLSCP) has been stated as "the development of techniques that may be applied to satellite observations of the radiation reflected and emitted from the Earth to yield quantitative information concerning land surface climatological conditions." To accomplish this objective a major field study called FIFE - the First ISLSCP Field Experiment - was conducted in 1987 on and near the Konza Prairie in Kansas. During that experiment two types of measurements were made, (1) long-term monitoring of basic meteorological parameters and (2) extensive surface and aircraft measurements made during four intensive field compaigns (IFC's). Among activities taking place during these IFC's is the determination of radiation fluxes, sensible and latent heat fluxes and the measurement of selected biophysical properties. This document describes results from pilot studies conducted in 1985 at the University of Nebraska Agriculture Research and Development Center and in 1986 at the FIFE site in Kansas to collect information and develop techniques contributing to successful measurement of selected parameters from these two measurement types.

Our basic overall objective in conducting these pilot studies was to document and understand certain important physical and biological conditions and processes which occur on the prairie site. To do this we made selected meteorological, plant and soil measurements to permit us to compare flux estimates with a plant simulation model, Cupid, with fluxes of radiation, sensible heat and latent heat calculated using micrometeorological techniques. Specifically, our objectives were (1) to determine the feasibility of using radio frequency transmitters and receivers to collect data from automated weather stations that will aid in determination of the meso- and micro-climatic variability at the FIFE site; (2) to measure and model reflected and emitted

radiation streams from various areas within the prairie site; (3) to make reliable estimates of sensible and latent heat fluxes over the prairie employing the eddy correlation technique and other micrometeorological methods and then to (4) evaluate the model Cupid for estimating the radiation, sensible and latent heat fluxes from routine atmospheric, plant and soil measurements. Such models offer a means to provide areal estimates of these fluxes from a limited number of point measurements.

Procedures and results of our research efforts on each of the four objectives specified above are presented in this report.

Objective (1) - Automated Data Collection Through Radio Frequency Communication

In 1985 equipment was procured to perform automated data collection via Radio Frequency (RF) communication. During the summer of 1985 the equipment was installed at the Agricultural Meteorological Laboratory at Mead, Nebraska for testing. Testing was carried out with an on-site IBM computer and an existing automated weather station at a nearby, permanent location. Linkage between the computer-modem-RF radio and the data logger-modem-RF radio was established and tests indicated that communication was satisfactory.

In 1986 additional equipment was purchased so that the field sites could be located on the Konza prairie. Three stations were installed to collect data in late July and early August 1986. A computer was installed at the Konza Prairie Headquarters building and an RF antenna was deployed on the roof. Descriptions for the three weather stations are given in Table 1. Stations #1 and #2 were located on the Konza Prairie while #3 was located just southeast of the Konza. Although the computer was only checked periodically (one to two times per week), the data collection process was reasonably successful as indicated in Table 2. The Konza #1 station utilized a CR21X data

Table 1. Description of the 3 surface weather stations deployed in 1986.

Instrument	Konza #1 426	Konza #2 400	Konza #3 400
Data logger	CR21X	CR21	CR21
RF-modem	yes	yes	no
RF-radio/antenna	yes	yes	no
Tape recorder	no	no	yes
Anemometer	yes	yes	yes
Wind vane	yes	yes	yes
Pyranometer	yes	yes	yes
Air temperature sensor	yes	yes	yes
Air relative humidity sensor	yes	yes	yes
Soil temperature probe	yes	yes	yes
Precipitation gauge	yes	yes	yes
Net radiometer	yes	no	no
PAR sensor	yes	no	no
Canopy temperature sensor - Nadir view	yes	no	no
Canopy temperature sensor - 30° view angle	yes	no	no

Table 2. Time period of data collection.

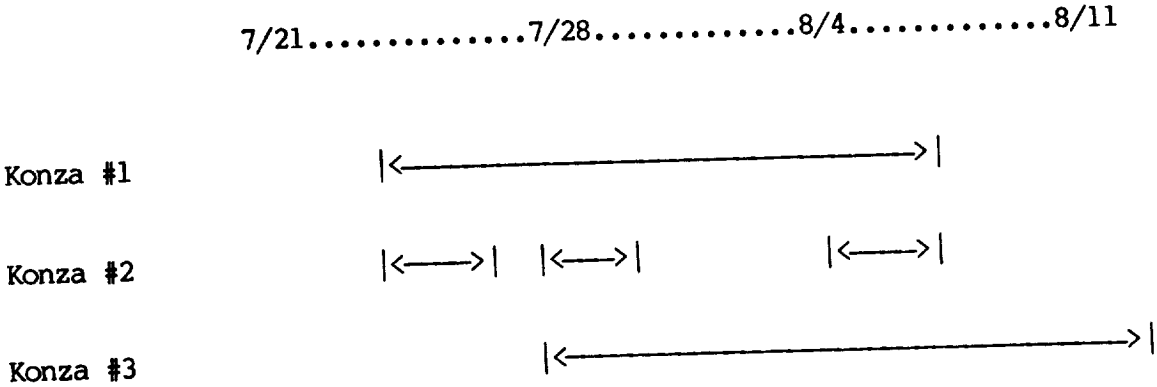

Experience with the CR21 in unattended mode would indicate that it worked well with the tape recorder (#3) but not with the RF-linkage (#2). The CR21X (#1 above) and RF-linkage gave an excellent performance.

logger which performed extremely well in the RF-linkage. Konza #2 utilized a CR21 data logger and would not operate continuously in RF-linkage. Konza #3 also had a CR21 data logger but was not part of the radio communication test (data were recorded on a cassette tape). The CR21X data logger manufactured by Campbell Scientific of Logan, Utah was conveniently employed, with no modifications, to collect sophisticated surface weather measurements on the Konza Prairie. We concluded that the CR21X data logger could be easily interfaced to additional sensors and used with RF-communications to establish a reliable weather network for FIFE. A CR10 data logger with RF linkage is now available. It is less expensive than the CR21X and could be used to obtain the parameters measured in this study.

Objective (2) - Measuring and Modeling Reflected and Emitted Radiation

Data collected to help meet this objective were obtained during late July and early August of 1986 at the FIFE site. We designed the study, in part, to help familiarize us with the topography and vegetative composition of the site and to test and develop equipment and procedures to be employed during the 1987 FIFE study. The major focus of our effort was to obtain reflectance and transmittance data from some of the dominant vegetative species and communities located within the FIFE site.

Instrumentation used to gather data on reflectance and transmittance included the Barnes model 12-1000 modular multiband radiometer (MMR), and a LI-COR model 1800-12 integrating sphere used with a specially designed radiometer. The Barnes MMR was used to collect reflectance data on vegetative communities along transects that may have differences due to topography--chiefly, slope and aspect. The integrating sphere was employed to collect data on reflectance and transmittance for individual blades of grass or leaves of forbs. Measurements of leaf area index (LAI) by destructive and nondes-

tructive methods along with sampling for vegetative dry matter were done for some of the locations where radiation measurements were made.

A. Leaf Transmittance and Reflectance:

Modeling of radiation fluxes requires knowledge of the transmissivities and reflectivities of leaves of the dominant plant species growing on the FIFE site. We measured the reflectivity and transmissivity of the leaves of several grass and forb species using a LI-COR integrating sphere fitted with a specially designed radiometer to collect data in the wavebands of the Barnes MMR. These wavebands are: (1) 0.45-0.52 μm, (2) 0.52-0.60 μm, (3) 0.63-0.69 μm, (4) 0.760.90 μm, (5) 1.15-1.30 μm, (6) 1.55-1.75 μm, and (7) 2.08-2.35 μm. Leaves of forbs or blades of grass were placed into the integrating sphere without detaching them from the plant; that is, the plants were studied nondestructively.

Of the hundreds of species of grasses and forbs found at the FIFE site, eleven of the most common ones were studied (six grass species and five forb species). The species name, common name of that species, whether it is a grass or forb, and the number of samples of that species for which data were collected are listed in Table 3.

Reflectances from the adaxial and abaxial (rft and rfb, respectively) of a blade of Andropogon gerardii as well as the transmittances through the top and bottom of the blade (tft and tfb, respectively, are depicted in Figure 1). The transmittances through both the top and bottom of the blade were essentially the same and were lower than the reflectances for the first three wavebands. In band 4 reflectances and transmittances were very similar for either side of a leaf. In bands 5 and 7 the reflectances from adaxial or abaxial surfaces tended to be within one or two percent (absolute values) of each other and were generally lower than the transmittances. Transmittance through

Table 3. Vegetation studied at the FIFE site.

Species	Common name	Species Type	Number or Samples
Andropogon gerardii Vitman	Big bluestem	Grass	3
Panicum virgatum L.	Switchgrass	Grass	2
Agropyron smithii Rydt.	Western wheatgrass	Grass	2
Eragrostis spectabilis (Pursh) Gread.	Purple lovegrass	Grass	1
Bouteloua curtipendula (Michx.) Torr.	Sideoats grama	Grass	1
Sorghastrum nutans (L.) Nash	Indiangrass	Grass	1
Salvia pitcheri Torr.	Pitchers sage	Forb	1
Vernonia baldwinii Torr.	Ironweed	Forb	1
Ambrosia psilostachya DC.	Western ragweed	Forb	1
Ceanothus americanus L.	New Jersey tea	Forb	1
Rhus glabra L.	Sumac	Shrub	1

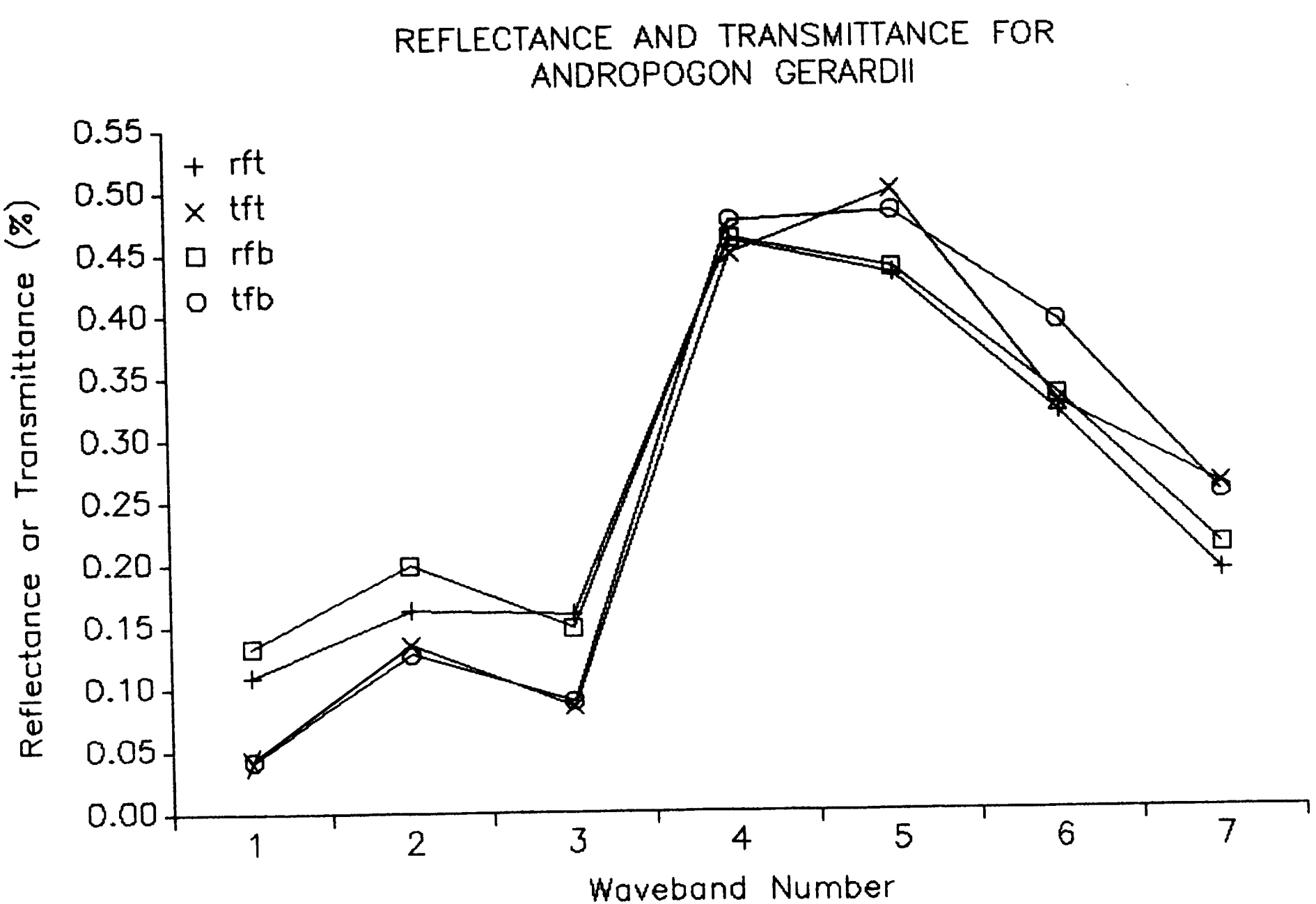

Figure 1. Leaf reflectance from the adaxial (rft) and abaxial (rfb) and transmittance through the adaxial (tft) and abaxial (tfb) in the MMR wavebands for Andropogon gerardii.

the top of the blade was essentially the same as reflectance from either the top or bottom of the leaf for band 6. Overall, the reflectances and transmittances in bands 1 through 3, which fall within that region of the electromagnetic spectrum known as the visible or photosynthetically active radiation (PAR) are much lower than those found in the remaining wavebands. In the PAR region actively growing plants are highly absorptive. Reflectances and transmittances in bands 4 through 7 fall within the infrared region and are much higher than those in the PAR region.

Three samples of A. gerardii exhibited similar reflectance characteristics in all bands (Fig. 2). In the PAR region reflectance and transmittance values peaked in band 2 (the green region), while in the infrared region reflectances peaked in band 4 (0.76-0.90 μm) and transmittances peaked in band 5 (1.15-1.30 μm). This pattern was true for all grasses.

Panicum virgatum (Fig. 3) exhibited trends very similar to A. gerardii. However, P. virgatum transmittances were slightly higher in all bands, except band 3, than A. gerardii. Reflectances for the two samples of P. virgatum behaved similarly, with one leaf showing consistently higher reflectance in all wavebands than the other (Fig. 4).

Data for Agropyron smithii (Fig. 5) depict values for transmittance and reflectance that were higher than those for P. virgatum but lower than A. gerardii in wavebands 1 through 3. In band 4, A. smithii peaked at higher reflectance than any other grass evaluated during the pilot study. Reflectances in bands 5 through 7 for A. smithii were greater than those observed for the previous two species. Reflectances for the two samples of A. smithii were very similar (Fig. 6).

Values of reflectance and transmittance for Bouteloua curtipendula are plotted in Fig. 7. Transmittances were much higher than reflectances in the

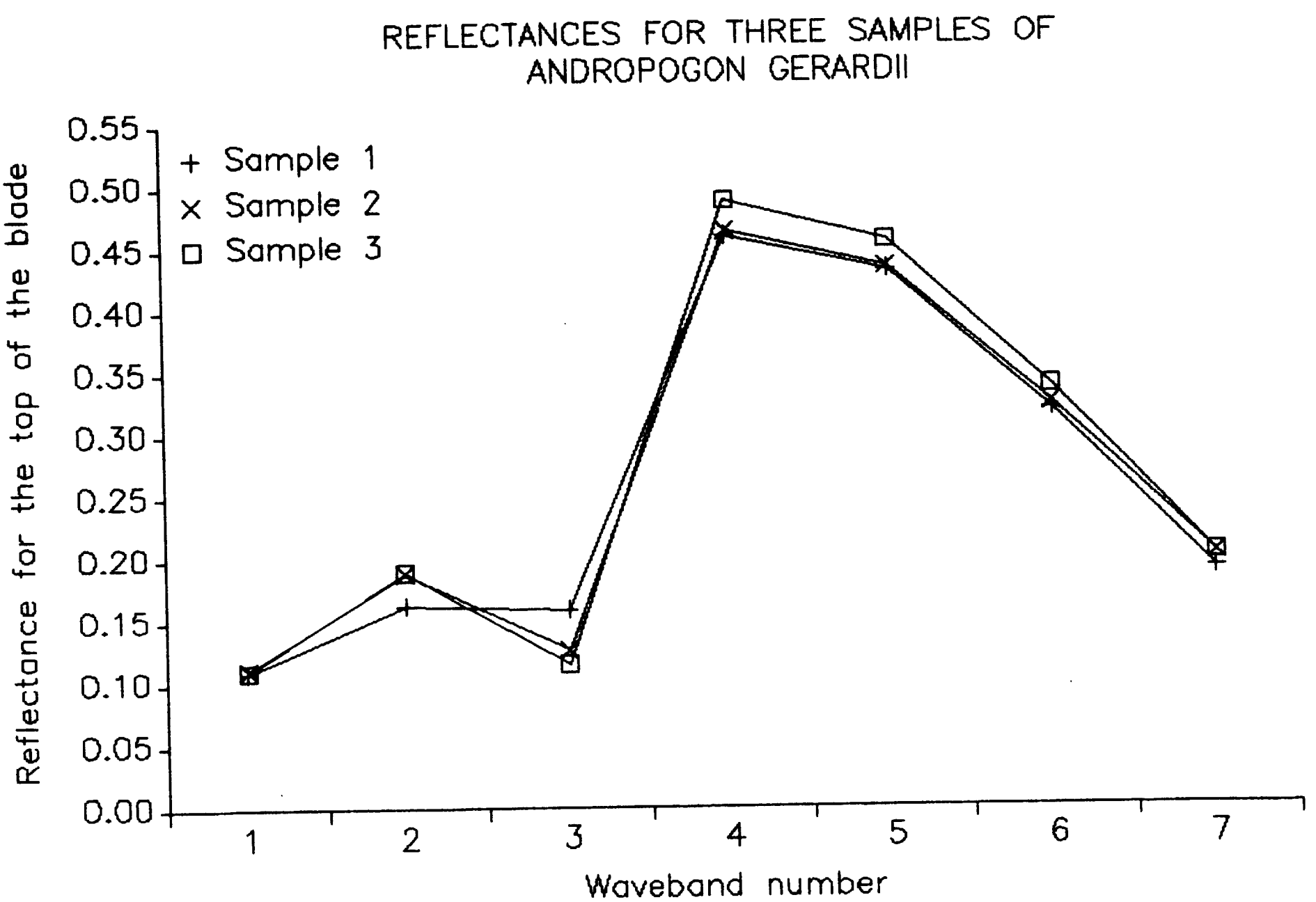

Figure 2. Comparison of leaf reflectances for leaves from 3 Andropogon gerardii plants.

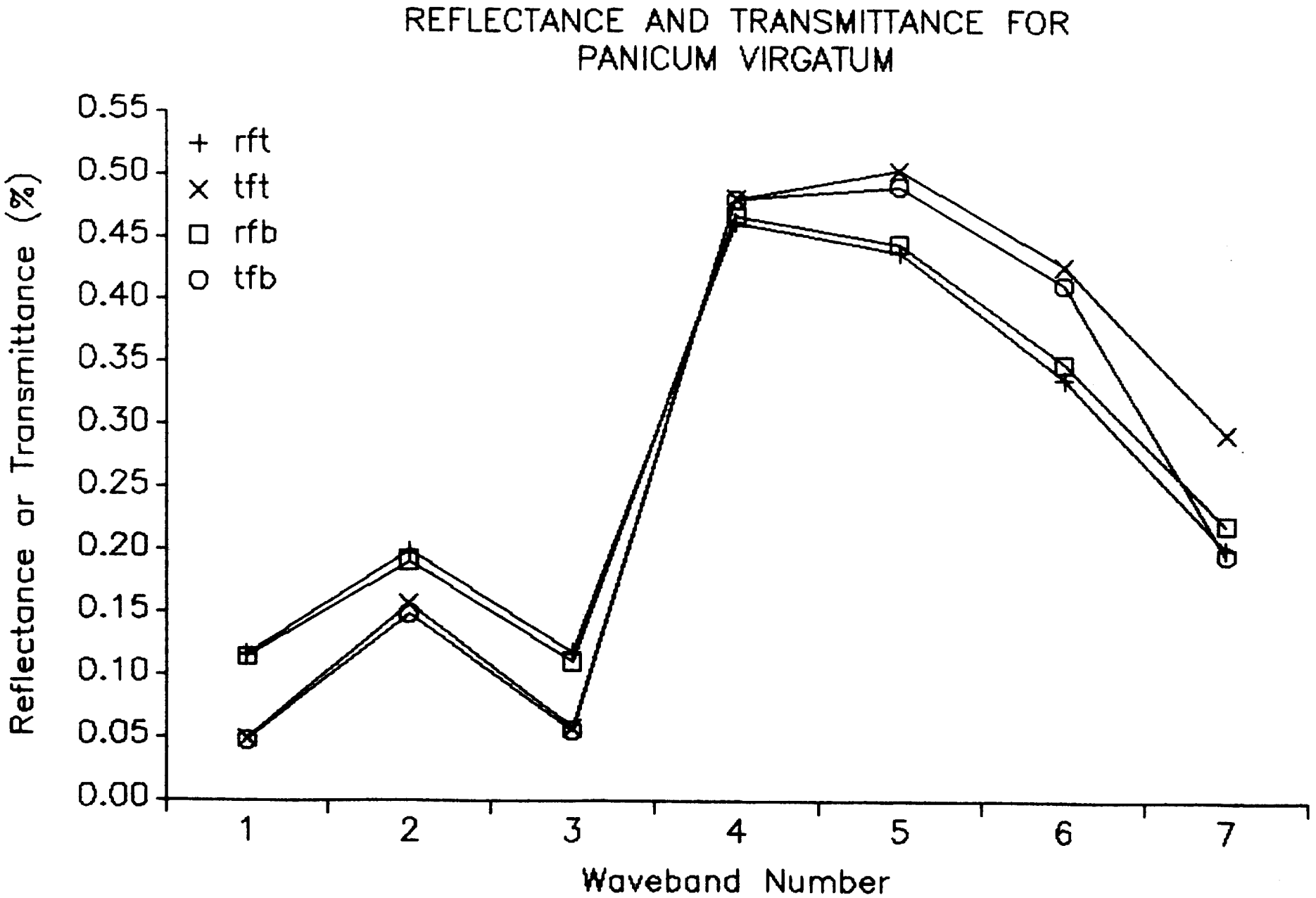

Figure 3. As in Fig. 1 for Panicum virgatum.

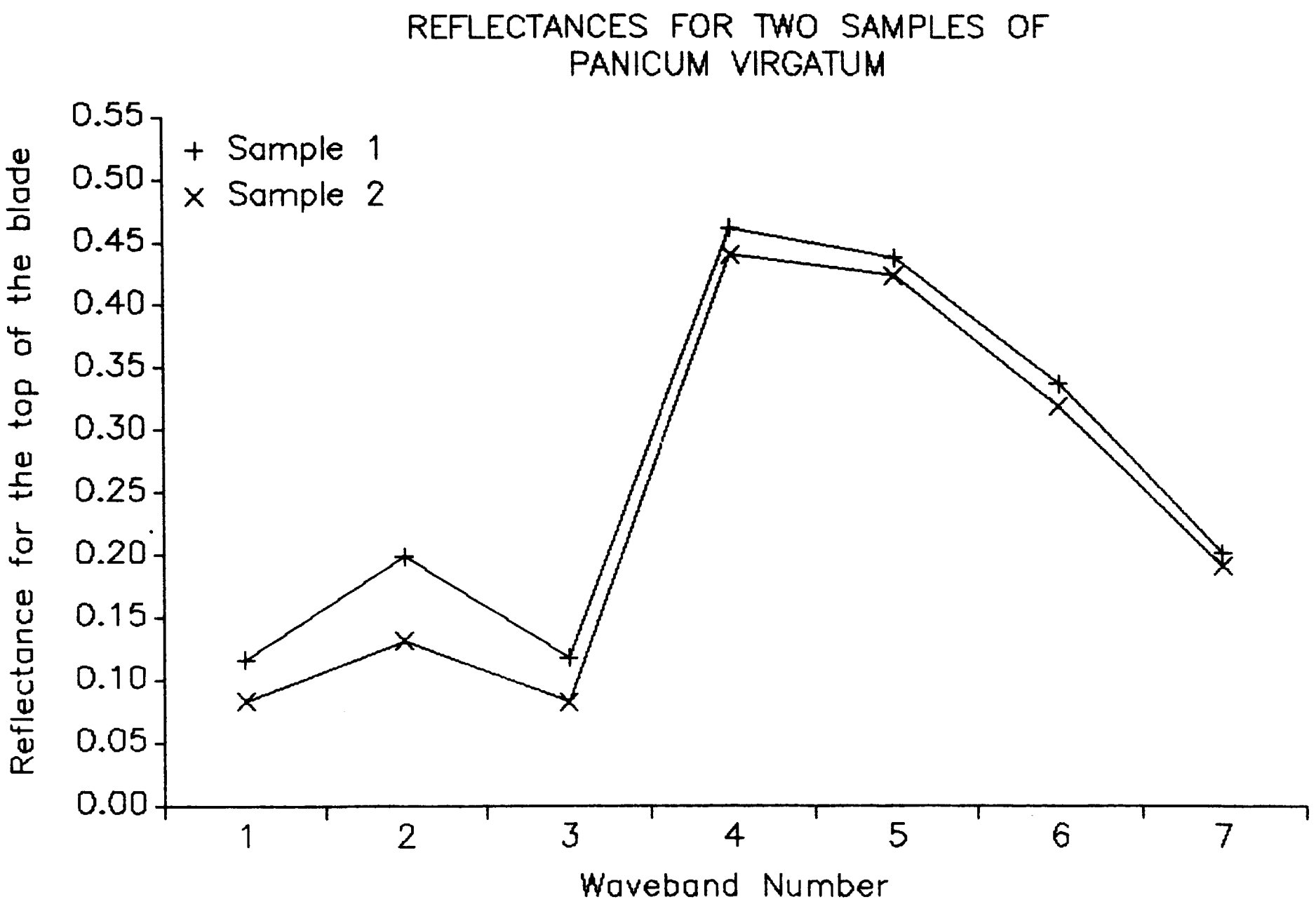

Figure 4. Comparison of leaf reflectances for leaves from 2 Panicum virgatum plants.

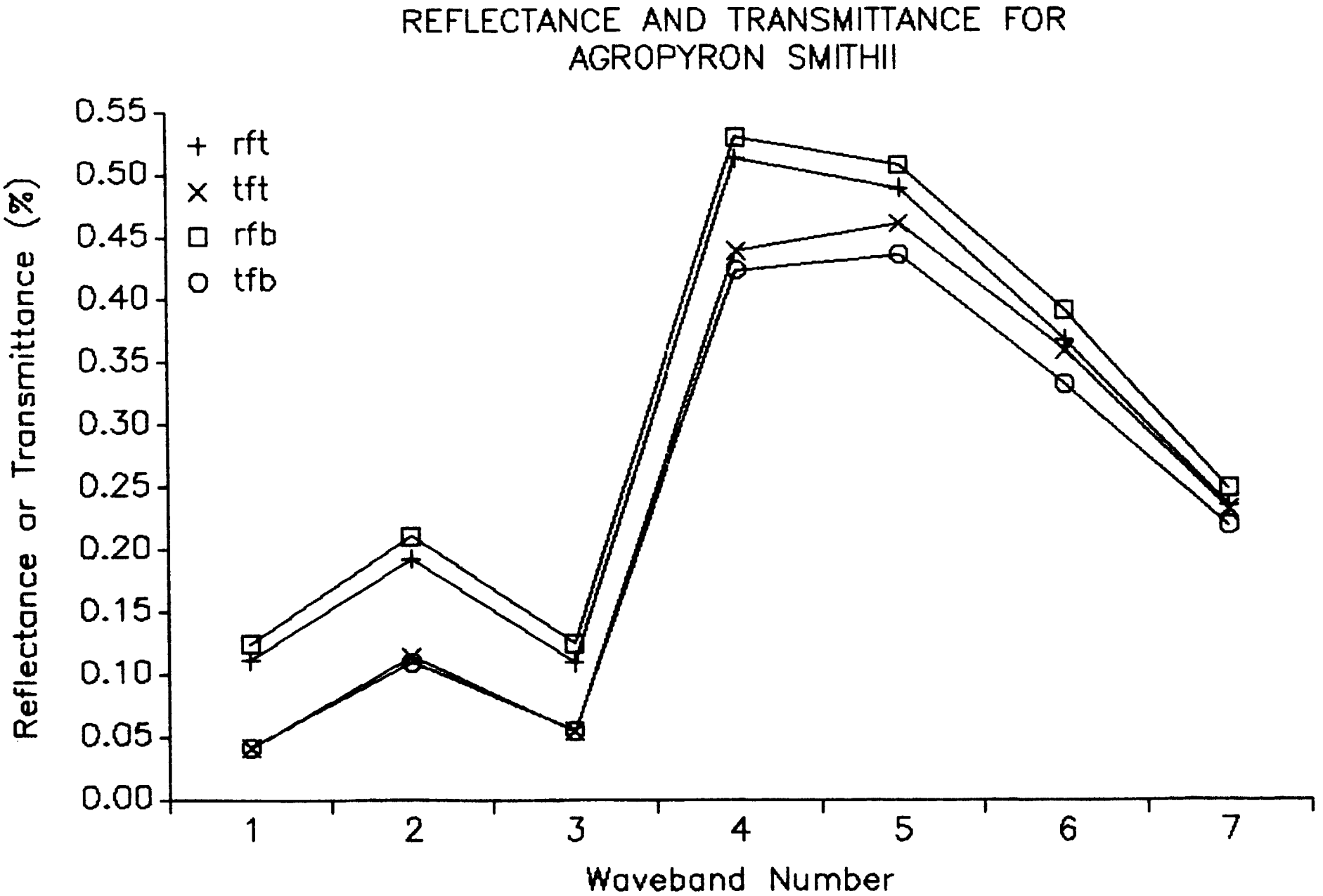

Figure 5. As in Fig. 1 for Agropyron smithii.

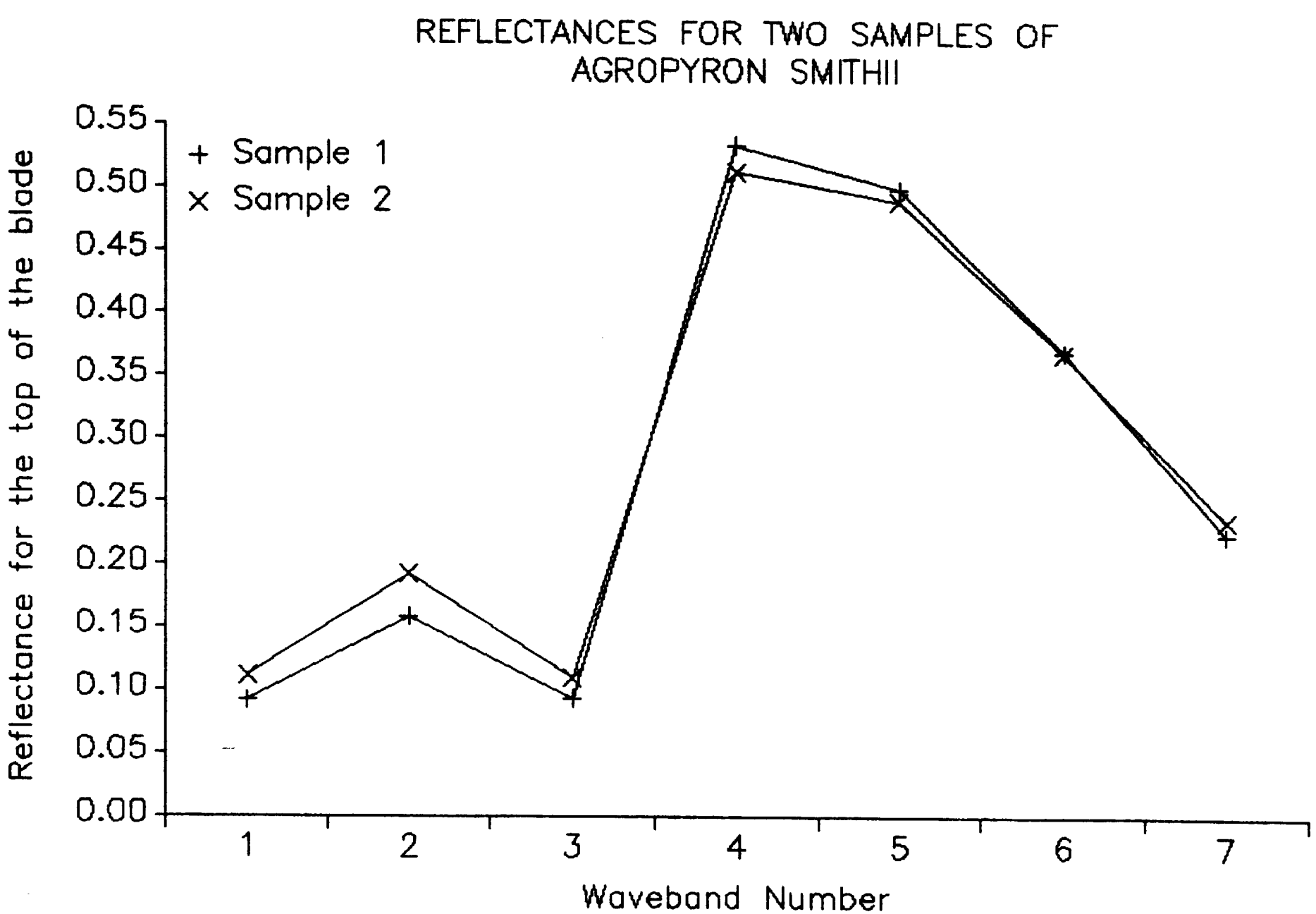

Figure 6. Comparison of leaf reflectances for leaves from 2 Agropyron smithii plants.

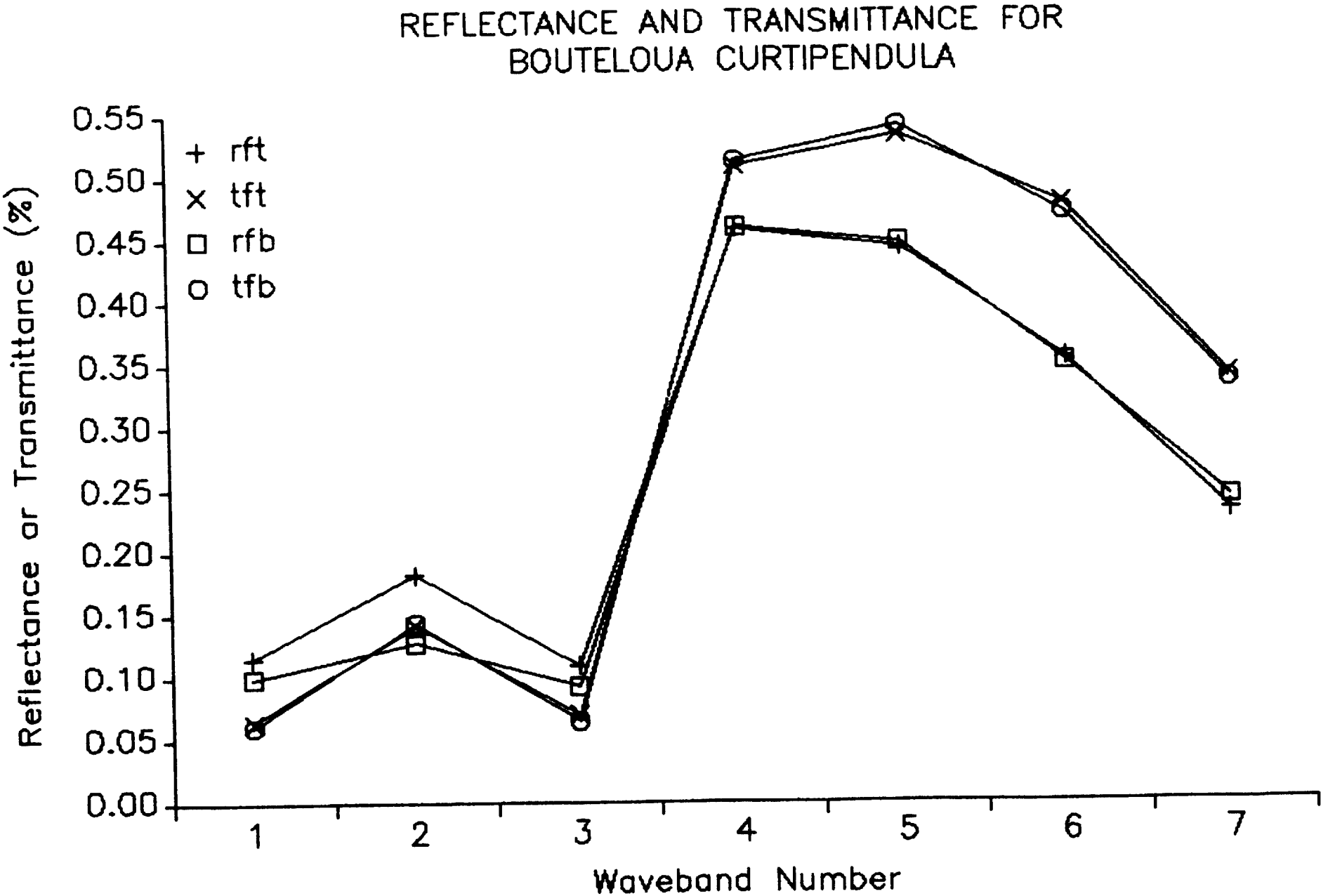

Figure 7. As in Fig. 1 for Bouteloua curtipendula.

longer wavelengths, a pattern also observed for Eragrostis spectabilis (Fig. 8). B. curtipendula and E. spectabilis had the highest transmittances in the longer wavelengths of all the grasses studied. Also E. spectabilis had the most irregular data (Fig. 8). It is not known if this is characteristic of this species or if the irregularities were due to measurement problems.

Figure 9 is a plot of the data for Sorghastrum nutans. The reflectance in band 4 was the second highest while transmittances in the visible wavebands were the lowest of the grasses evaluated.

Reflectances from the adaxial surfaces of all grass species followed the same general pattern; that is, peak reflectances in the visible portion of the spectrum in band 2 and peak reflectance in the NIR spectrum in band 4 (Fig. 10). Some species differ from each other in some wavebands, yet are similar in others. Because of this, it is important to identify the dominant grass species and characterize their reflectance and transmittance properties in order to better model the surface radiation fluxes. Our data suggest that measurements from both the top and bottom of grass leaves may not be required since transmittances and reflectances on either side are within three to five percent in absolute terms.

As was the case for grasses, forbs displayed a peak reflectance and transmittance value in band 2 of the visible region (Figs. 11-15). However, in the infrared region transmittance peaked in either band 5 or band 4, while the reflectance usually peaked in band 4 but tended to be "flat" between bands 4 and 5.

In contrast to the grasses, reflectances and transmittances of some forbs varied according to the leaf surface. For example, transmittances through the top and bottom surfaces of Vernonia baldwinii (Fig. 12) and the shrub Rhus glabra (Fig. 14) were very different in the visible region but similar in the

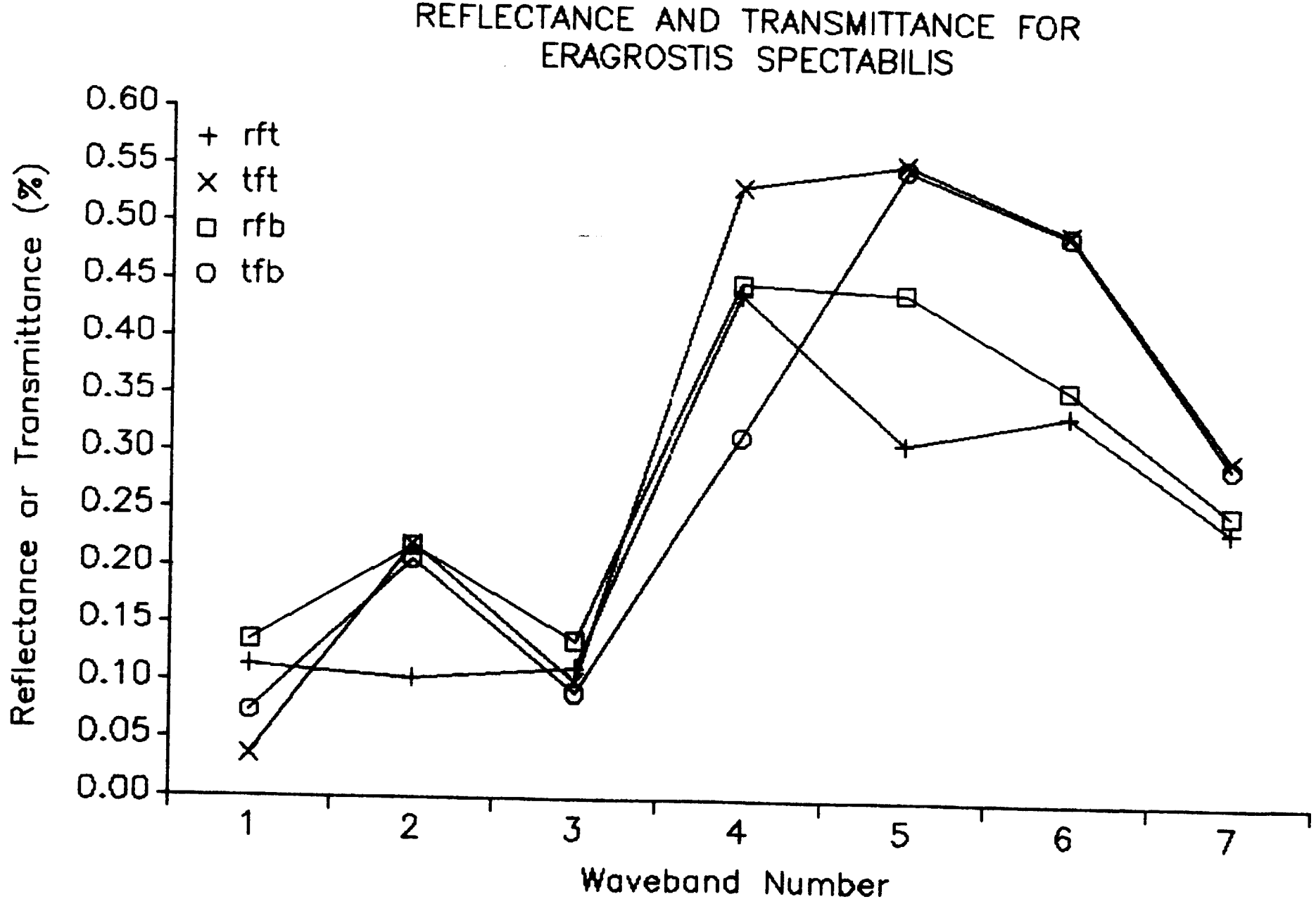

Figure 8. As in Fig. 1 for Eragrostis spectabilis.

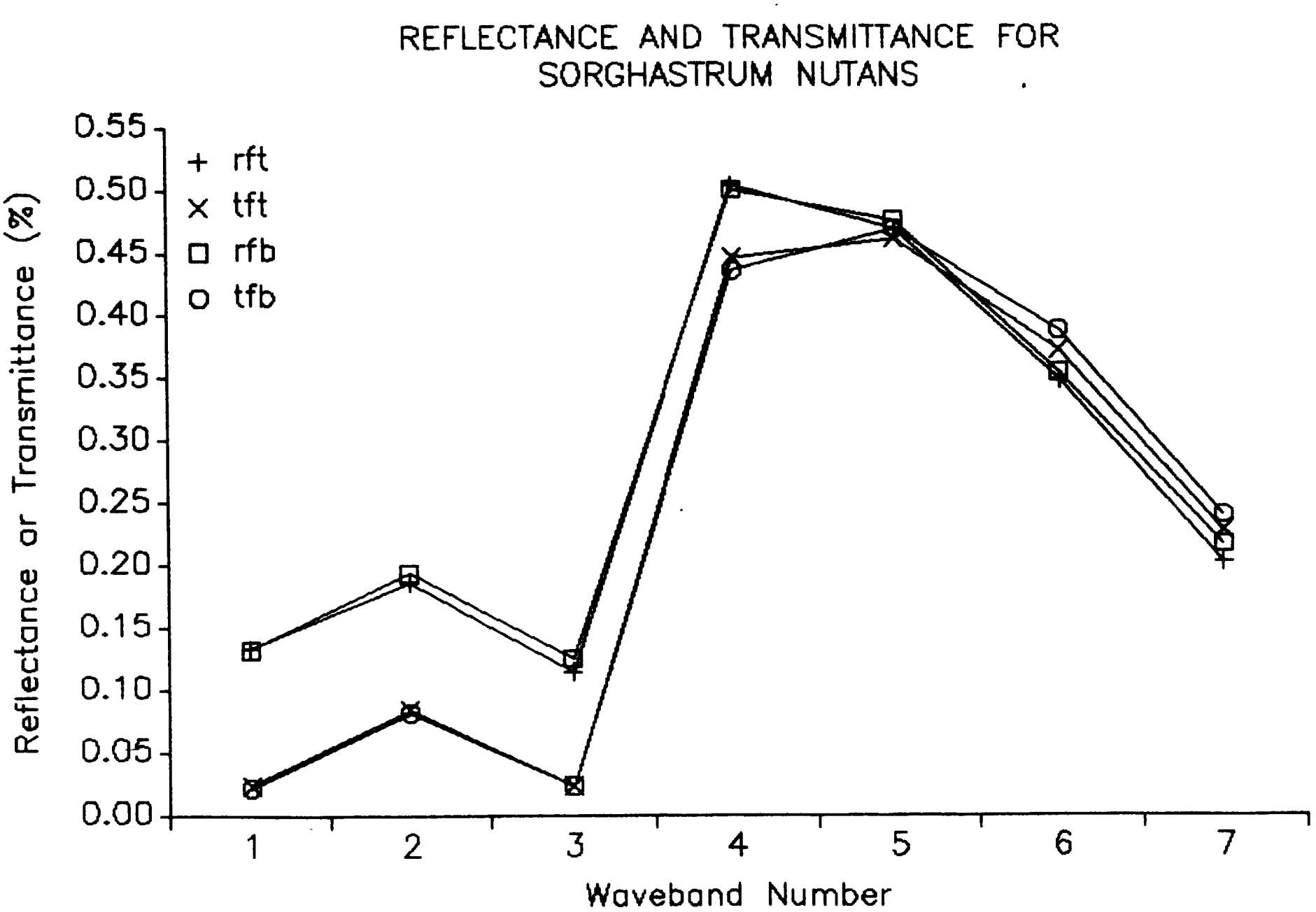

Figure 9. As in Fig. 1 for Sorghastrum nutans.

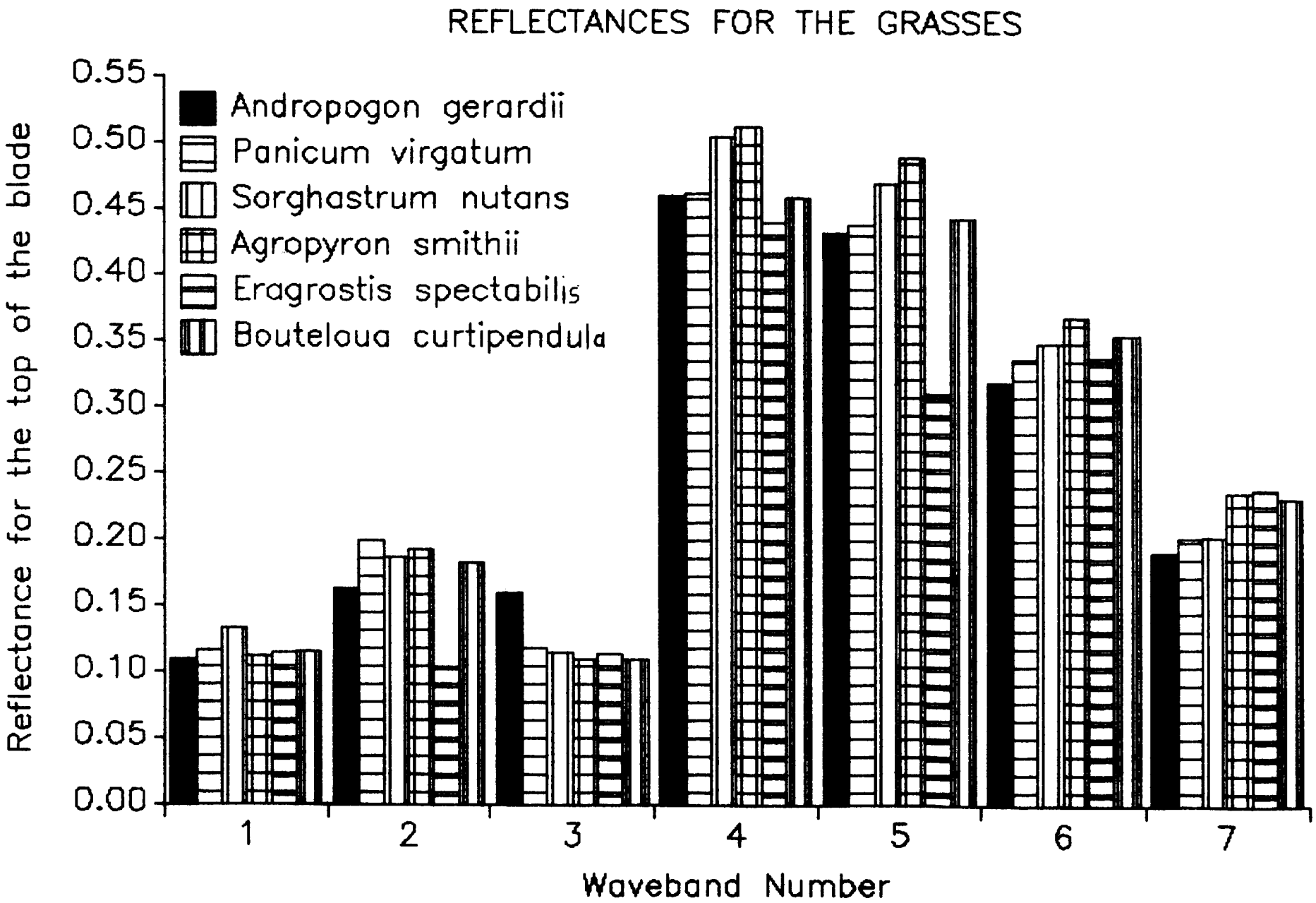

Figure 10. Comparison of reflectances in the MMR wavebands for all grasses measured in the study.

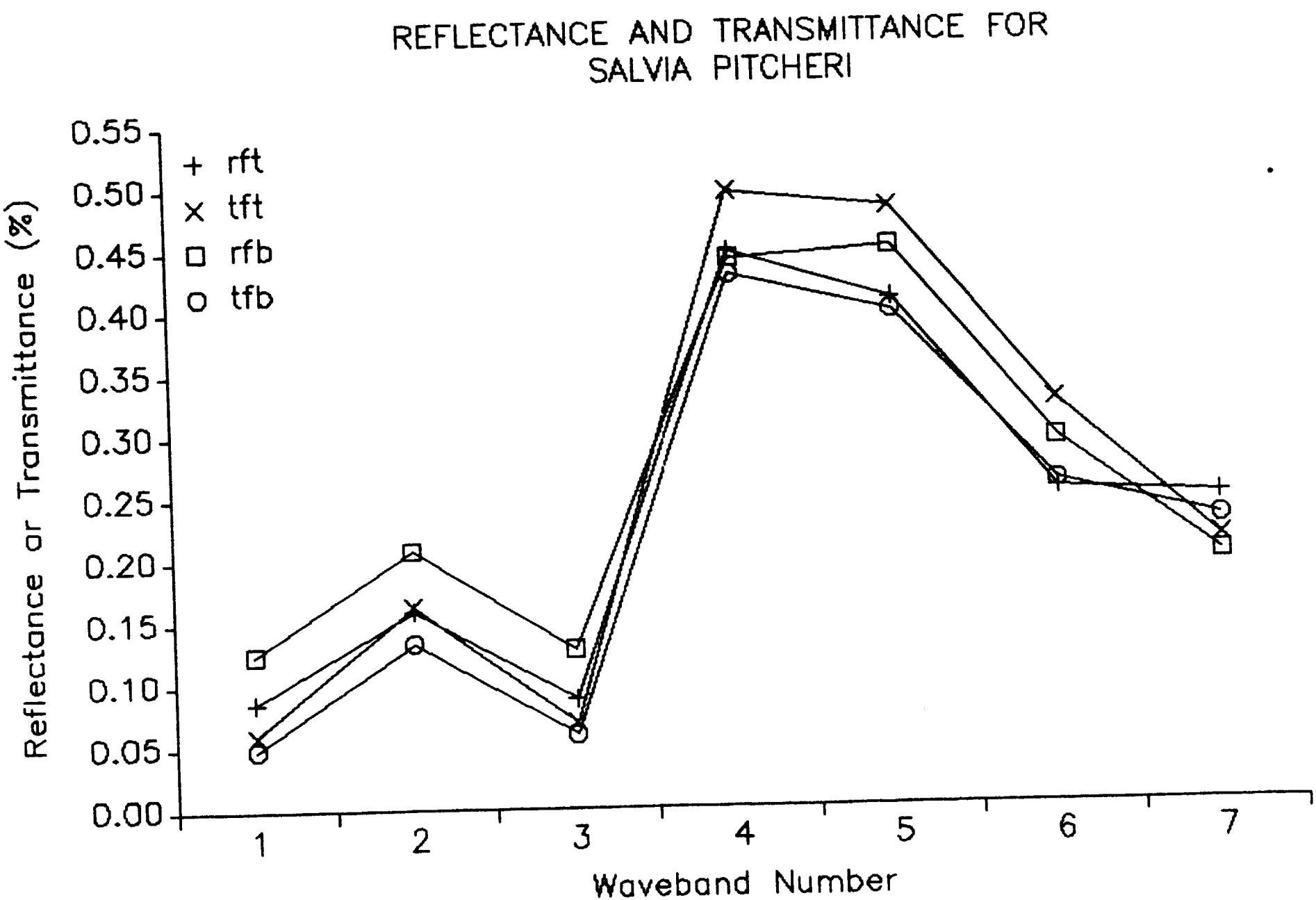

Figure 11. As in Fig. 1 for Salvia pitcheri.

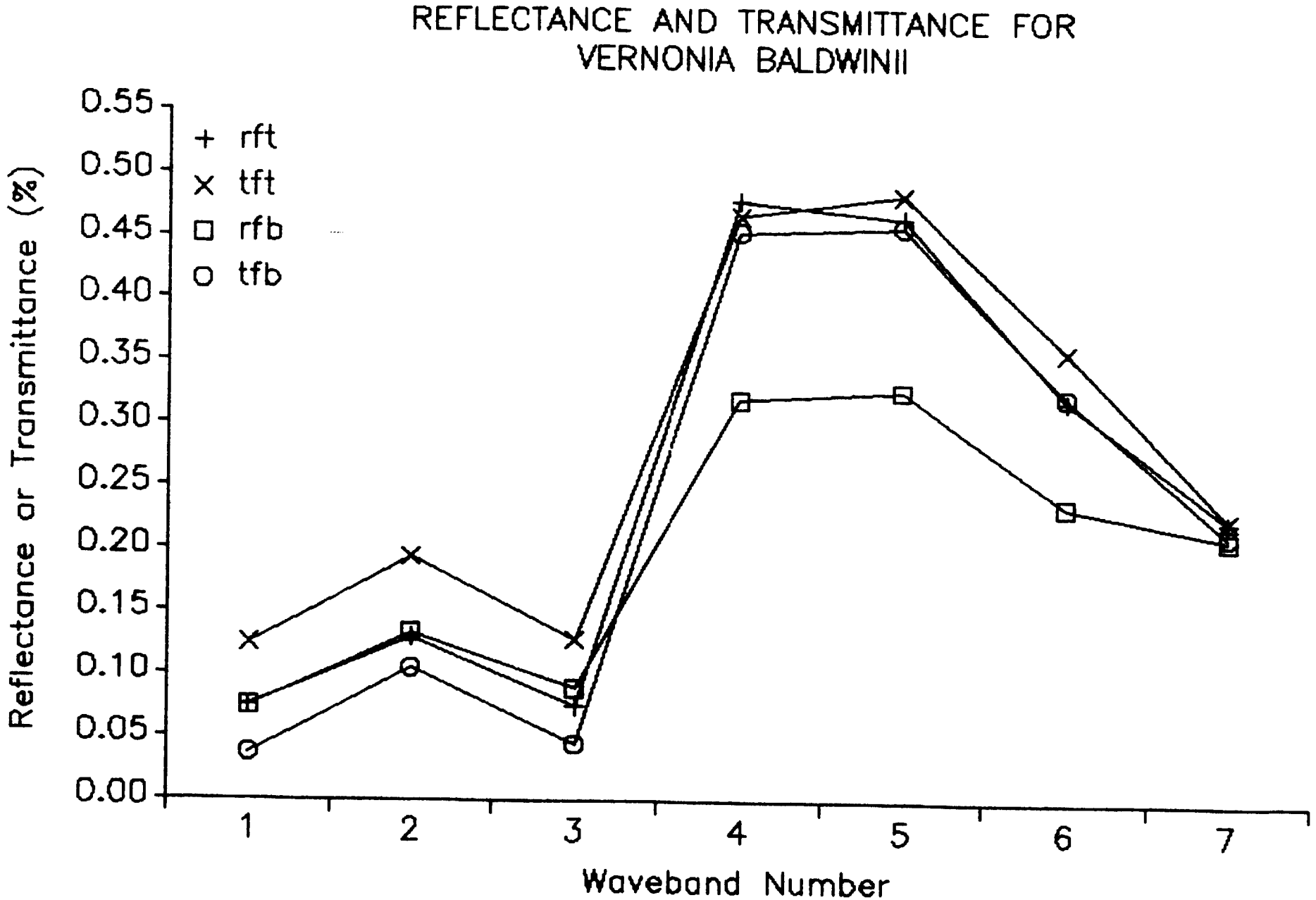

Figure 12 As in Fig. 1 for Vernonia baldwinii.

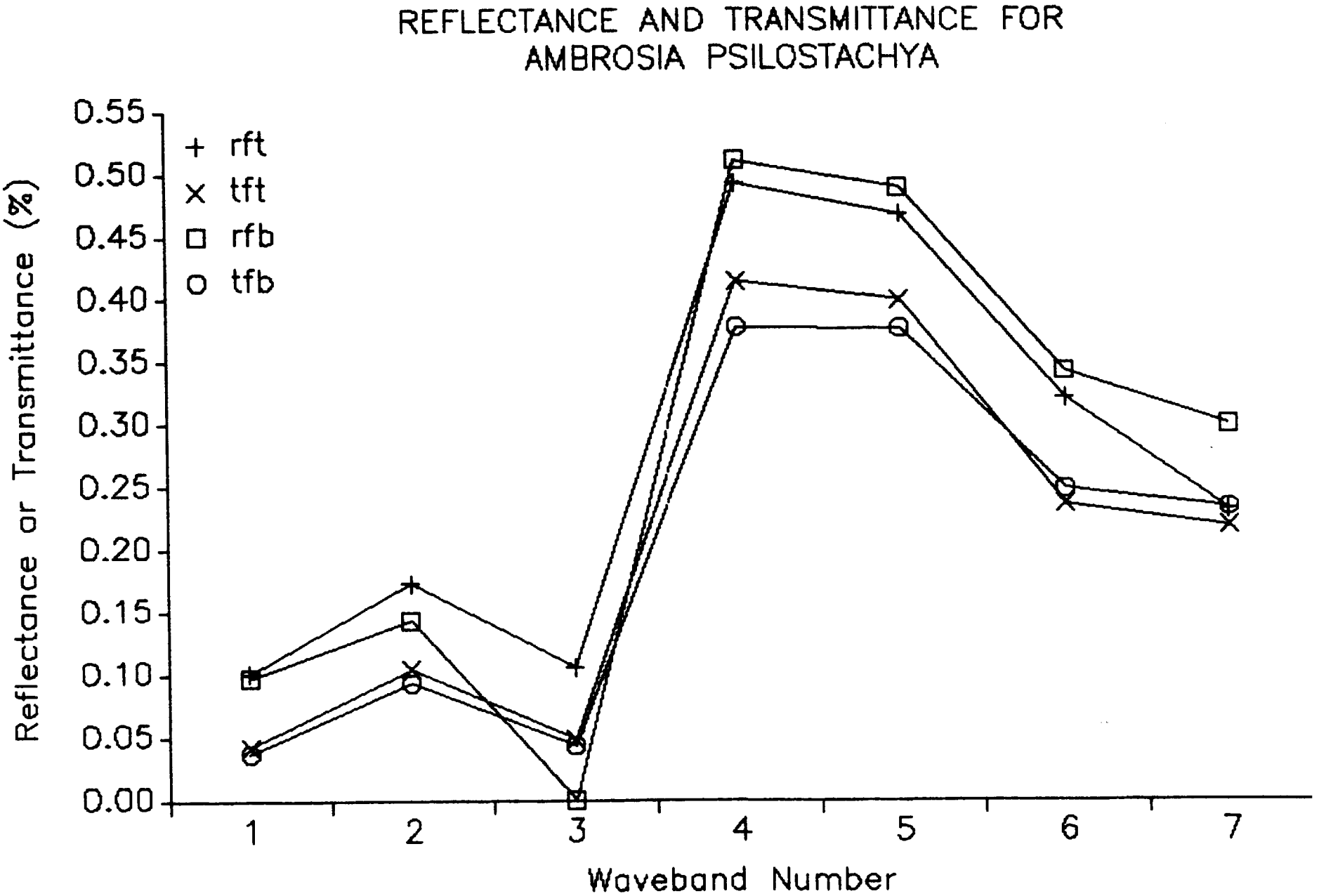

Figure 13. As in Fig. 1 for Ambrosia psilostachya.

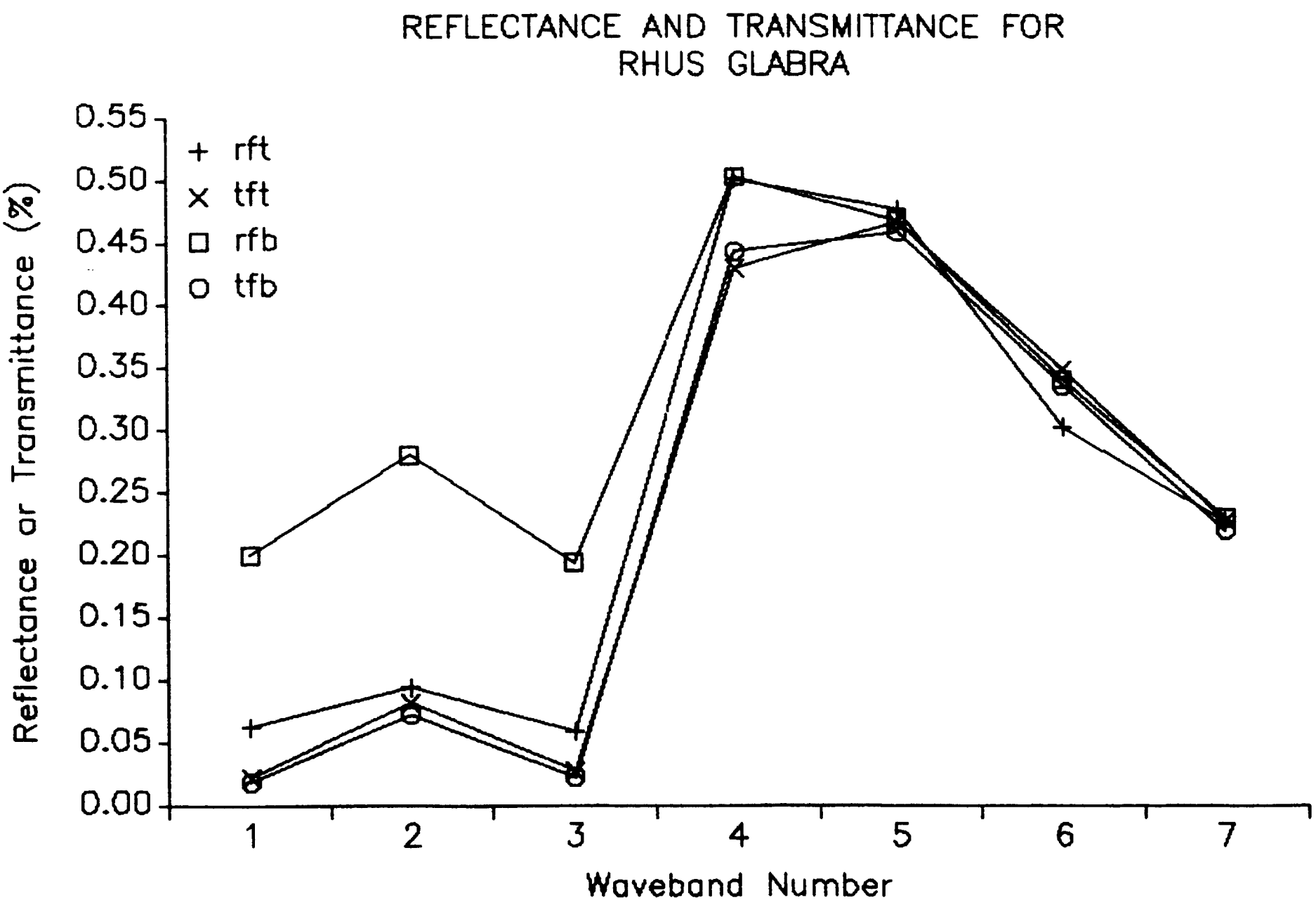

Figure 14. As in Fig. 1 for Rhus Glabra.

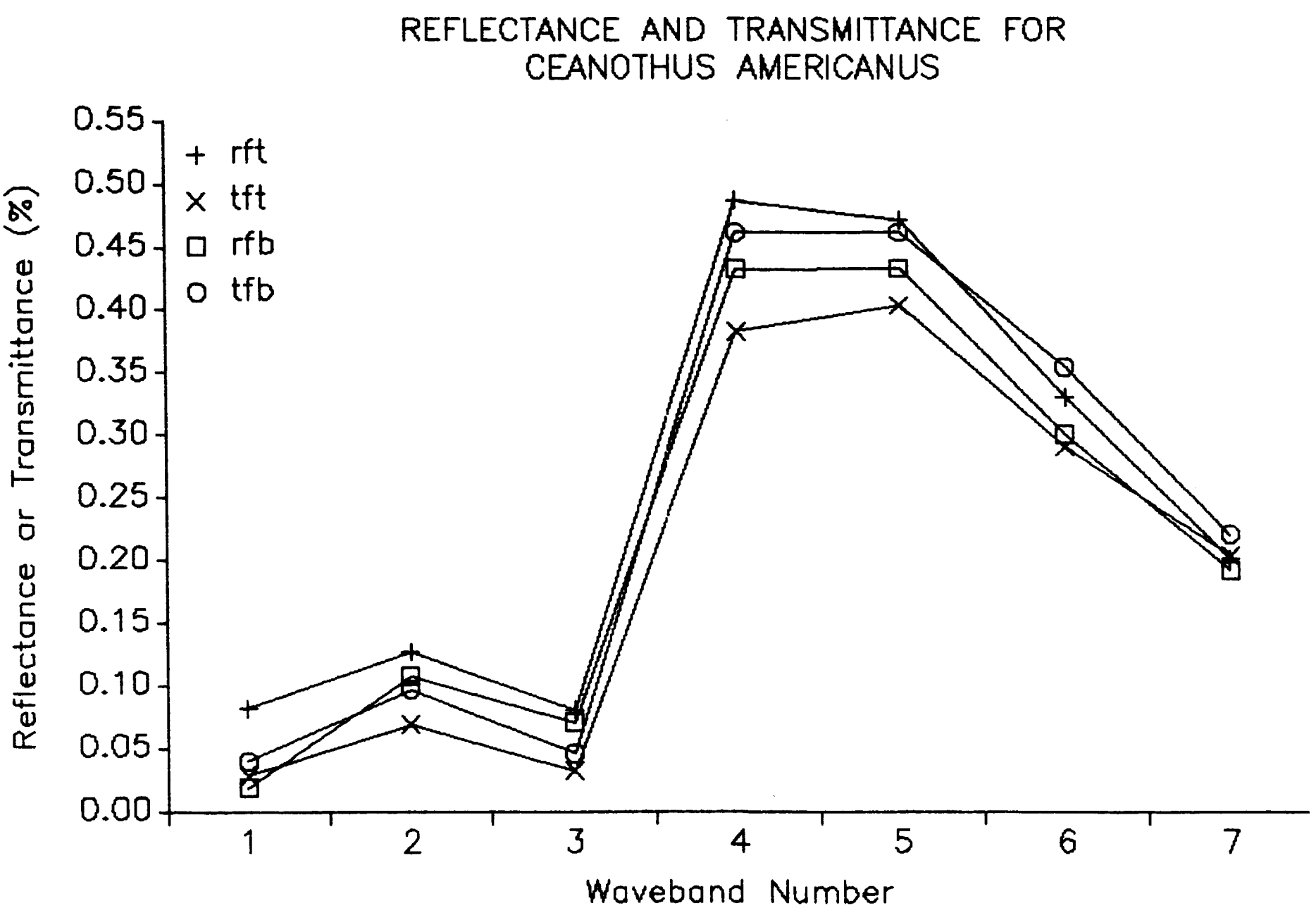

Figure 15. As in Fig. 1 for Ceanothus americanus.

NIR region. Reflectance from the adaxial surface of the leaf was much lower than from the abaxial in wavebands 4 through 6. However, some species of forbs did not display such large differences in reflectances and transmittances for the different leaf surfaces as shown, for example, by Ceanothus americanus (Fig. 15). Reflectance and transmittance properties of the forbs, except for Salvia pitcheri, are very similar in the infrared wavebands, but are not similar to each other in the visible wavebands (Fig. 16). Forbs may not make up a very significant portion of a satellite pixel, but the contribution of forb reflectance to the overall surface reflectance at various locations within the FIFE site needs evaluation.

B. Bidirectional Reflectance and Emittance:

Reflected spectral radiation from prairie surfaces was measured with a Barnes MMR model 12-1000. It was necessary to take MMR measurements using a portable mast because of restrictions placed on driving vehicles on the Konza prairie. The mast allowed us to take measurements along predetermined transects, and enabled us to record changes in spectral properties of vegetative communities that may have resulted from changes in slope and aspect, or changes in species composition.

The portable mast (Fig. 17) was designed to hold the MMR approximately 3.1 m above the soil surface. At this height the radiometer viewed a spot size of about 0.75 m in diameter at nadir. Measurements were made from seven different view angles. These angles were nadir and 20°, 30°, and 50° to either side of nadir. The mast was oriented so that readings were made in or near the principal plane of the sun.

Data were collected on a total of twenty-three plots on transects at two different sites. The first site was located on the Konza Prairie southeast of the headquarters building in the NE 1/4 of section 24 and SE 1/4 of section 23

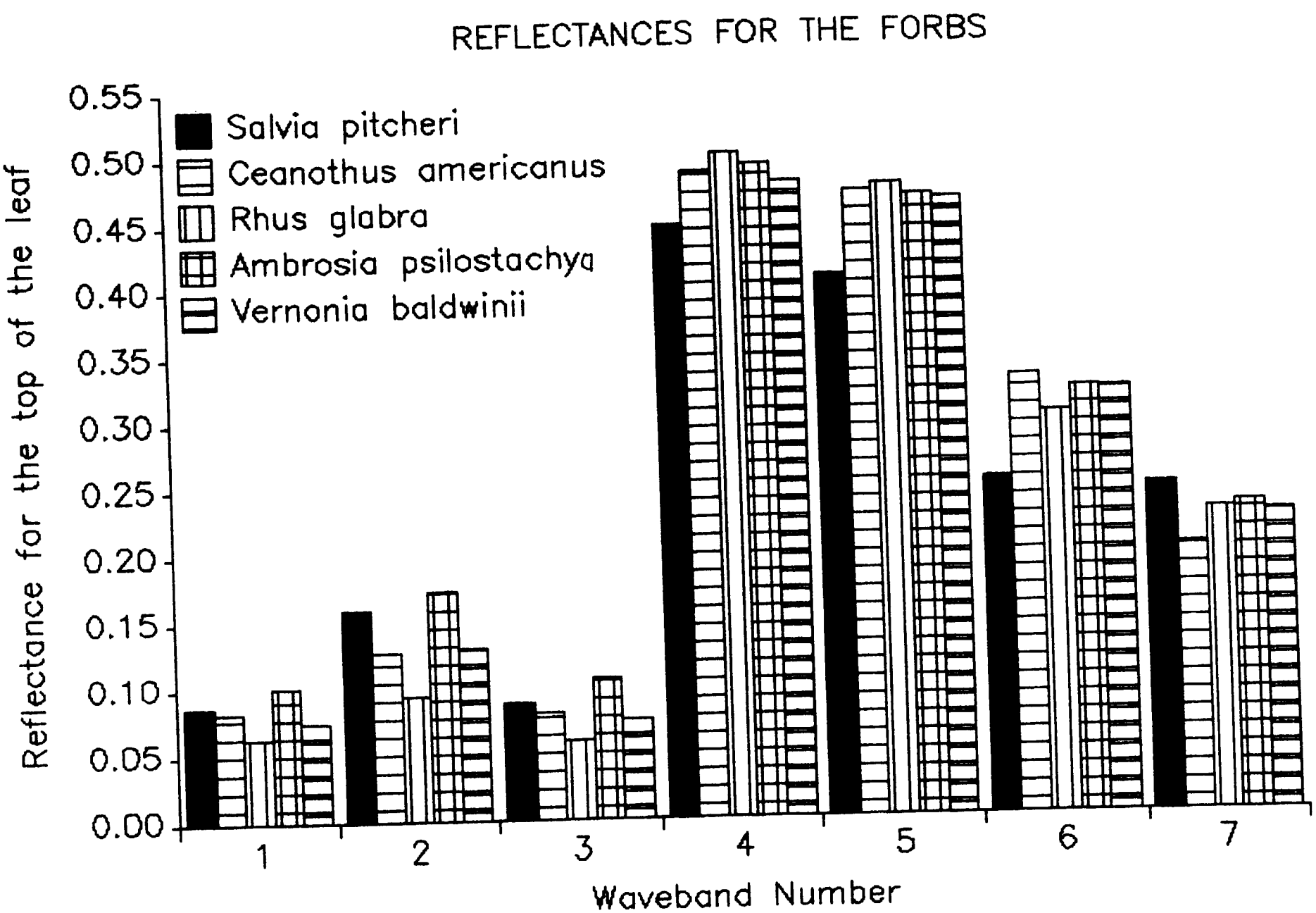

Figure 16. As in Fig. 10 for forbs.

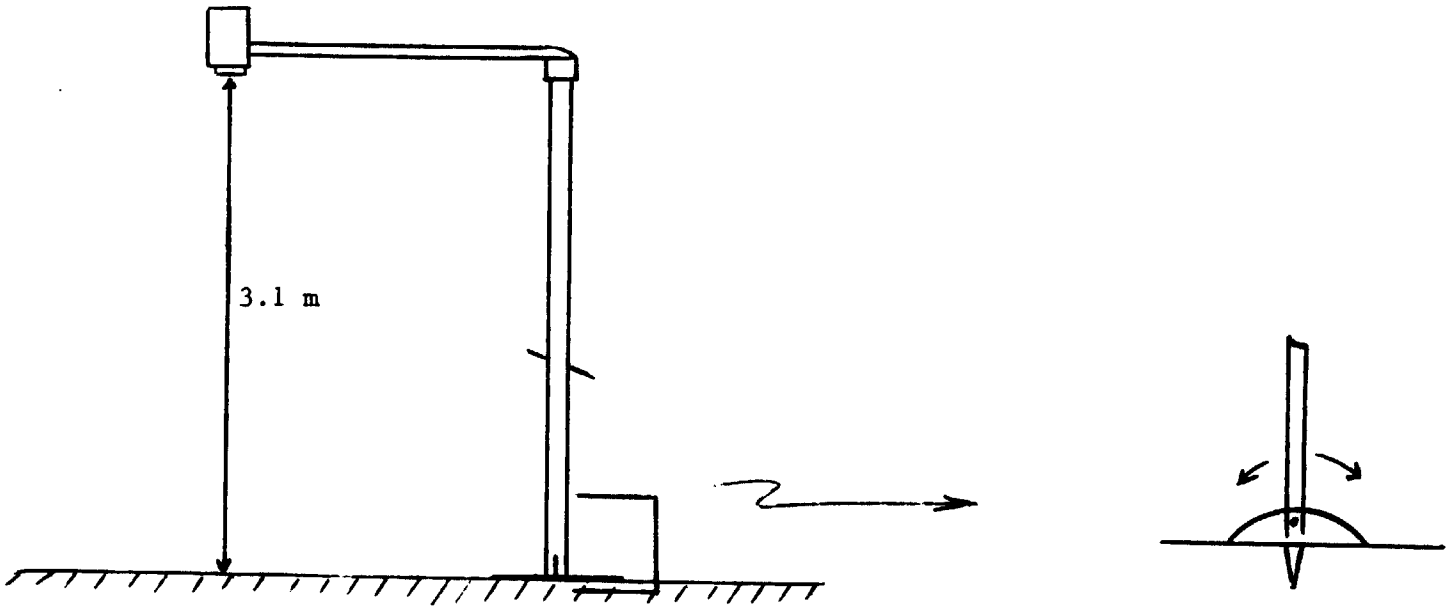

Figure 17. Schematic of portable mast for the Barnes MMR. At right is a drawing of the base of the mount, which allows measurements off-nadir.

in the Swede Creek quadrangle. It is referred to as Konza 1 on the figures. The second transect was located on a gently sloping area near the flux site referred to as site 11, 16, 18 in the 1987 FIFE study. It is referred to as Konza 2 on the figures. These transects were chosen to exhibit differences in topography and species composition. Data were taken from Konza 1 and Konza 2 on July 29 and July 30, 1986, respectively.

MMR voltages were recorded on an Omnidata polycorder and converted to reflectance factors (RF's) using the procedure described by Gardner (1983). These RF values were plotted and examined as a function of view angle and also used in the calculation of albedoes and vegetation indices.

1. Reflectance as Function of View Angle.

a. Konza 1 Site: The influence of slope, time of day and species composition on bidirectional reflectance factor distributions for grassland surfaces in the principal plane of the sun are shown in Figures 18-23. The dips in the curves in the backscatter direction are probably caused by instrument shadowing of the surface viewed by the MMR. Without exception, backscatter reflectance was greater than forward scattered reflectance. The minimum reflectance occurred not at nadir, but rather at view angles of about 20° or 30° for all measurements made on the north-facing slope (Figs. 18, 19, 20 and 22) and at nadir for the south facing slope (Fig. 23).

Reflectance decreased as the solar zenith angle decreased, especially as the view angles approached nadir. The effects were most pronounced for NIR reflectances (bands 4, 5) although visible reflectances (bands 1, 2, 3) also decreased with decreasing solar zenith angle and view angles near nadir.

Some general conclusions for reflectance curves from the Konza 1 transect are summarized as follows:

1) The general order of reflectance was, in order of increasing values, bands 1, 3, 7, 2, 6, 5 and 4.

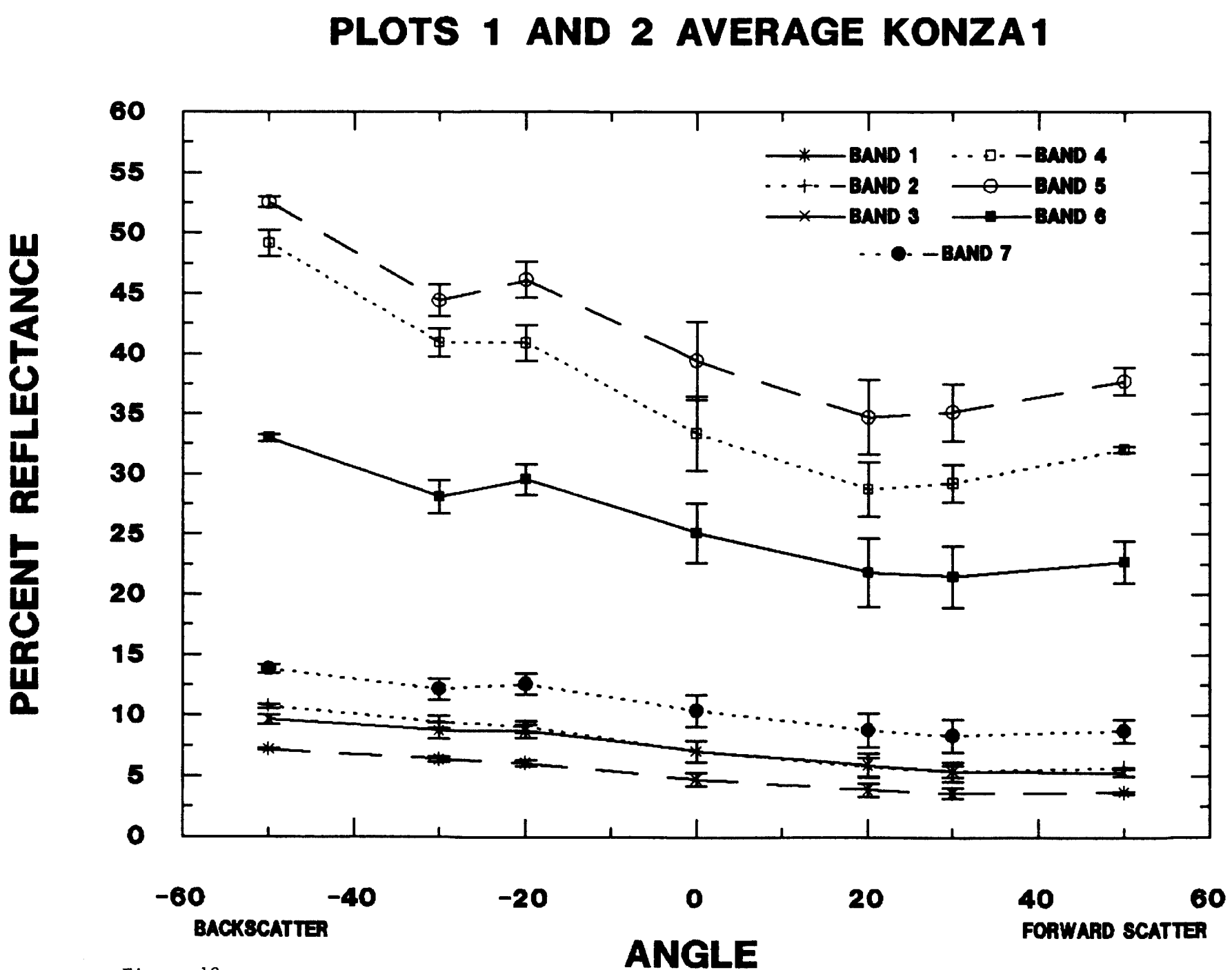

Figure 18. Percent reflectance as a function of view angle for plots 1 and 2 at the Konza 1 site on day 210 (July 29, 1986). The solar zenith angle was 41°, leaf area index was about 2.0 and 0° slope.

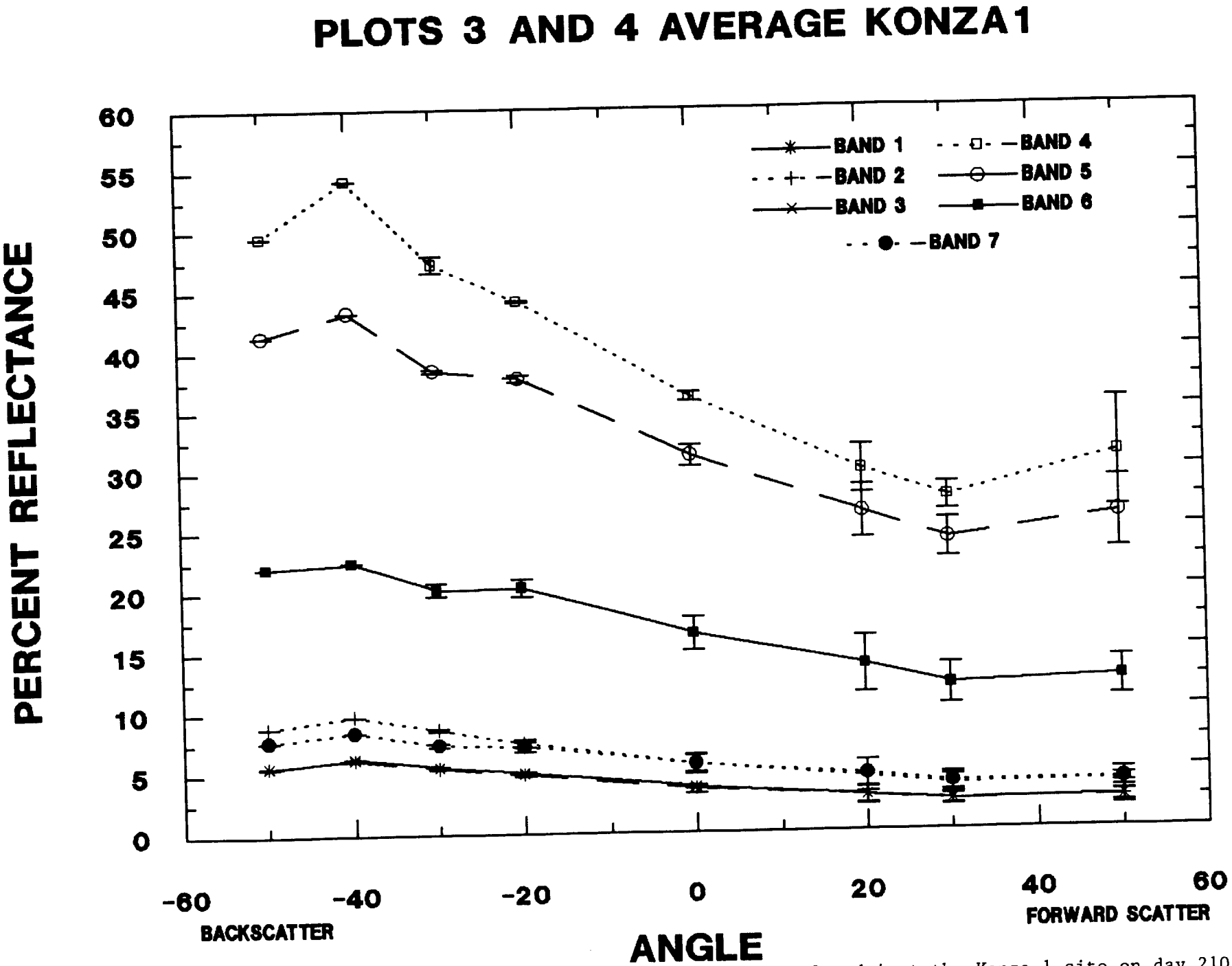

Figure 19. Percent reflectance as a function of view angle for plots 3 and 4 at the Konza 1 site on day 210. The solar zenith angle was 35°, leaf area index was about 4.0 and a north-facing slope of 20°.

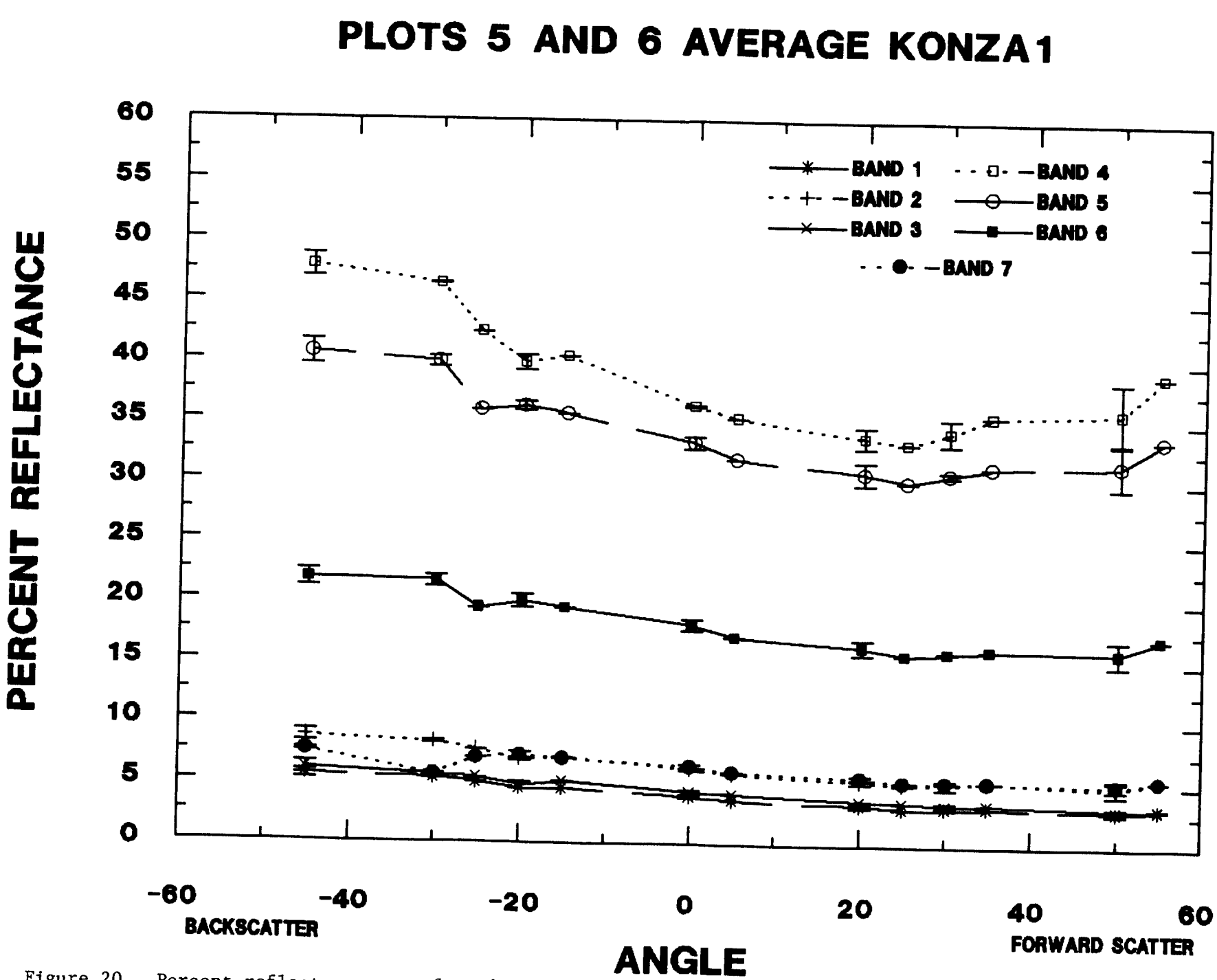

Figure 20. Percent reflectance as a function of view angle for plots 5 and 6 at the Konza site 1 on day 210. The solar zenith angle was 31°, leaf area index was about 3.5 and a north-facing slope of 5°.

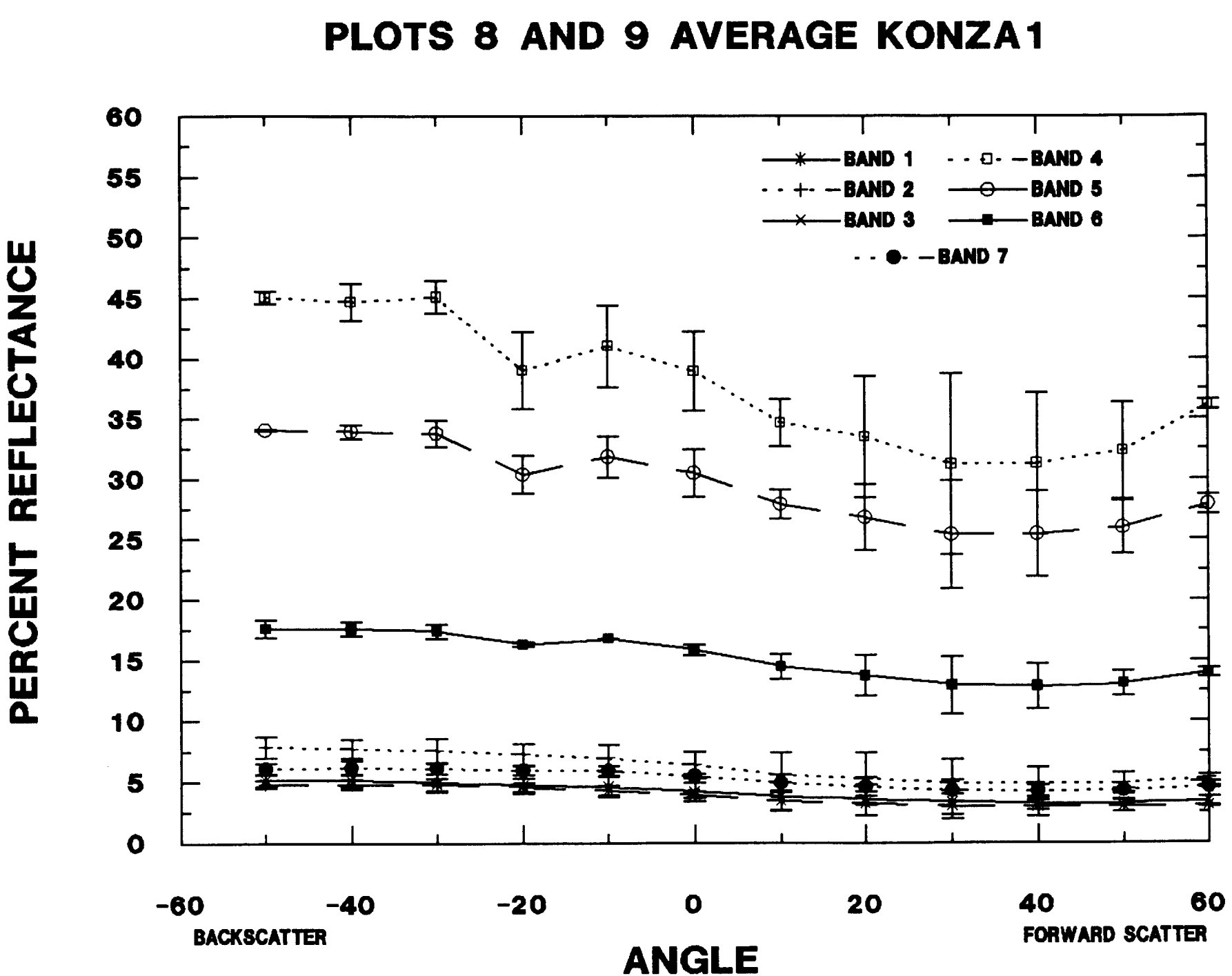

Figure 21. Percent reflectance as a function of view angle for plots 8 and 9 at the Konza 1 site on day 210. The solar zenith angle was 20°, leaf area index of 3.5 and north-facing slope of 10°.

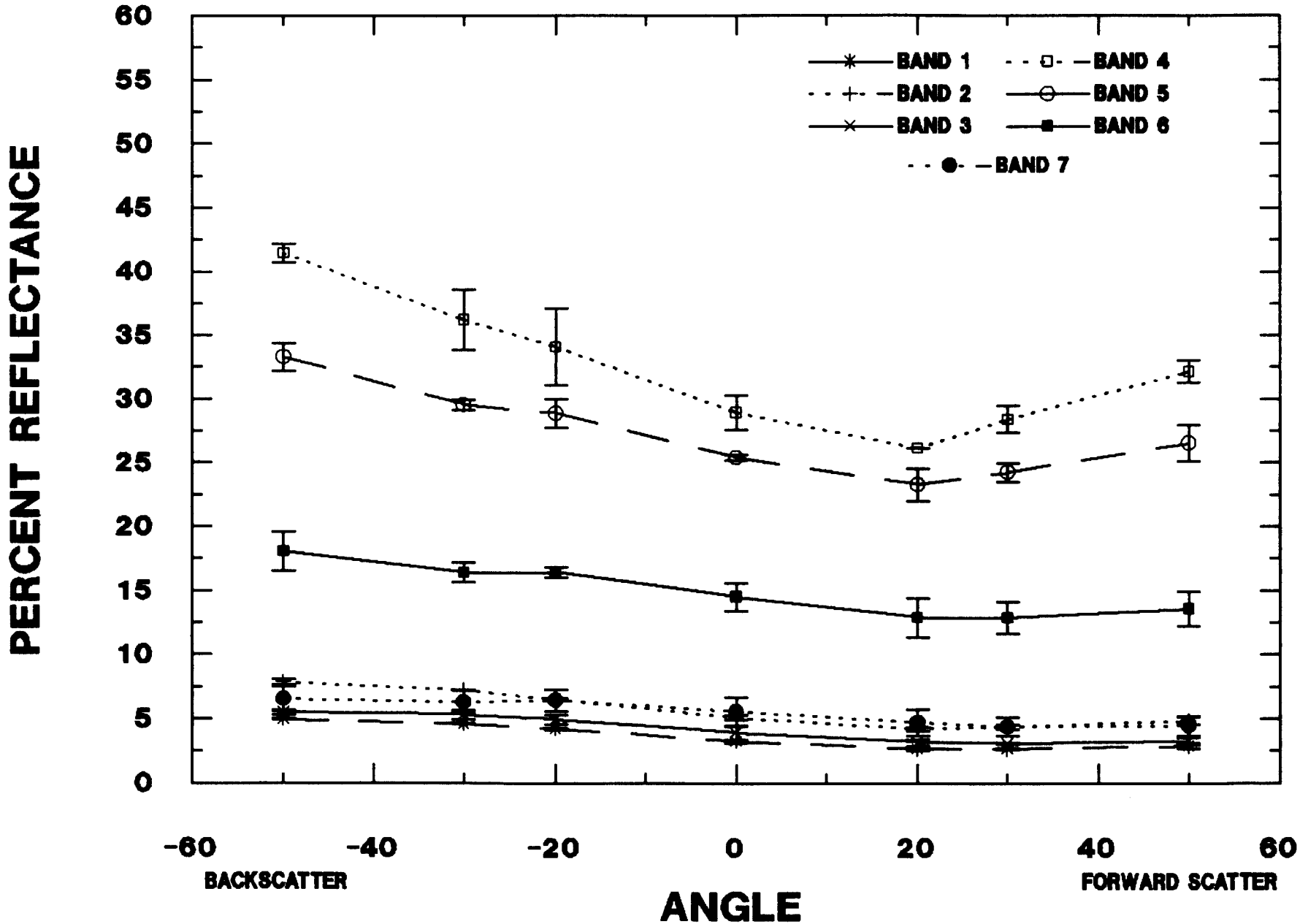

Figure 22. Percent reflectance as a function of view angle for plots 10 and 11 at the Konza site 1 on day 210. The solar zenith angle was about 22°, leaf area index was 4.0 and 0° slope.

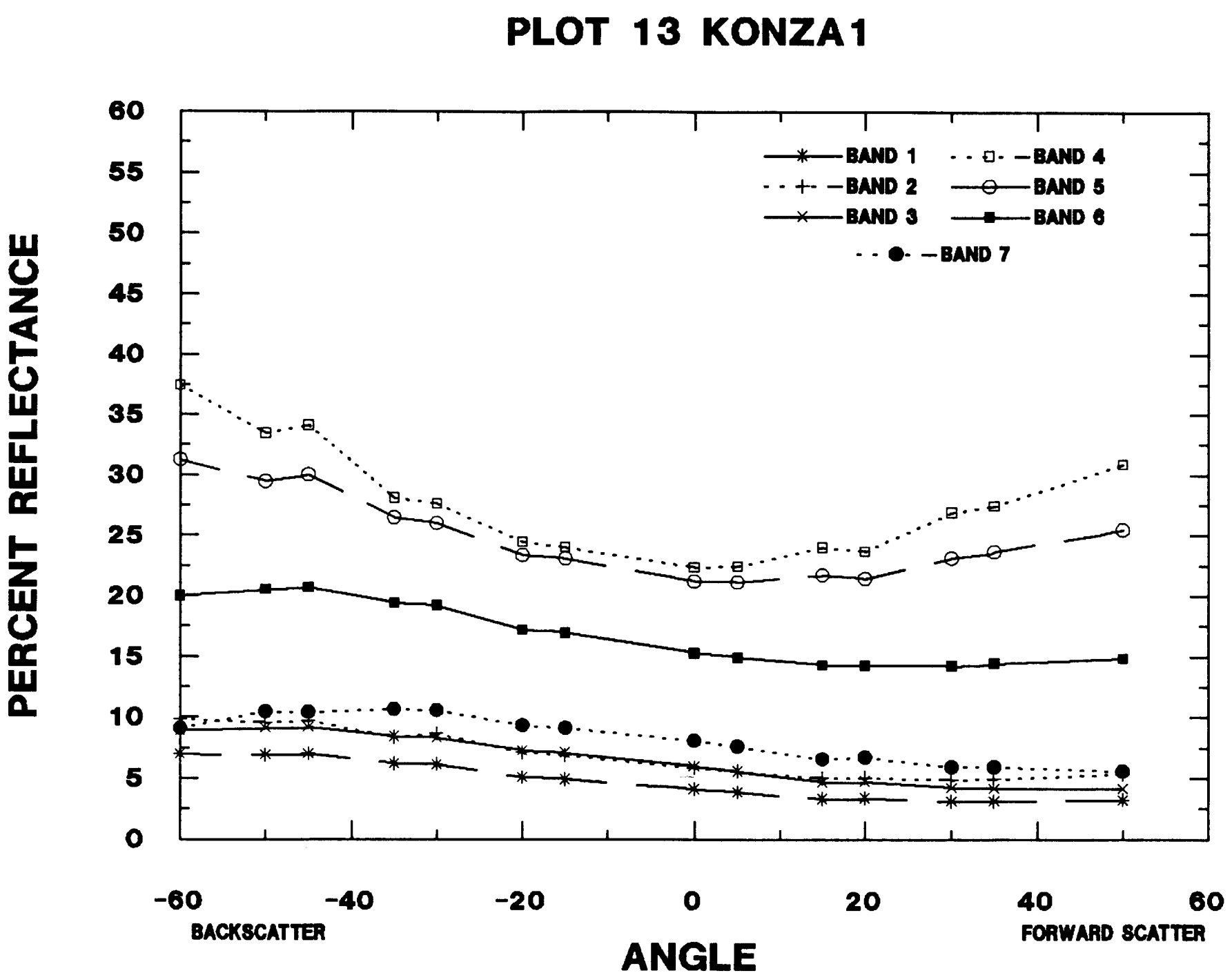

Figure 23. Percent reflectance as a function of view angle for plot 13 at the Konza site 1 on day 210. The solar zenith angle was 28°, leaf area index was about 1.5 and a south-facing slope of 15°.

2) Reflectance magnitudes and patterns were very similar for the visible bands of 1 and 3 which are located in the chlorophyll absorption bands and for band 2 (visible) and band 7 (mid-IR).

3) Minimum near-IR reflectance occurred at 20-30° in the forward scatter direction and maximum at 50° in the backscatter direction. Forward scatter reflectance at 50° was generally 10-20% (15-30% relative difference) lower than backscatter at 50°. Minimum values were 15-30% (30-50% relative) lower than the maximum values.

4) Visible reflectance generally decreased from the backscatter direction at -50 to the forward scatter at 50°. Forward scatter was generally 2-5% lower (30-50% relative difference) than backscatter with a minimum some 3-5% (30-60% relative) lower than the maximum.

b. Konza 2 Site: Data from Konza 2 provided an opportunity to examine the effect of sun zenith angle on bidirectional reflectance (Figs. 24 and 25). Reflectances in the visible wavebands 1 and 3 changed very little as the solar zenith angle decreased from 44 to 22°, particularly in the forward scattering direction. There was about a 1% change in reflectance (absolute terms) at nadir and at the backscatter angles. The effect of solar zenith angle on reflectance in band 4 was not clear. The highest reflectances for band 6 were measured at the lowest solar zenith angle. Canopy reflectances measured at the 34° solar zenith angle were consistently lower than reflectances measured at the 44° and 22° angles. Because reflectances can be influenced by changes in canopy and leaf structures and properties which could mask solar zenith effects measurements such as leaf water potential, effective LAI and leaf angle distributions would provide useful information for helping to characterize changes in canopy reflectance over time.

The effects of increasing LAI on bidirectional reflectance is demonstrated in Figs. 26-28. Three different leaf area coverages are illustrated with

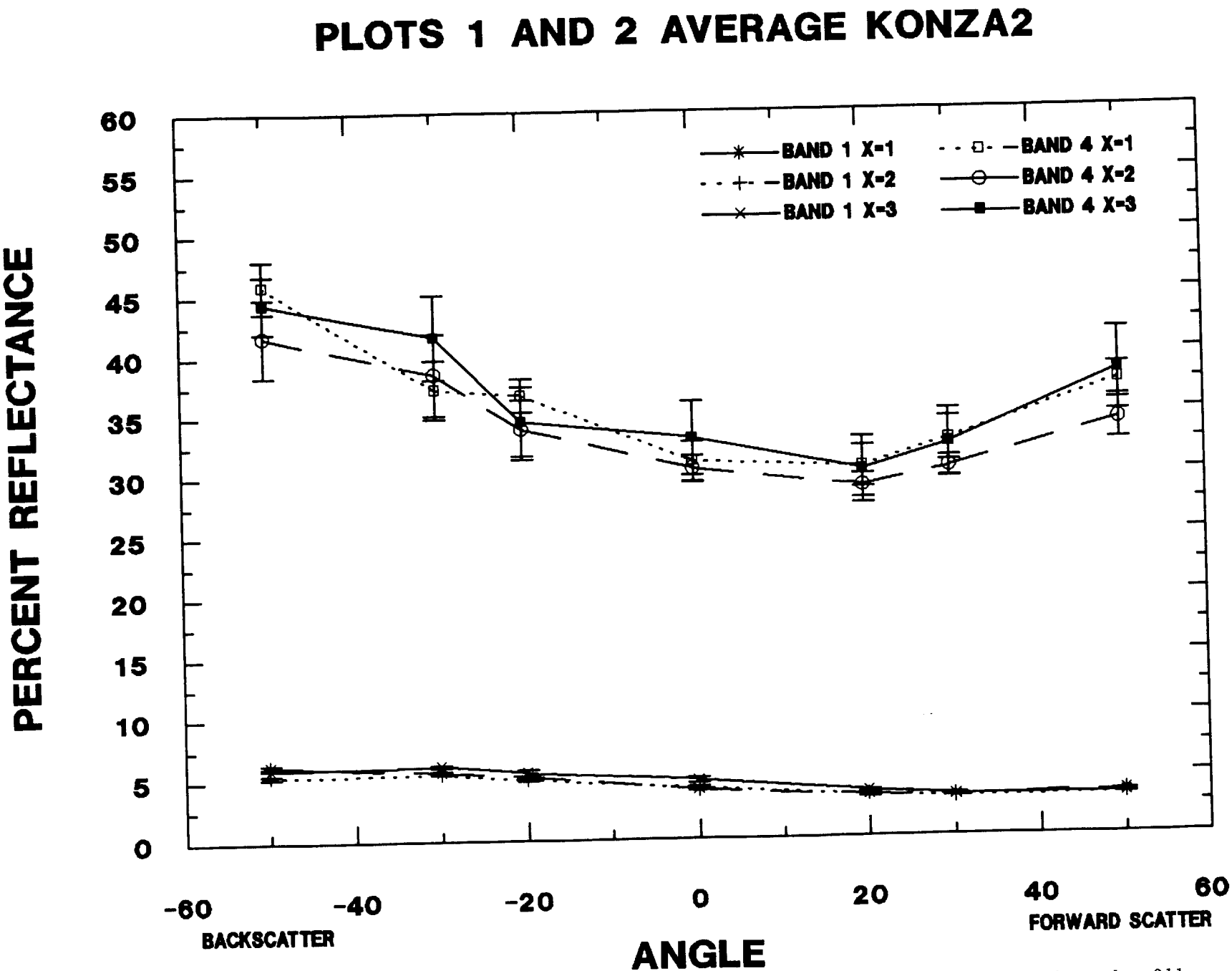

Figure 24. Percent reflectance of MMR bands 1 and 4 for plots 1 and 2 at the Konza site 2 on day 211. Solar zenith angles were 44°, 34° and 22° for X = 1, 2, 3, respectively, and leaf area index of about 1.8 and 0° slope.

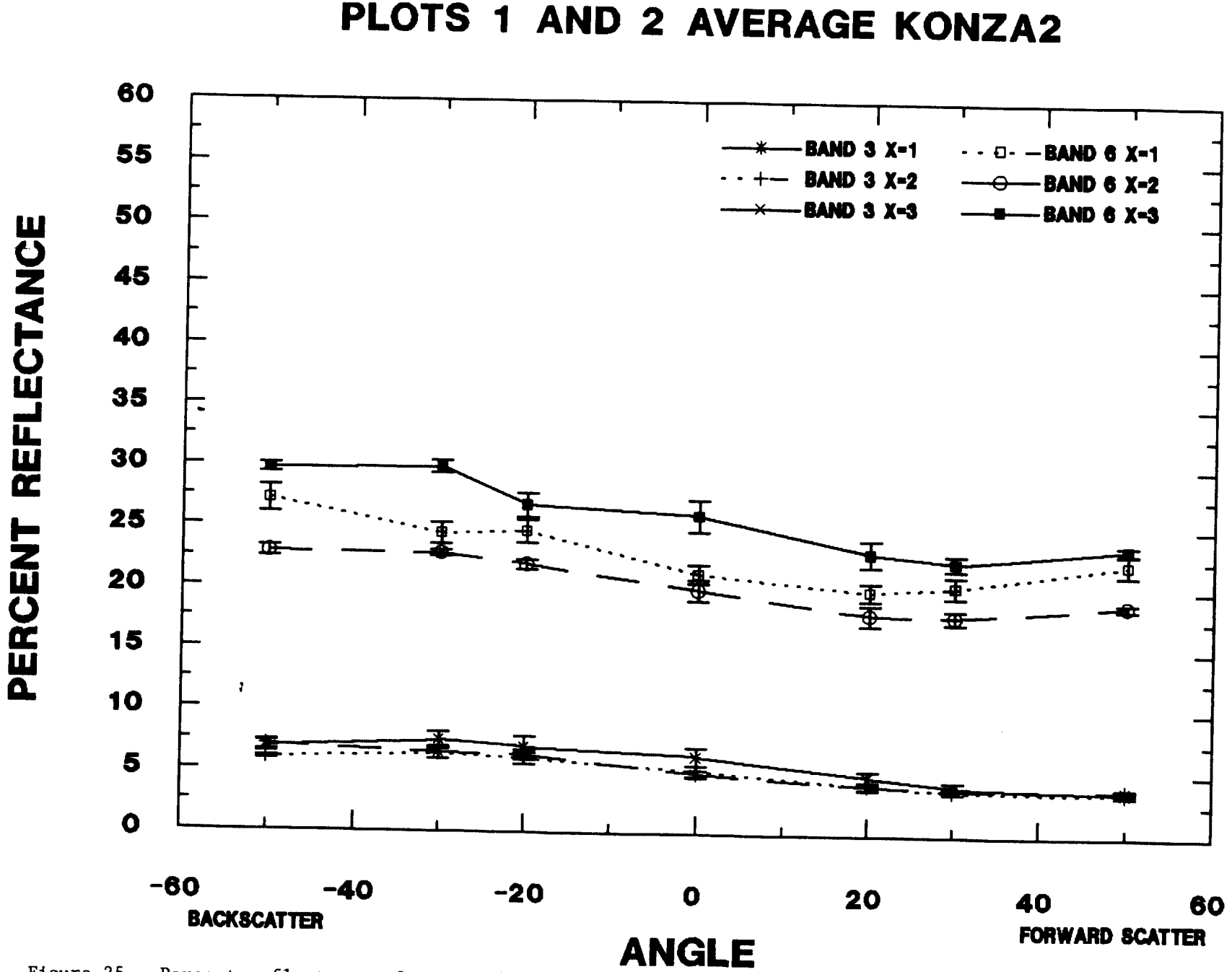

Figure 25. Percent reflectance of MMR bands 1 and 3 for plots 1 and 2 at the Konza site 2 on day 211. Solar zenith angles are 44°, 34° and 22° for X = 1, 2, 3, respectively, and leaf area index of about 1.8 and 0° slope.

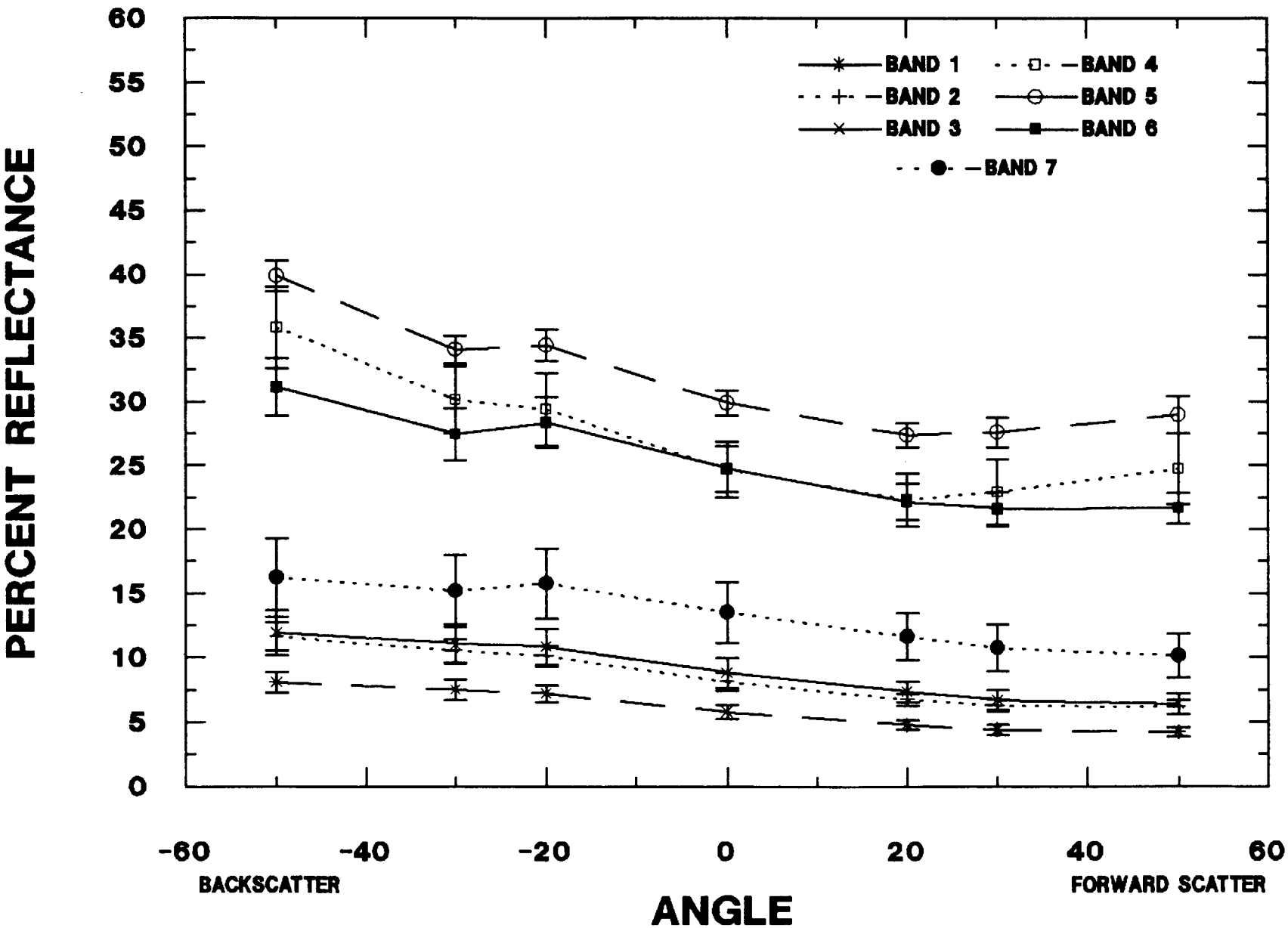

Figure 26. Percent reflectance as a function of view angle for plots 3 and 4 at the Konza 2 site on day 211 (July 30, 1986). The solar zenith angle was 40°, leaf area index was about 0.5 and 0° slope.

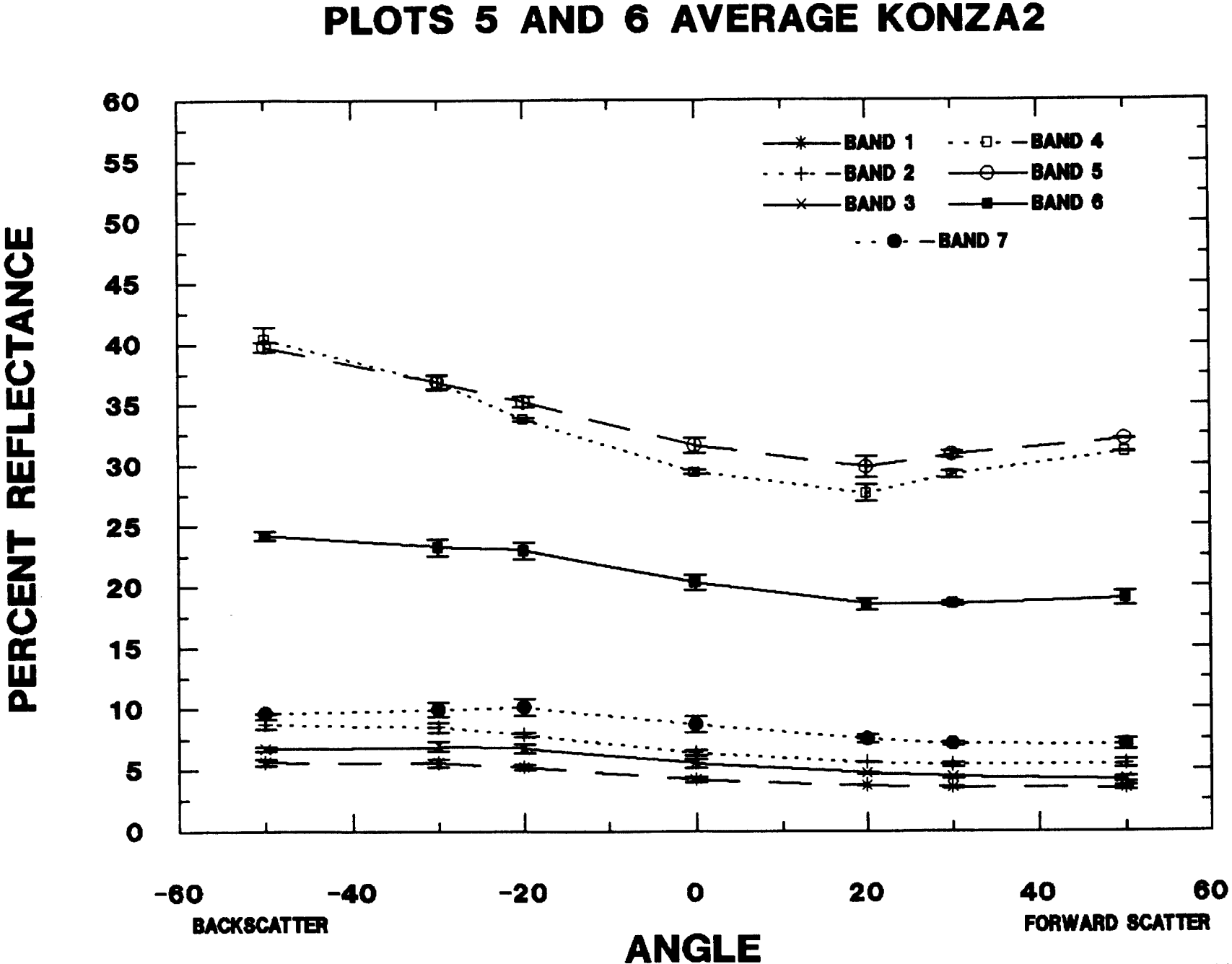

Figure 27. Percent reflectance as a function of view angle for plots 3 and 4 at the Konza 2 site on day 211. The solar zenith angle was 37°, leaf area index about 1.7 and 0° slope.

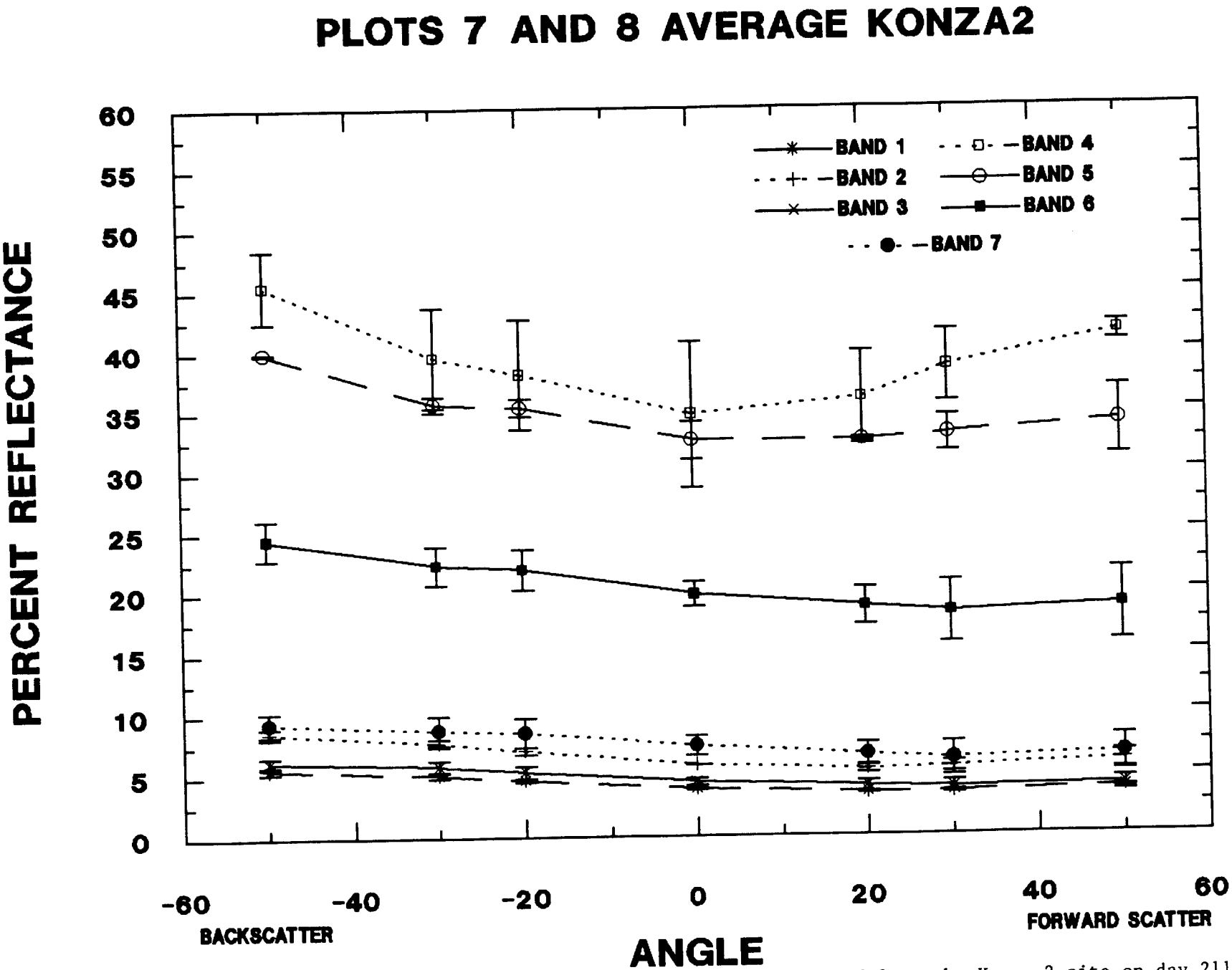

Figure 28. Percent reflectance as a function of view angle for plots 7 and 8 at the Konza 2 site on day 211. The solar zenith angle was 24°, the leaf area index about 4.2 and 0° slope.

LAI values of 0.5, 1.7 and 4.2. The contribution of soil reflectance to canopy reflectance decreased with increasing leaf area. This decrease is seen in the reflectance measurements. Visible and mid-IR reflectance decreased as leaf area increased while near-IR reflectance increased. Visible and mid-IR bidirectional reflectances did not differ between the areas with LAI of 1.7 and those with LAI = 4.2 (Figs. 27, 28). Areas with LAI of 1.7 apparently covered as much soil as those with LAI of 4.2 so that the reflection of radiation in these wavebands to the canopy reflectance was similar.

An examination of all bidirectional reflectance data collected at Konza site 2 resulted in the following general conclusions:

1) Reflectances in band 5 were generally higher than for band 4. This differs from the measurements made at Konza site 1 where reflectances were consistently higher for band 4. Changes in species composition or the influence of radiation from the soil may be a factor.
2) Reflectance generally increased in the order of bands 1, 3, 2, 7, 6, 4, 5.
3) The minimum NIR reflectance occurred at 0 to 20° in the forward scattering direction with maximum reflectance at 50° in the backscatter direction. Forward scatter at 50° was generally 5-10% (10-20% relative) lower than backscatter at the same angle.
4) Minimum reflectance in the visible wavebands occurred in the 20 to 30° forward scattering directions with the maximum in the 50° backscatter direction. The minimum was generally 3-5% (35-49% relative) lower than the maximum.
5) Maximum reflectance in channel 7 occurred in the 30 to 50° backscatter direction and minimum in the 30 to 50° forward scatter direction.

2. Albedo Calculations.

Albedo is defined as the percentage of incident solar energy reflected away from a surface (Lougeay, 1978; Rosenberg et al., 1983). It is an important quantity in the determination of the radiation balance of earth surfaces (Kriebel, 1979; Eaton and Dirmhirn, 1979; Rosenberg et al., 1983). The importance of albedo in the calculation of net radiation (Rn) is illustrated by equation (1):

$$Rn = (1-r)(Rsw\downarrow) + (Rlw\downarrow - Rlw\uparrow) \quad (1)$$

where

Rn = net radiation ($W\ m^{-2}$)
r = albedo (%)
Rsw↓ = incoming shortwave radiation ($W\ m^{-2}$)
Rlw↓ = incoming longwave radiation ($W\ m^{-2}$)
Rlw↑ = outgoing longwave radiation ($W\ m^{-2}$)

Albedoes may be different from one another and generally change with time (Kriebel, 1979). Albedo was expected to vary from place to place because the FIFE site presents variations in topography, management practices, vegetative communities, litter cover, soil exposure, and vegetation density.

One of our ultimate goals is to calculate the net radiation of a surface employing data acquired by remote sensing instrumentation. The albedo must be known to quantify the shortwave balance (Eq. 1). Investigation into the utility of employing remotely sensed data from the MMR to calculate albedo was performed. These calculations of albedo utilized three components: 1) reflectance factors derived from the MMR data, 2) the Walthall et al. (1985) bidirectional reflectance equation, and 3) the solar radiation curve of Moon (1940). The actual algorithm used to calculate the albedo is:

$$r = \sum_{i=1}^{7} Wi\ Rhi \quad (2)$$

where

r = albedo
Wi = a weighting factor
Rhi = hemispherical reflectance for channel i as determined by the model of Walthall et al. (1985).

A description of the reflectance factor calculations may be found in Gardner (1983) as elaborated upon by Bauer et al. (1981). Moon's (1940) solar radiation data provided solar irradiation in W m^{-2} μm^{-1} for the region 0.295-2.14 μm for a surface at sea level with an optical air mass of two. The data of Moon were plotted and the MMR bandwidths were noted on the graph.

To determine the albedo for a given surface using remotely sensed data, the bandwidths must account for all the radiation in the spectral curve constructed from the Moon (1940) data. Therefore, each band of the MMR was extended to cover a little larger region of the spectrum than they actually measure (Table 4).

Table 4. Weighting factors assigned to each MMR waveband based on the data of Moon (1940).

Band	Original Width (μm)	Extended Width (μm)	Energy in Each Band (W m^{-2})	Weighting Factor Wi
1	.45- .52	.295- .520	140	0.1884
2	.52- .60	.520- .615	112	0.1511
3	.63- .69	.615- .700	96	0.1309
4	.76- .90	.700-1.025	228	0.3072
5	1.15-1.30	1.025-1.360	106	0.1435
6	1.55-1.75	1.360-1.800	49	0.0665
7	2.08-2.35	1.800-2.140*	9	0.0125

*Moon's data showed no energy past 2.140 μm.

Weighting factors are determined by dividing the energy in each band by the total energy under the curve (approximately 740 W m-2) (Moon, 1940).

Hemispherical reflectances (Rhi) calculated for each channel for each sample plot are multiplied by their respective weighting factors (Wi) and then summed to provide the albedo for the sample plot. Albedos for a selected number of sample plots from the Konza 2 site were calculated and are shown in Table 5.

Table 5. Albedo values calculated by equation 2 for several plots at the off-Konza site.

Plot #	Time	Albedo
1	1026	24
1	1126	21
1	1247	24
2	1034	25
2	1119	22
2	1255	25
3	1044	20
4	1053	21
5	1101	22
6	1108	21
11	1340	25

Estimated albedoes fall in the range of 20-25% which are reasonable albedo values for vegetative surfaces (Rosenberg et al., 1983). However, independent measurements of albedo for the sample plots were not made, therefore, it is difficult to say that the determined values of albedo are correct.

During the intensive field campaigns (IFCs) supporting measurements of net radiation, albedo, and canopy temperatures will be made in order to compare the albedo and net radiation values calculated from remotely sensed data. More recent and accurate solar radiation curves or models will be sought to improve albedo calculations.

Objective (3) - Measurement of Sensible and Latent Heat Fluxes

Measurements were made over a winter wheat crop (Triticum aestivum L., Colt) at Mead, Nebraska on selected days during the 1985 growing season. The incoming shortwave radiation (Rs) was measured with a pyranometer. Net radia-

tion (Rn) was measured using Swissteco net radiometers. Soil heat flux (S) was measured with heat flow sensors. Soil temperature was measured with thermocouples. Surface soil heat flux (S) was computed from soil heat flow sensor and soil thermocouple data employing a combination method. Mean wind speed profiles were measured with a set of three-cup anemometers. Profiles of mean air temperature and humidity were measured with ceramic wick psychrometers.

Soil moisture was measured gravimetrically and with a Campbell Nuclear Pacific neutron probe. Crop height, leaf area index and dry matter were monitored. Water potential and stomatal resistance of flag leaves were also measured.

Fluxes of sensible (H) and latent (LE) heat were computed by means of the Bowen-ratio technique. The data have been analyzed, tabulated and graphed. The following data sets were used to compare Cupid estimated fluxes with measured values.

Variables	Measurement Dates (1985)
a) Meteorological: Rs, Rn, S, H, LE, air temperature, vapor pressure deficit, wind speed, soil temperature	May 22, 23, 25, 28, 29, 30; June 7, 8, 13, 14 and 20
b) Soil Moisture:	May 21, 23, 28; June 3, 6 8, 10, 12, 17, 18 and 24
c) Plant height, leaf width, height of most dense region, height of lowest leaves, leaf area index, dry matter:	April 20, 24; May 6, 14, 17, 20, 22, 23, 24, 28, 29, 30; June 3, 5, 7, 8, 10, 12 13, 14, 17, 18, 21 and 24
d) Leaf water potential and stomatal resistance:	May 20, 21, 22, 23, 24, 28, 29, 30, 31; June 3, 5, 6, 7, 8 and 10

Fluxes of water vapor and sensible heat were calculated using the eddy correlation technique for a tall grass prairie location within the FIFE site

near Manhattan, Kansas on a few selected days during July-August, 1986. Vertical velocity fluctuations were measured with a sonic anemometer, air temperature and humidity fluctuations were measured with fine wire thermocouples and a Lyman-alpha hygrometer. These measurements were made 2.25 m above the ground. Supporting data on net radiation, mean horizontal wind speed profiles, soil heat flux, mean air temperature and humidity, and soil temperature were also obtained. Micrometeorological data were collected when the wind was south to east, resulting in approximately 200 m of upwind fetch over reasonably flat terrain. Volumetric soil water was determined gravimetrically in the upper 0.6 m soil layer.

Signals from the eddy correlation sensors were recorded on an IBM PCAT microcomputer using an analog to digital converter. These signals were low-pass filtered with 8-pole Butterworth active filters (12.5 Hz cutoff frequency) and recorded at 25 Hz. The slow-response signals were recorded on an IBM PCXT microcomputer. Data were averaged for the first 45 min of each solar hour. The last 15 minutes were reserved for sensor calibration and checks.

Energy Fluxes

The energy balance over the prairie vegetation can be approximated by[1]:

$$Rn + LE + H + S \approx 0 \qquad (3)$$

Values of Rn and S were measured with slow-response sensors (net radiometers and heat flow transducers). On the other hand, LE and H were measured with fast-response eddy correlation sensors. Ideally, -(LE+H) should be balanced by (Rn+S). The sum of latent and sensible heat fluxes [-(LE+H)] measured by

[1]Fluxes directed away from the surface are negative.

the eddy correlation technique generally agreed well with the sum of the net radiation and soil heat flux (Rn+S), measured independently (Fig. 29).

Diurnal patterns of the energy balance components over the tall grass prairie measured on 30 July 1986 are shown in Fig. 30a. The vegetation was at the heading stage and the leaf area index (LAI) was about 2.0.

Except for a few early morning clouds, 30 July was clear with high solar radiation. Midday air temperature and vapor pressure deficit on this day ranged from 33 to 37°C and from 3.3 to 4.2 kPa, respectively (Fig. 31). Fluxes H, LE and S followed diurnal patterns similar to that of Rn. Net radiation reached its maximum of about 570 W m^{-2} at solar noon and decreased in the afternoon. Sensible and soil heat fluxes reached peak magnitudes of about 130 W m^{-2} and 90 W m^{-2} at solar noon, respectively. Both fluxes were directed away from the surface throughout the day. The latent heat flux reached a peak magnitude of 410 W m^{-2} around 1100 hrs and then decreased later in the day.

The diurnal patterns of the energy balance components on a partly cloudy day (6 August 1986), at the same stage of growth, are shown in Fig. 30b. This day was mostly to partly cloudy in the morning hours and clear in the afternoon. Midday air temperature and vapor pressure deficit ranged from 27 to 30°C and from 018 to 1.3 kPa, respectively. Values of Rn varied, depending on the degree of cloud cover, from 460 to 580 W m^{-2} during the midday. Diurnal patterns of LE, H and S followed that of Rn quite closely. The latent heat flux was reduced due to lower Rn and atmospheric evaporative demand (lower air temperature, vapor pressure deficit and wind speed) on this day as compared to those on 30 July (see Fig. 31). A greater proportion of Rn was partitioned into sensible heat. Midday magnitude of H varied from 140 to 190 W m^{-2}. Magnitude of LE during the midday ranged between 210 to 340 W m^{-2}. Midday S was about 80 W m^{-2}.

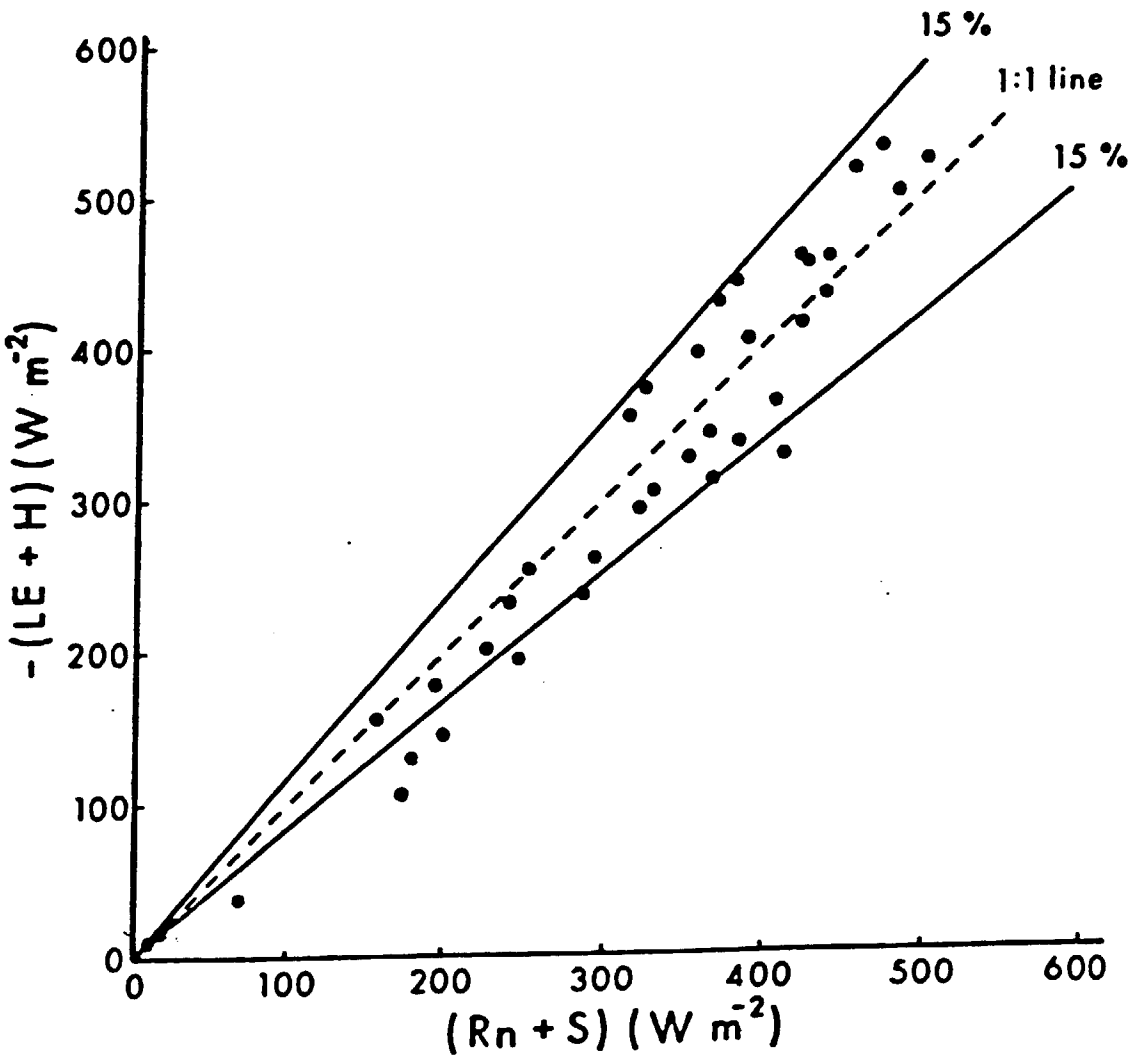

Fig. 29. Balance of energy budget terms. LE and H measured by eddy correlation. Rn and S measured with net radiometer and heat flow transducer. Dotted lines indicate 15% deviation from 1:1 line.

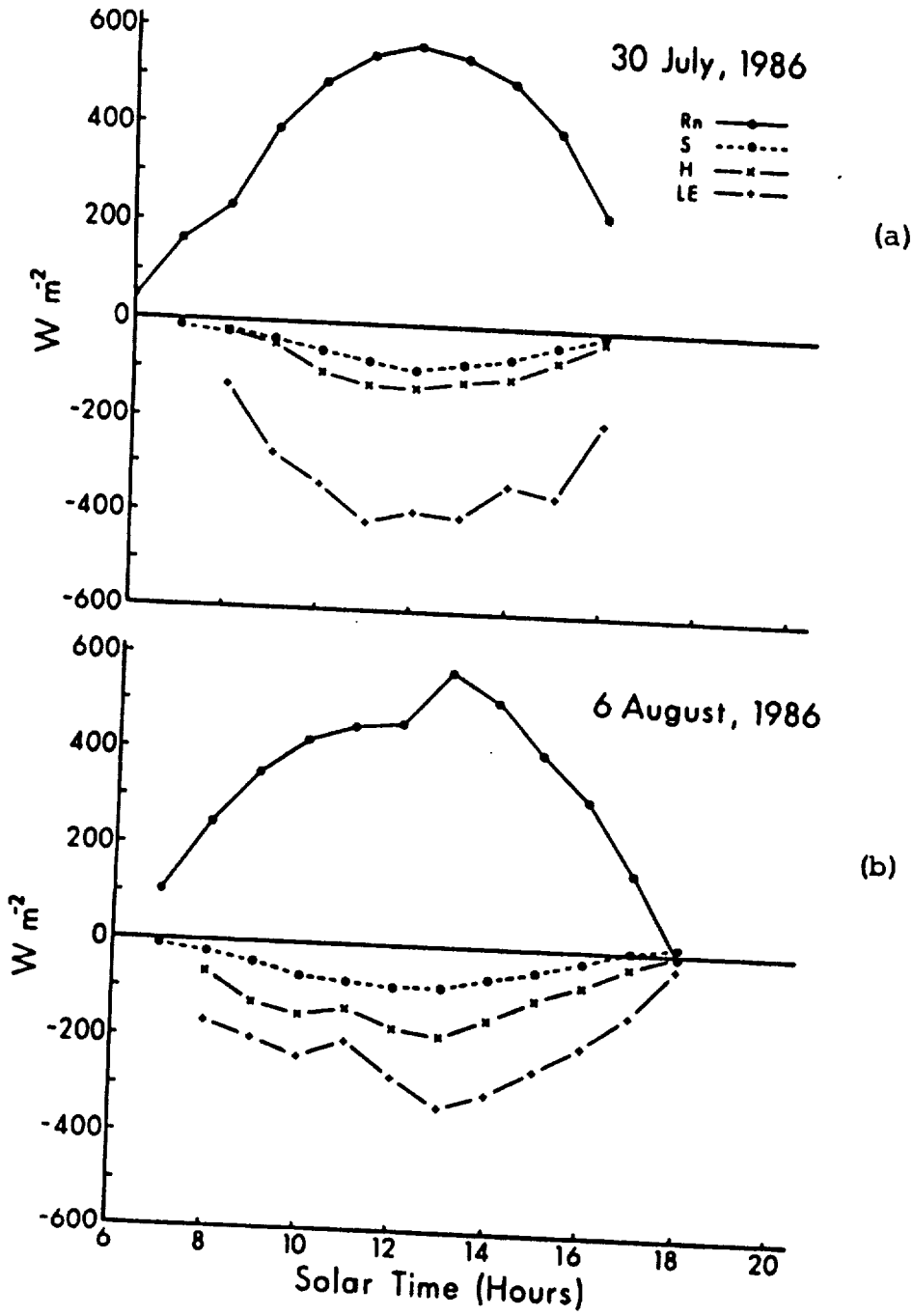

Fig. 30. Diurnal patterns of net radiation (Rn), soil heat flux (S), sensible heat flux (H), and latent heat flux (LE) over a tall grass prairie near Manhattan, Kansas. (a) 30 July 1986; (b) 6 August 1986.

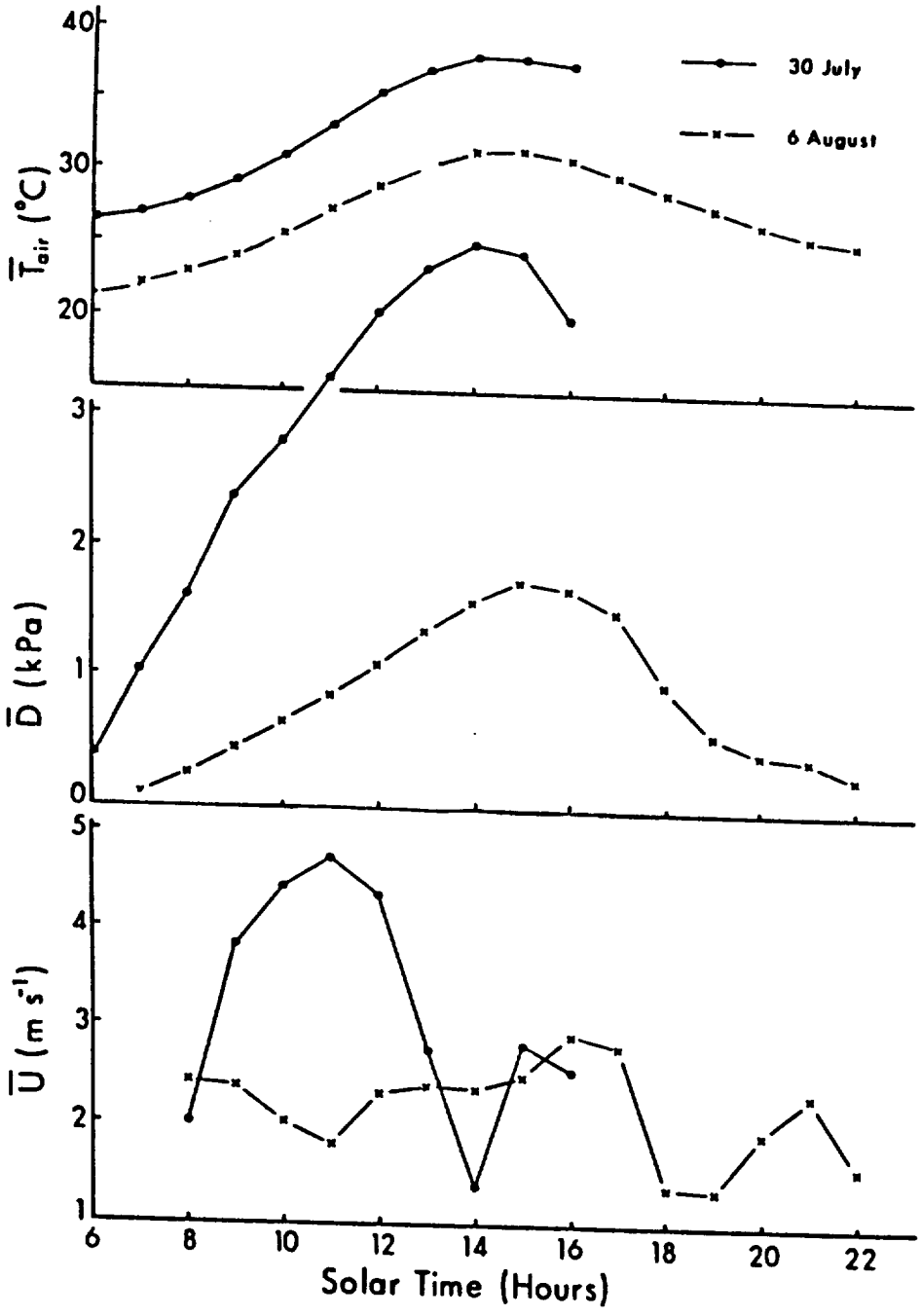

Fig. 31. Diurnal patterns of mean air temperature ($\bar{T}$), mean vapor pressure deficit ($\overline{VPD}$), and mean wind speed ($\bar{U}$) over a tall grass prairie near Manhattan, Kansas. These measurements were made at 1.25 m above ground. 30 July and 6 August 1986.

Profiles of volumetric soil water content in the upper 0.6 m, measured during 29 July - 6 August, are shown in Fig. 32. These data show that there was more water available in the soil on 6 August than on 30 July; therefore, the greater partitioning of Rn into H was not likely due to increased water stress at this later date.

Objective (4) - Modeling Radiation, Sensible and Latent Heat Fluxes

A. Estimated LAI and Mean Leaf Angles:

Experimental and theoretical studies have demonstrated that the structure of a vegetative canopy can have a significant effect on its reflective properties in the visible and NIR portions of the spectrum (Pinter 1985, cited by Jackson and Pinter 1986). Canopy architecture information can provide considerable aid in the interpretation and prediction of remotely sensed data. Direct measurements of canopy structure can be rather time consuming. The nature of the research to be conducted during FIFE will require a relatively rapid means of obtaining canopy structural measurements.

An indirect non-destructive measure of LAI and leaf angle distribution was introduced by Norman et al. (1983). The method employs the relationship between the extinction of radiation beneath a canopy and the canopy structure. The relationship described mathematically is:

$$T = e^{-k(\theta, \alpha)\ LAI} \qquad (4)$$

T represents the transmission of radiation for a canopy, θ is the sun or view zenith angle and k is the extinction coefficient given by:

$$k(\theta, \alpha) = \int_{o}^{\pi/2} g(\alpha) \cos\delta\ d\alpha \qquad (5)$$

$g(\alpha)$ is the fraction of leaves with inclination angle α to the horizontal, δ is the angle between the leaf normal and the given sun direction, and θ is

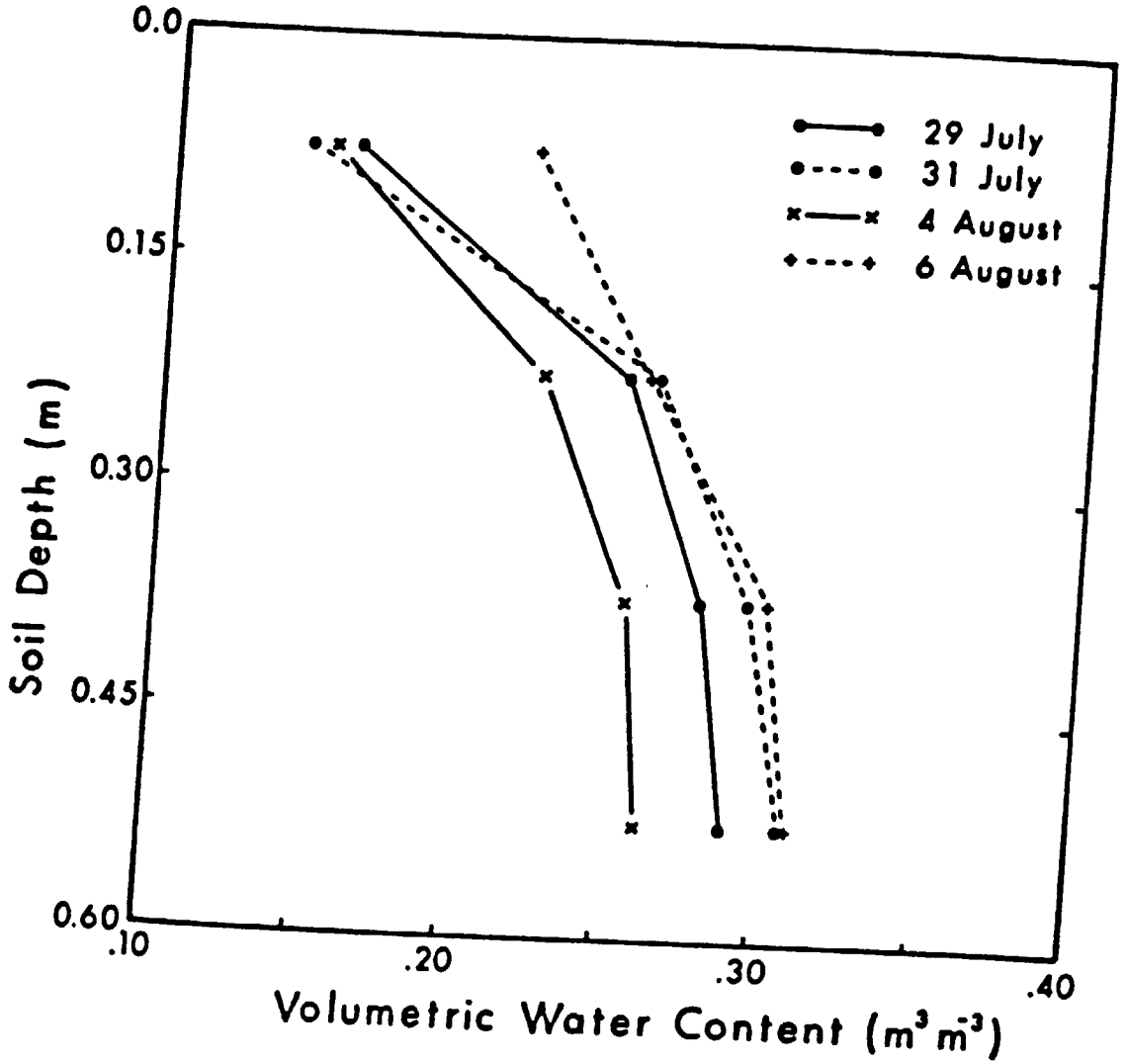

Fig. 32. Change in volumetric water content at selected depths measured during the experimental period in a tall grass prairie.

the zenith angle of the sun. The penetration of radiation is dependent on the number and distribution of gaps in the canopy. Thus, canopy light penetration measurements contain a wealth of information on the vegetative structure.

Using the relationship in Eq. (4) and given values of T and θ, values of k and LAI can be inferred (Norman et al., 1979; Lang et al., 1985). Recently, Norman and Campbell (1987) proposed an inversion routine describing the canopy leaf angle distribution as an elliptical distribution. The ellipsoid can vary in horizontal and vertical axes describing most leaf angle distributions. The extinction coefficient, k, is defined as a function of LAI and x (the ratio of vertical to horizontal axes of the ellipse) and then solve for x and LAI such that:

$$f = \sum (\ln T_i + k_i \, LAI)^2 \quad \text{is minimum.} \tag{6}$$

The bisection method is used to find the solution where the RMS error is minimized.

Canopy structure information has been inferred using photographic techniques and sunfleck measurements below a canopy with success in turf grass, corn and soybean canopies (Lang et al., 1985; Perry, 1985; Kopeck, 1987). The view zenith angle is varied in the photographic method while the source zenith angle is varied in the sunfleck method.

Cone sensors have been developed which sense diffuse light entering at a variety of angles (Norman et al., 1983). Two cone sensors were used in this research. One was a multi-cone sensor which measures diffuse light at angles 12°, 33°, 49°, 65° and 81° (Norman et al., 1983). The second was a prototype sensor developed by LI-COR which measures diffuse light at 7°, 25°, 40° and 58°.

Ten measurements above and below the canopy were made in each plot. The LI-COR sensor required correction of raw data for corruption of light detected

by one or more sensors. The ratio of corrected measurements below the canopy with measurements above represent the fraction of diffuse light penetrating the canopy. The 10 ratios from each plot were averaged to give a mean gap fraction at each angle. These values were used as input values for the inversion routine.

Part of the 1986 field experiment included testing the suitability of the multi-cone sensor in a grassland environment. LAI estimates inferred using the multi-cone sensor data were compared to LAI estimates inferred from the LI-COR cone data. Multi-cone LAI estimates were generally lower than LI-COR cone LAI estimates (Fig. 33). The lower values of the multi-cone LAIs are due, in part, to the height of the cone (approximately 0.1 m) so that the leaf area below the height of the cones was not viewed. Canopy heights were as low as 0.30 m in some plots. A shorter cone like the LI-COR instrument is desirable for grassland applications. Also the multi-cone sensor is more sensitive in the green portion of the spectrum, thereby sensing more scattered radiation. The canopy appears to be brighter at greater zenith view angles where it should be darker; this results in higher calculated values of gap fraction at these lower angles. The distribution of gap fractions with cone angle were exemplary of canopies with lower leaf area and more horizontally inclined leaves than actually existed. In most cases, the multi-cone sensor data resulted in lower LAI and lower mean leaf angle estimates than those derived from the LI-COR sensor. Estimates of LAI, as well as additional canopy structural measurements, are given in Table 6.

Inferred LAI was plotted against dry leaf weight and canopy height (Figs. 34, 35). The relationship is described with an exponential equation from Landsberg (1977) of the form:

$$LAI(s) = A(1 - \exp^{B(x+C)}) \qquad (7)$$

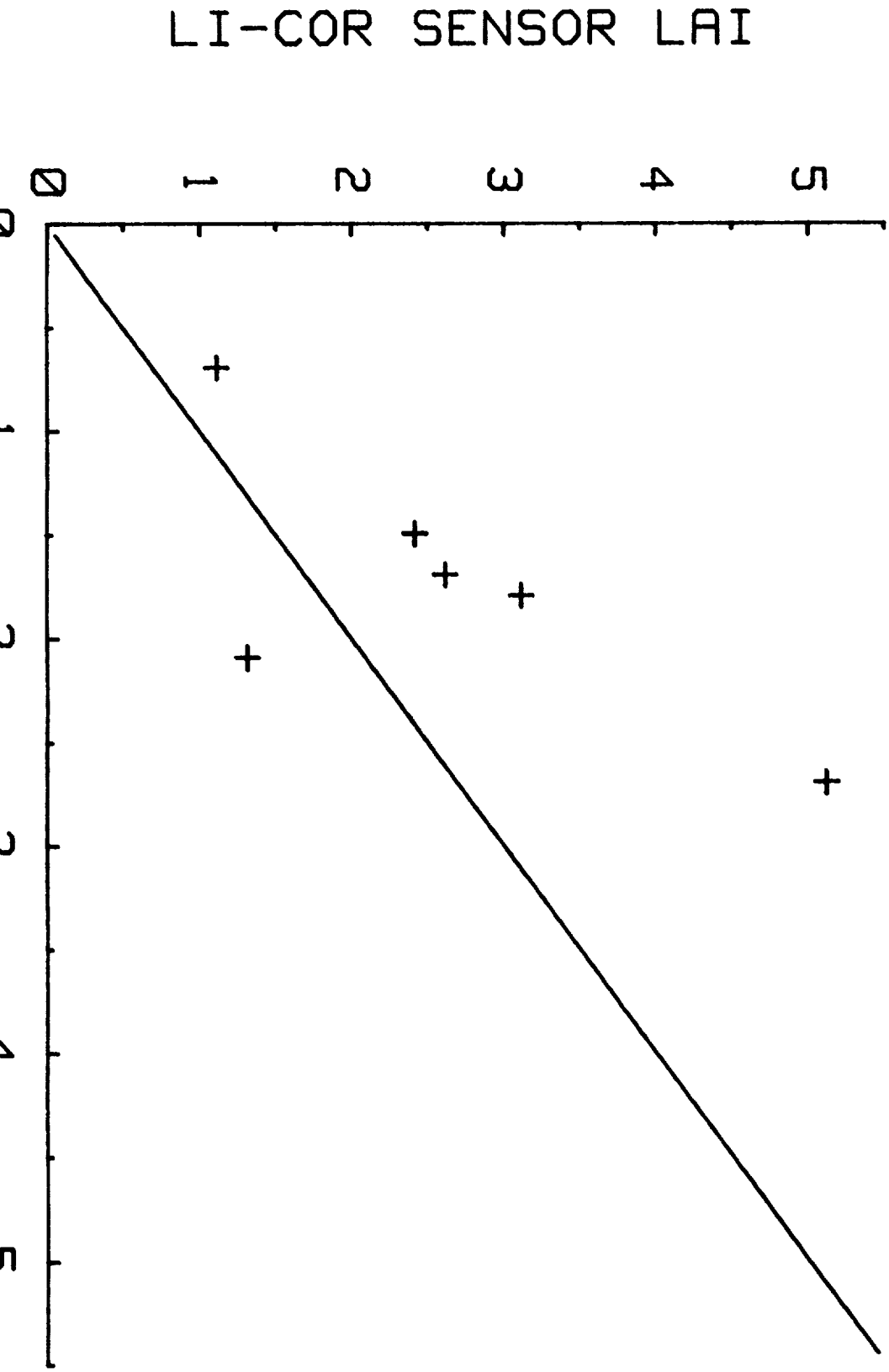

Figure 33. Comparison of estimated LAI values from the multicone sensor with the LI-COR sensor.

Table 6. Canopy structure characteristics, FIFE pilot study. July, August, 1986.

Plot #	Location	Dry Weight (g)	Height (cm)	Inferred LAI	Mean Leaf Angle
1	KONZA 2	64.0	35	2.4	62.5
2	KONZA 2	81.4	35	2.6	62.5
3	KONZA 2	60.1	30	1.1	74.9
4	KONZA 2	64.5	30	1.3	69.3
5	KONZA 2	92.1	40	2.4	64.1
6	KONZA 2	71.1	35	3.1	59.4
7	KONZA 2	149.8	65	5.1	50.2
8	KONZA 2	131.8	45	3.4	53.3
9	KONZA 2	113.6	50	4.4	57.9
10	KONZA 2	93.7	40–45	3.7	55.8
11	KONZA 2	104.8	30–35	3.4	64.1
21	KONZA 1	106.7	35	2.6	46.0
22	KONZA 1	77.7	35	2.0	50.9
23	KONZA 1	160.5	70	3.7	56.7
24	KONZA 1	195.9	70	4.5	55.0
25	KONZA 1	200.4	65	2.9	62.5
26	KONZA 1	114.4	65	3.5	62.5
27	KONZA 1	129.8	60	3.4	54.1
28	KONZA 1	119.0	70–75	3.6*	
29	KONZA 1	93.7	50	2.9*	
30	KONZA 1	137.1	60	4.8*	
31	KONZA 1	112.5	45	3.5*	
32	KONZA 1	57.3	30	1.4*	

*Approximate LAI; values extrapolated from curve.

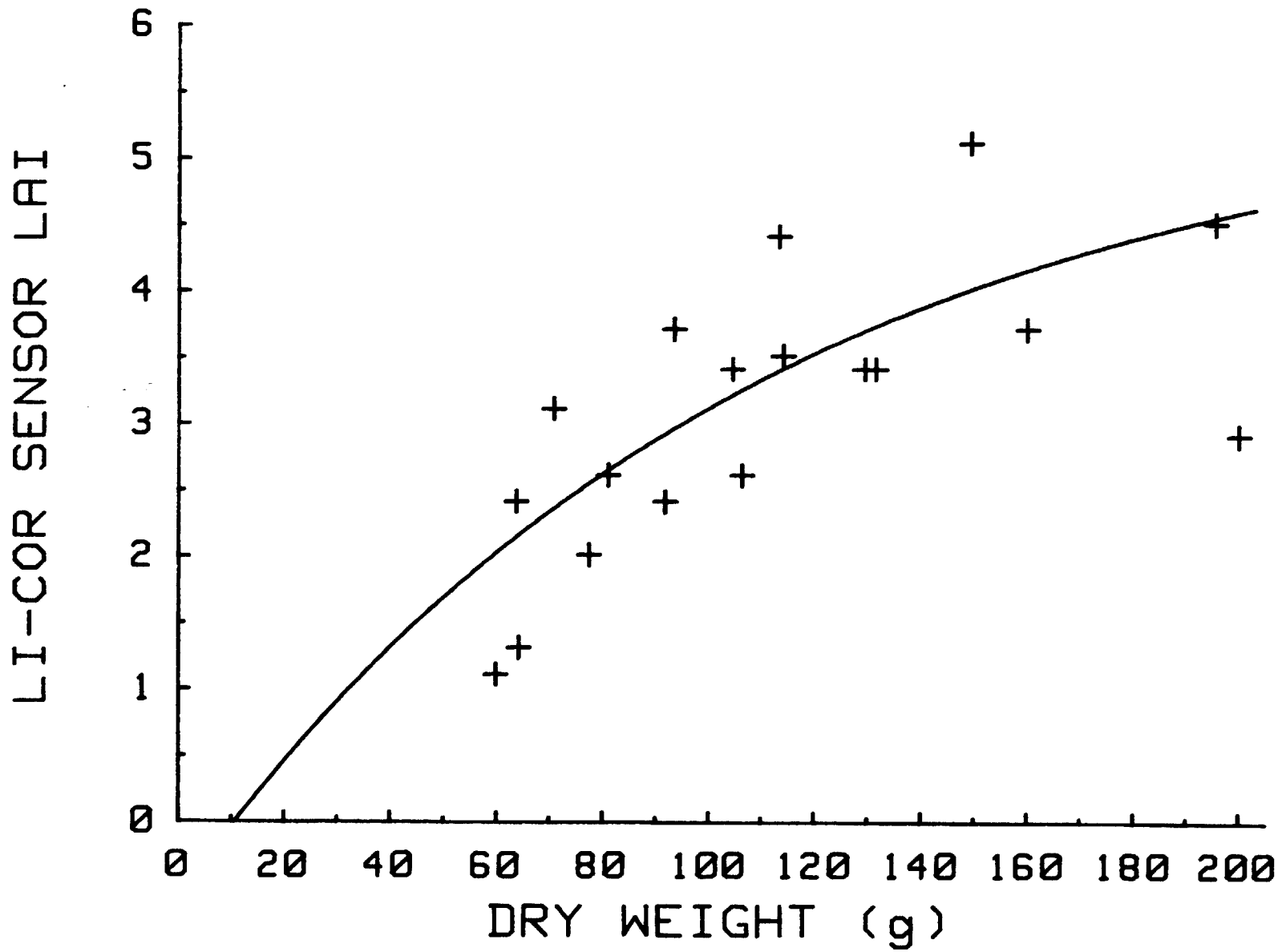

Figure 34. Relationship between measured dry weight of plant biomass and estimated LAI from LI-COR sensor.

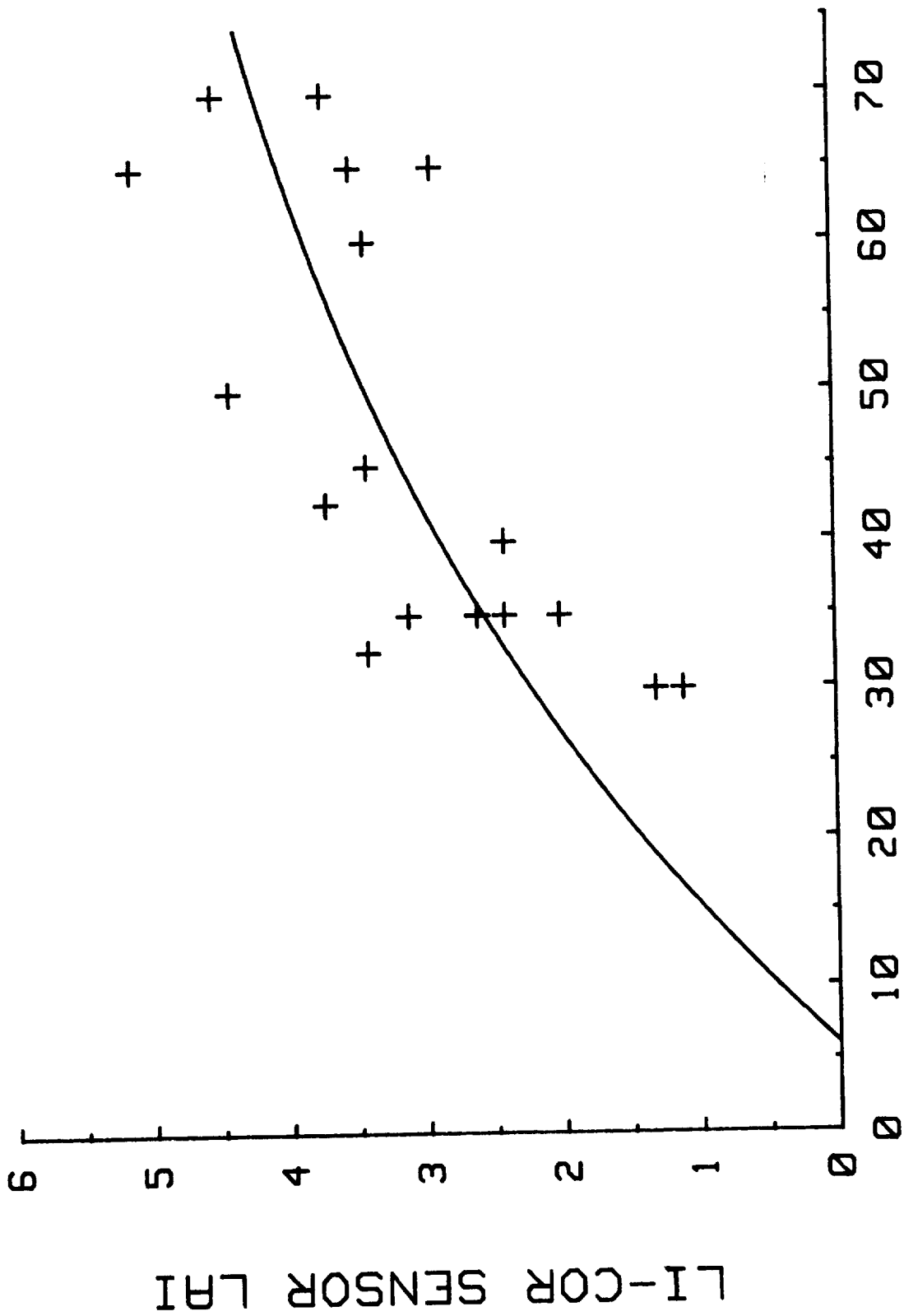

Figure 35. Relationship between measured canopy height and estimated LAI from LI-COR sensor.

where x is the leaf or total biomass dryweight in grams or canopy height in cm. Such relationships can be useful in estimating LAI from the dry biomass or, conversely, estimating biomass from estimates of LAI which can be made quite rapidly using sensors such as the one developed by LI-COR.

B. Model Simulations of Wheat Canopy Fluxes:

Coordinated measurements of biological characteristics, hourly climatic data and fluxes made over a wheat canopy at Mead, Nebraska in May and June, 1985 and over a site on the FIFE pilot study area periodically from July 29 through August 6, 1986 provided opportunities to test the performance of the model, Cupid (Norman, 1982) for agronomic and natural grassland communities.

Cupid is a comprehensive plant-environment model, including many environmental and plant factors. The model requires a number of input values which make the model versatile. Input information includes hourly measurements of solar radiation, air temperature, relative humidity, wind speed, precipitation and soil temperature. Hourly inputs were available from the automated weather stations located at the study areas. Canopy input information on soils and vegetation makes the model independent of surface cover. Soil inputs include bulk density, soil texture, volumetric soil moisture at some reference depths, soil emissivity and soil reflection properties in the visible, near-infrared (NIR) and thermal portions of the spectrum. Vegetation input includes leaf area index, canopy height, mean leaf angle, leaf reflectance and transmittance (in the visible, near-NIR and thermal), and vegetation emissivity. Stomatal characteristics for the wheat canopy were taken from Denmead and Millar (1976) while those for the FIFE site were determined from field measurements.

C. Wheat Canopy Fluxes:

We examined measured and predicted fluxes of Rn, LE, H and S over a wheat canopy for four days in 1985: May 22 (Day 142), May 30 (Day 150), June 7 (Day 158) and June 13 (Day 164). These represent four days of contrasting weather and canopy conditions.

Soils at Mead are a Sharpsburg silty clay loam. Wheat row spacing was 0.18 m with a plant spacing of 0.03 m. Leaf area index of the canopy decreased with time. The LAI for the four days were 4.5, 3.0, 1.2 and 0.3, respectively. Radiation, wind, temperature and vapor pressure input were available from the Mead automated weather station, providing hourly input over a 24-hour period (Figs. 36-39). No precipitation was recorded on any of these days.

There was very good agreement between measured and simulated Rn, LE and H fluxes for May 22 and May 30 (Figs. 40-43), clear and partly cloudy days with high but decreasing LAI. Measured and simulated fluxes of Rn for June 7 and June 13 were also in good agreement although simulated LE and H fluxes were in poor agreement (Figs. 44-47). The poor agreement probably results from the senescing stages of wheat and a significant decrease in green leaf area. Although LAI had decreased considerably by day 164, wheat heads probably contributed more to the biomass than was represented by the model. Characterizing the wheat heads in the model should improve simulations.

D. Natural Grassland Canopy Fluxes:

Measured and predicted fluxes of Rn, LE, H and S for two days: July 30 (Day 211) and August 3 (Day 215) were examined. These represent days of contrasting weather conditions. LAI was about 2.9 on both dates. July 30 was mostly sunny with temperatures as high as 40°C (Fig. 48). August 3 was cloudy near solar noon with lower temperatures than July 30 (maximum - 29.2°C) (Fig. 49). Winds of 6 m/s were recorded during the early morning hours.

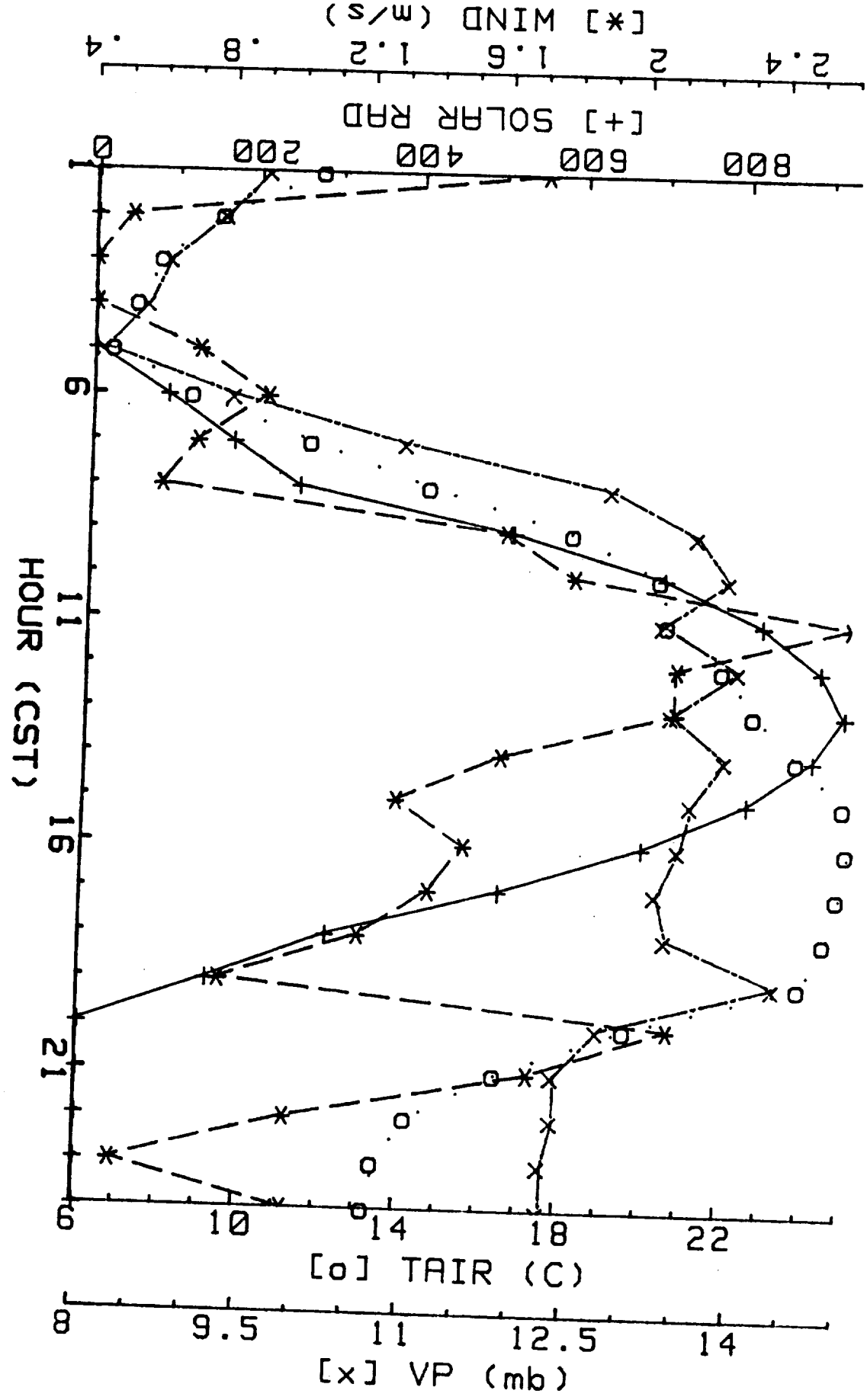

Figure 36. Hourly values of solar radiation, wind speed, air temperature and vapor pressure on May 22, 1985 (Day 142).

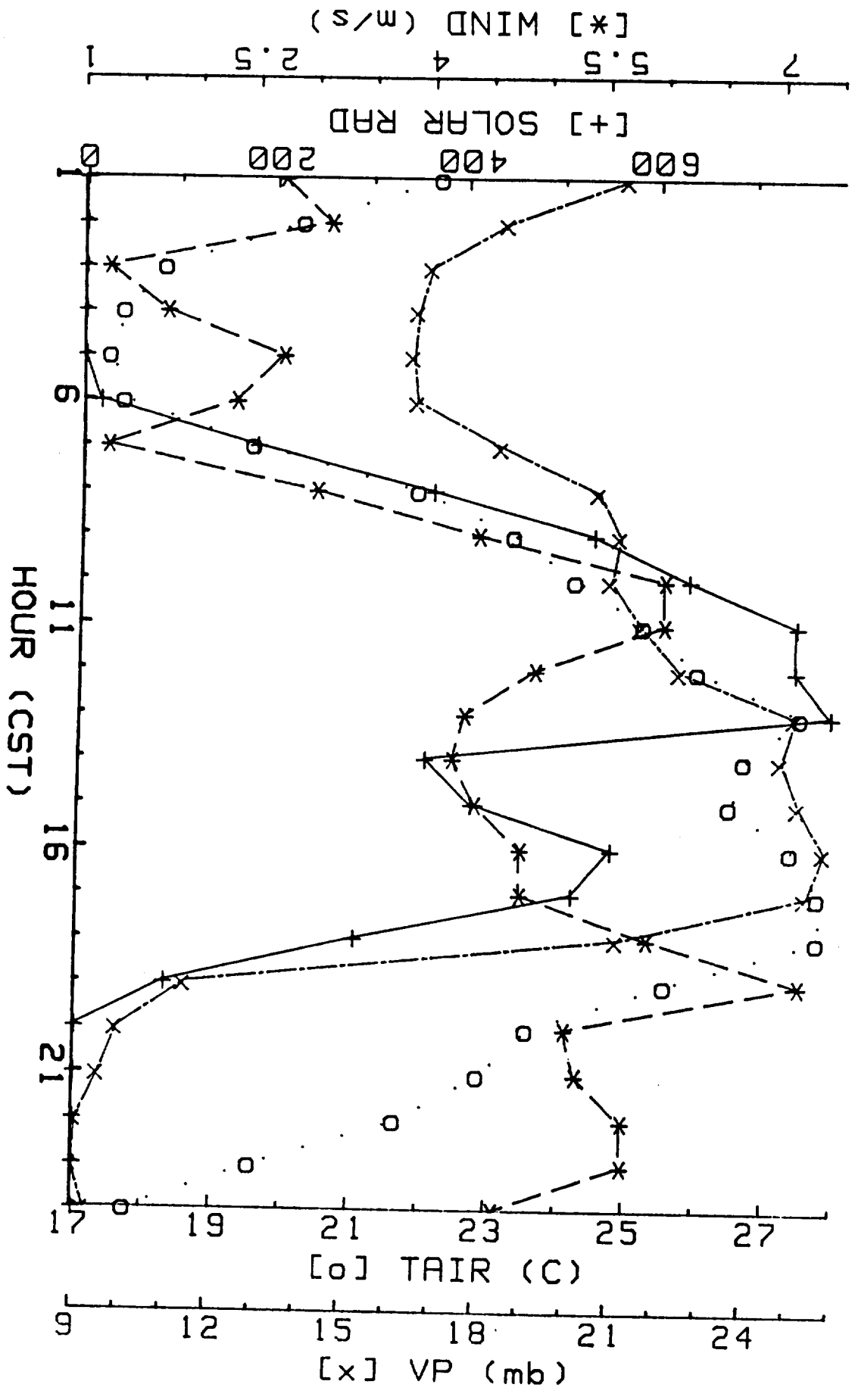

Figure 37. Hourly values of solar radiation, wind speed, air temperature and vapor pressure on May 30, 1985 (Day 150).

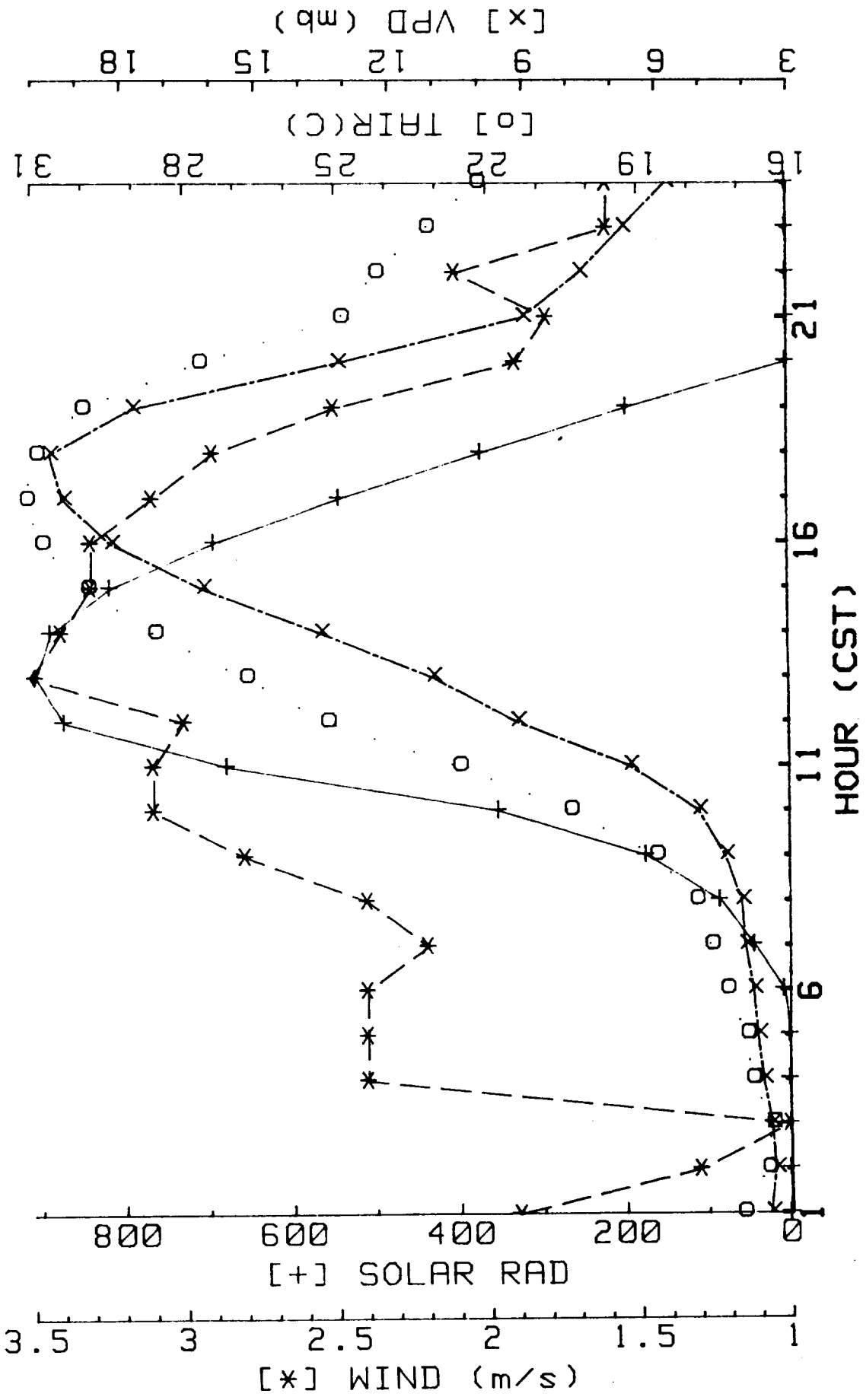

Figure 38. Hourly values of solar radiation, wind speed, air temperature and vapor pressure on June 7, 1985 (Day 158).

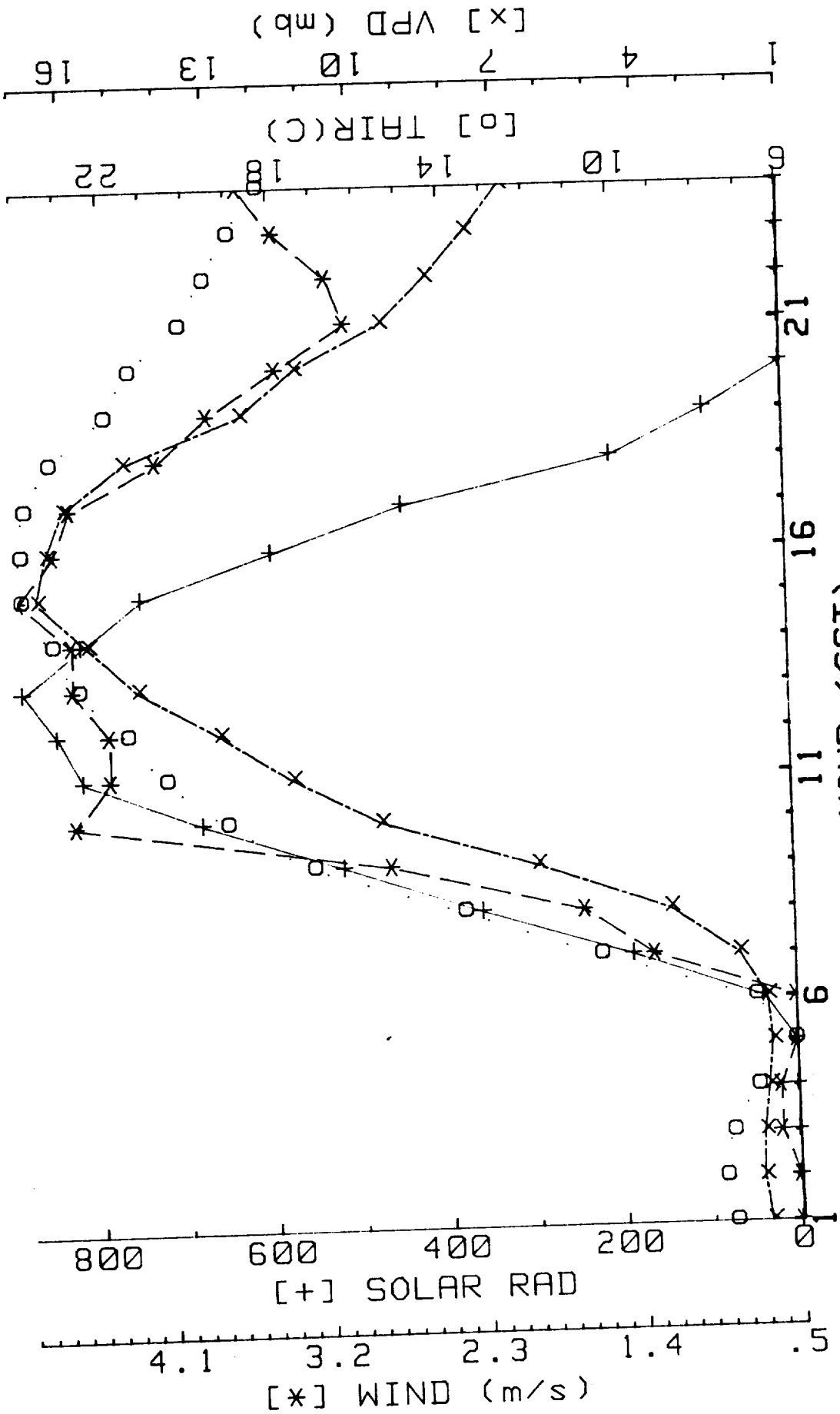

Figure 39. Hourly values of solar radiation, wind speed, air temperature and vapor pressure on June 13, 1985 (Day 164).

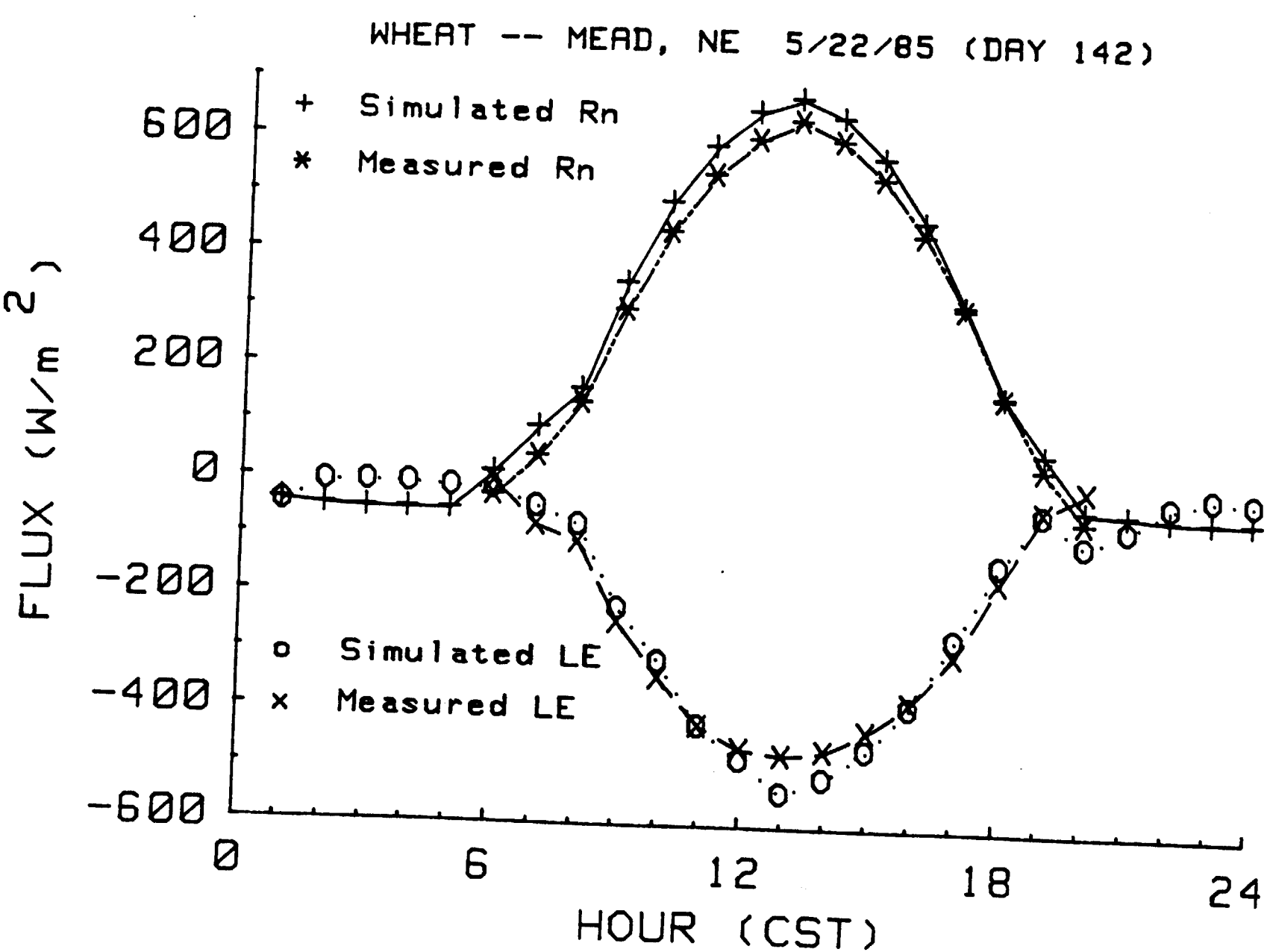

Figure 40. Comparison of measured and simulated Rn and LE fluxes on May 22, 1985 (Day 142).

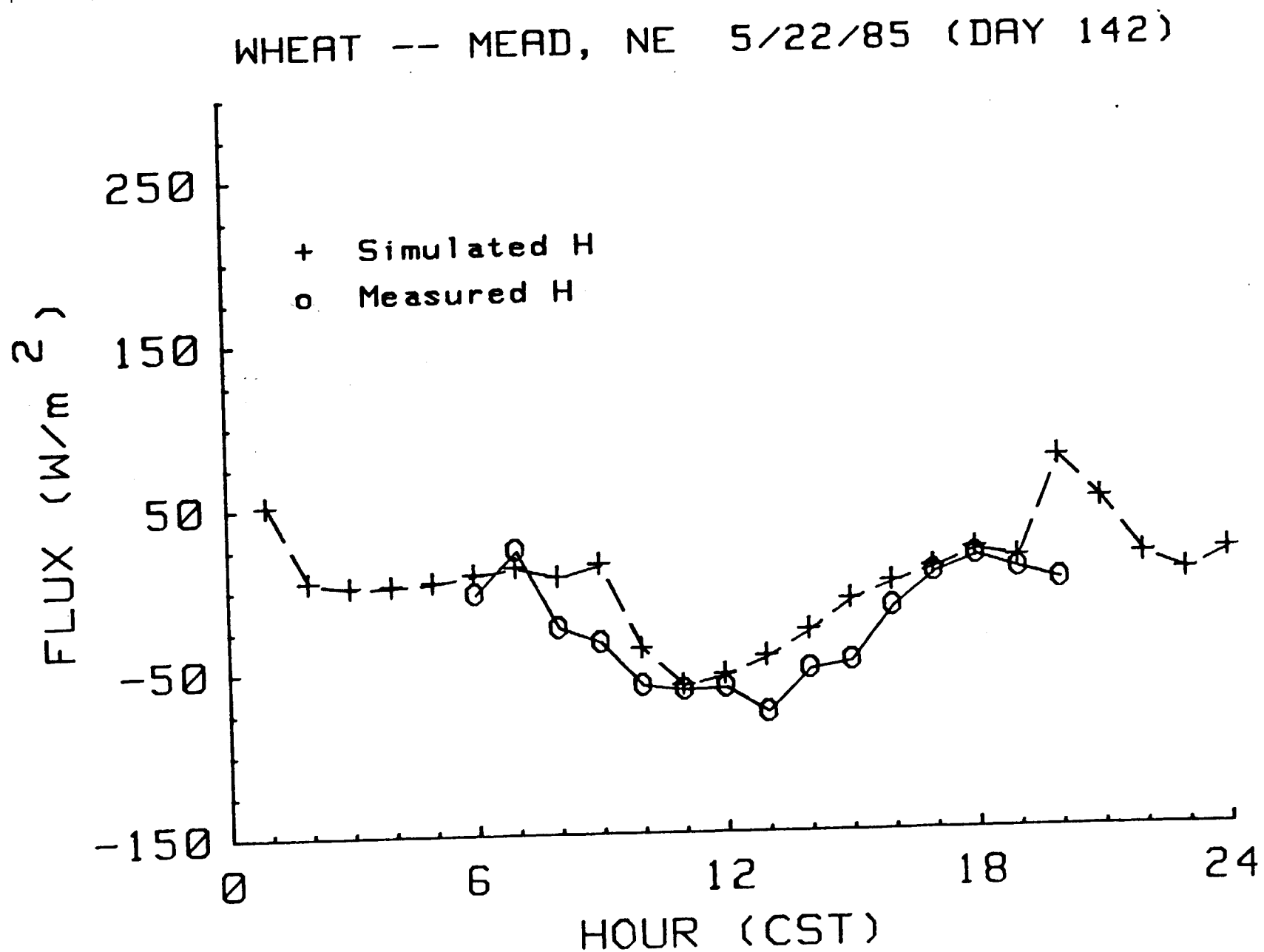

Figure 41. Comparison of measured and simulated H fluxes on May 22, 1985 (Day 142).

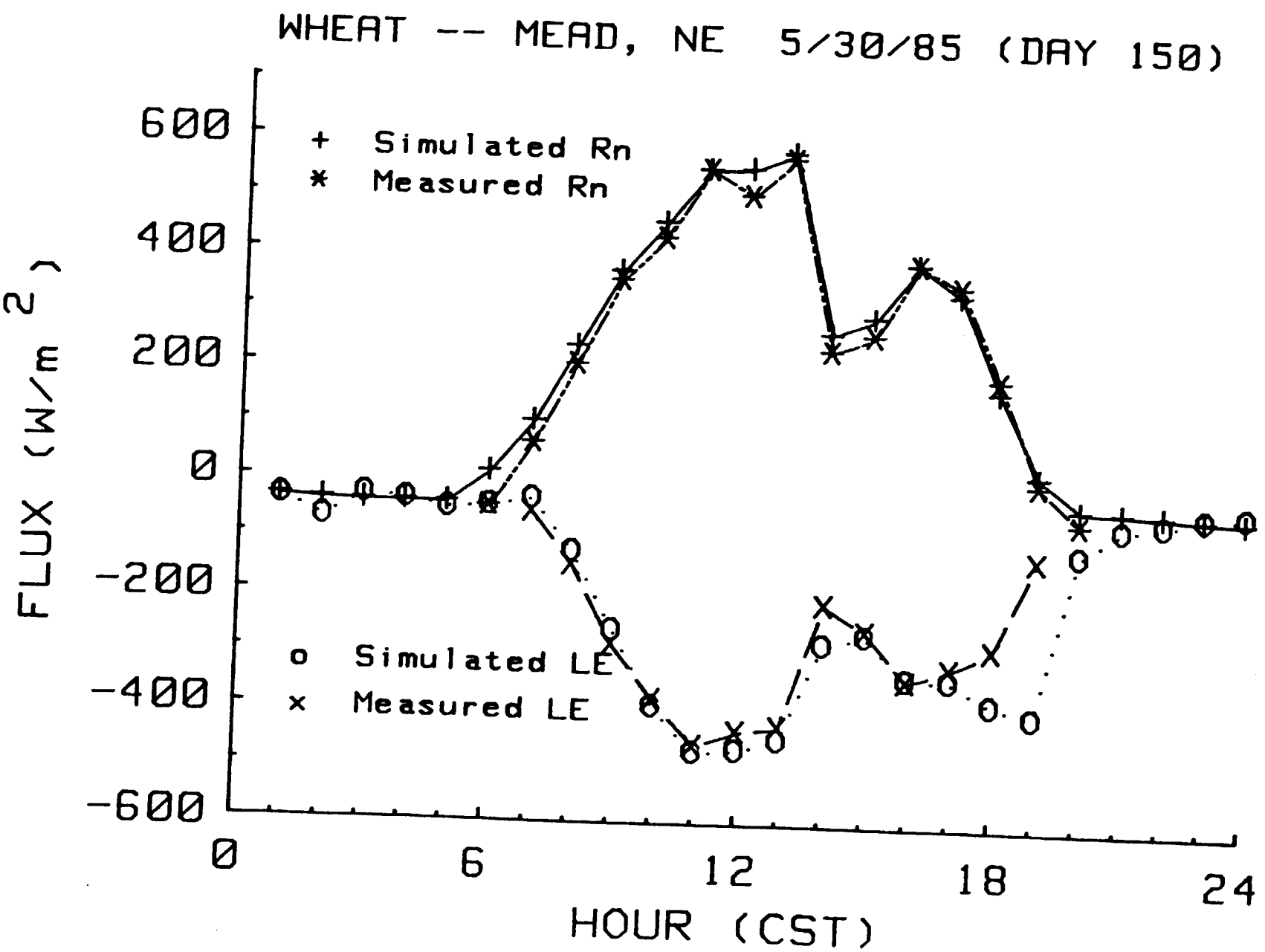

Figure 42. Comparison of measured and simulated Rn and LE fluxes on May 30, 1985 (Day 150).

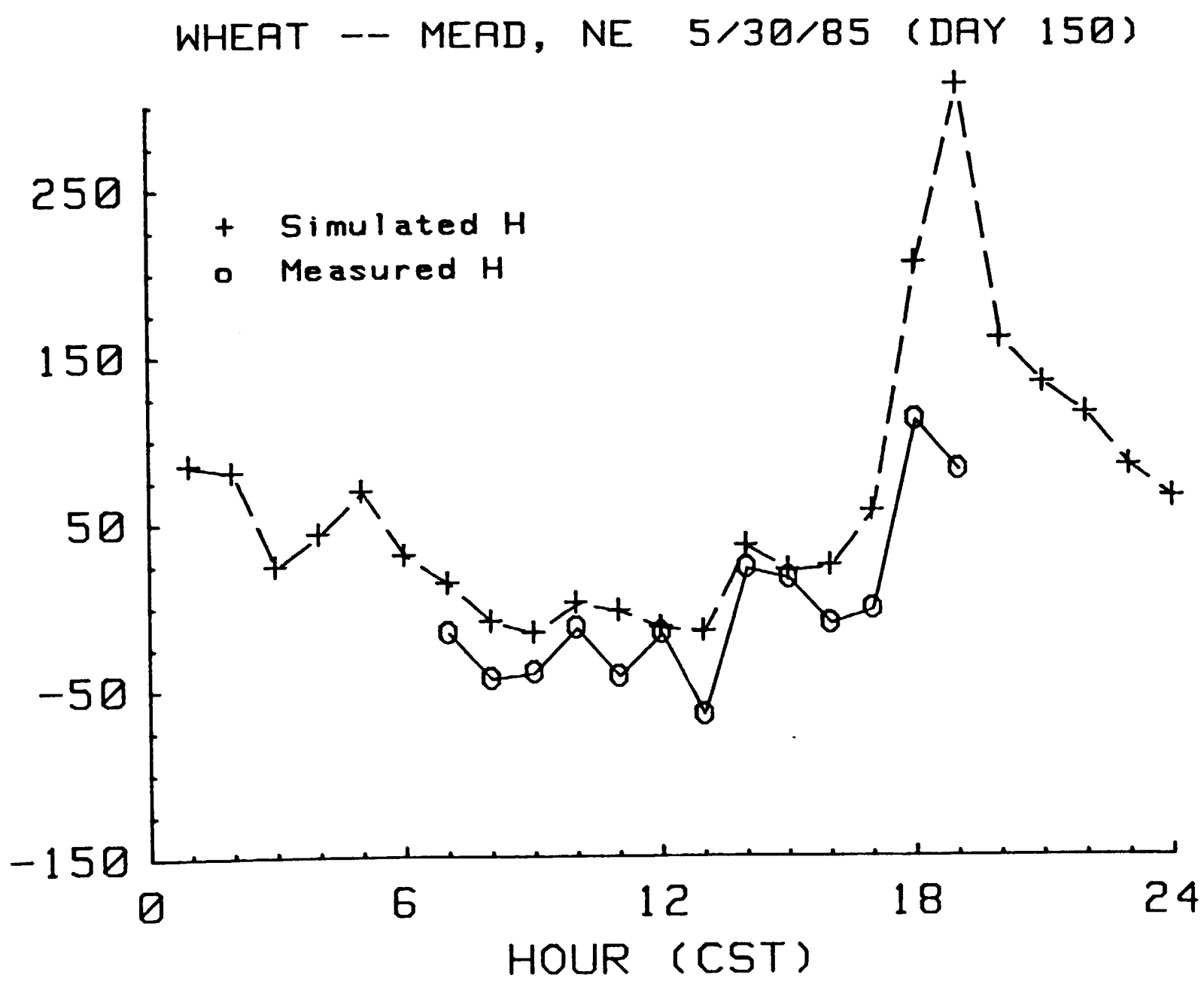

Figure 43. Comparison of measured and simulated H fluxes on May 30, 1985 (Day 150).

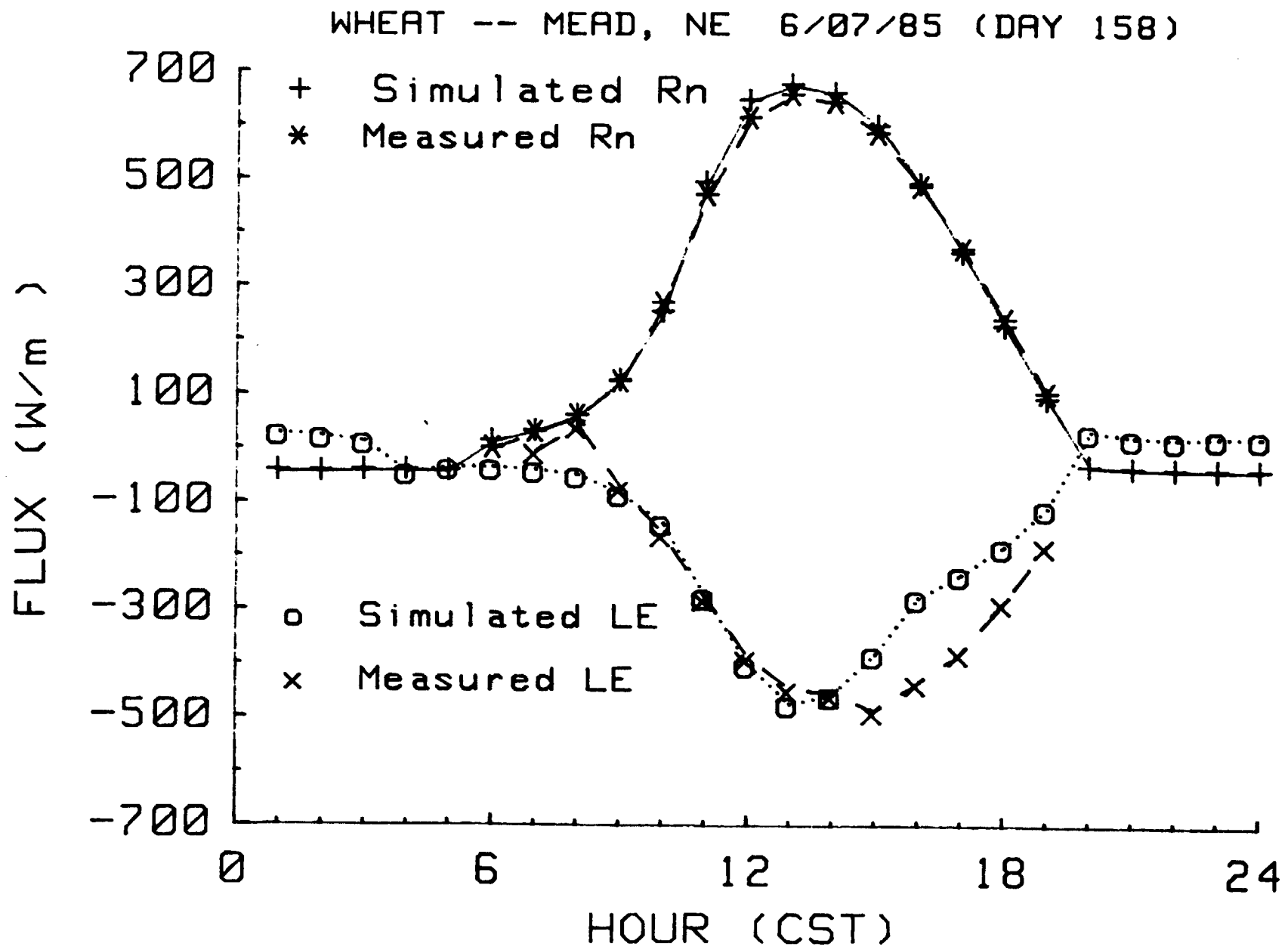

Figure 44. Comparison of measured and simulated Rn and LE fluxes on June 7, 1985 (Day 158).

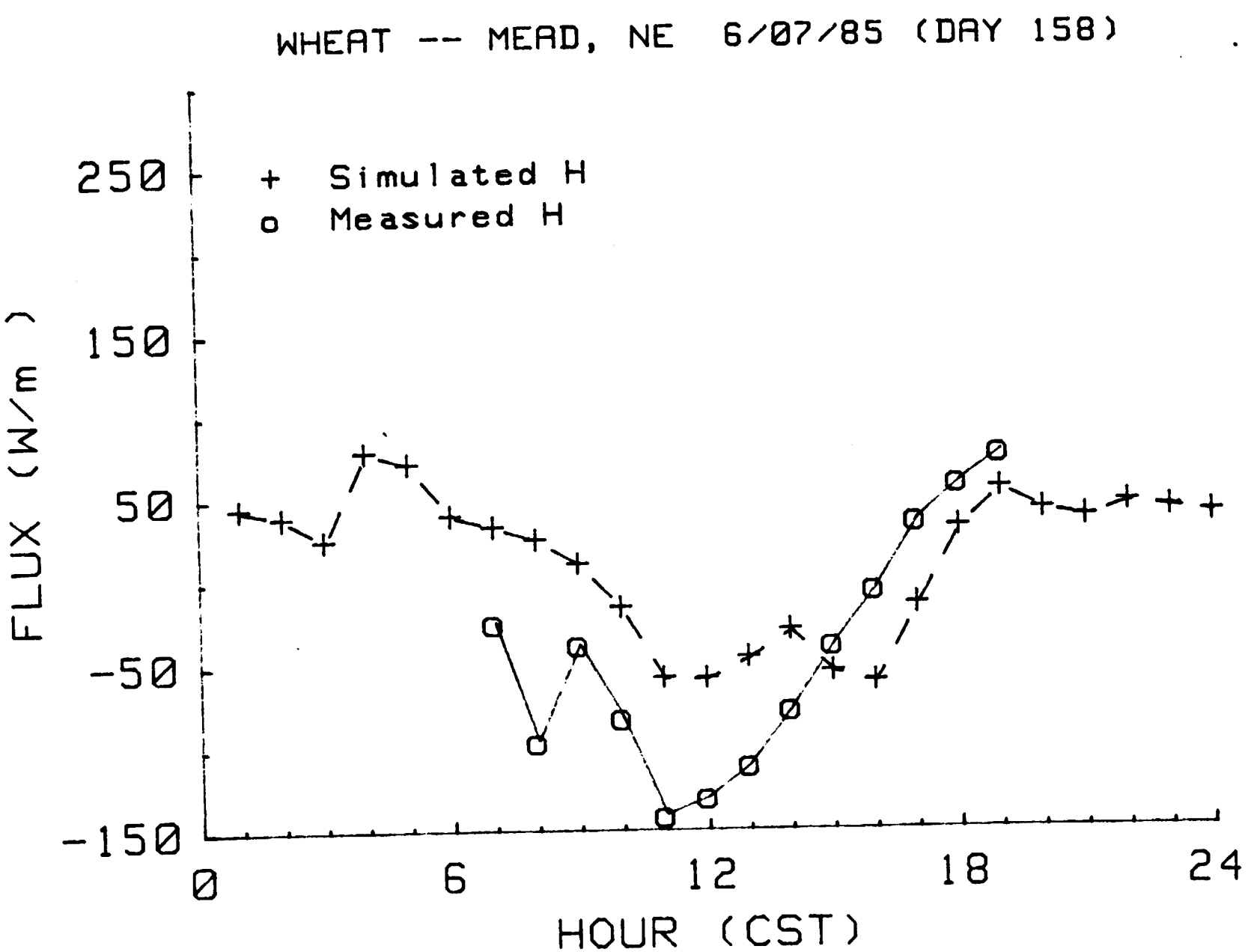

Figure 45. Comparison of measured and simulated H fluxes on June 7, 1985 (Day 158).

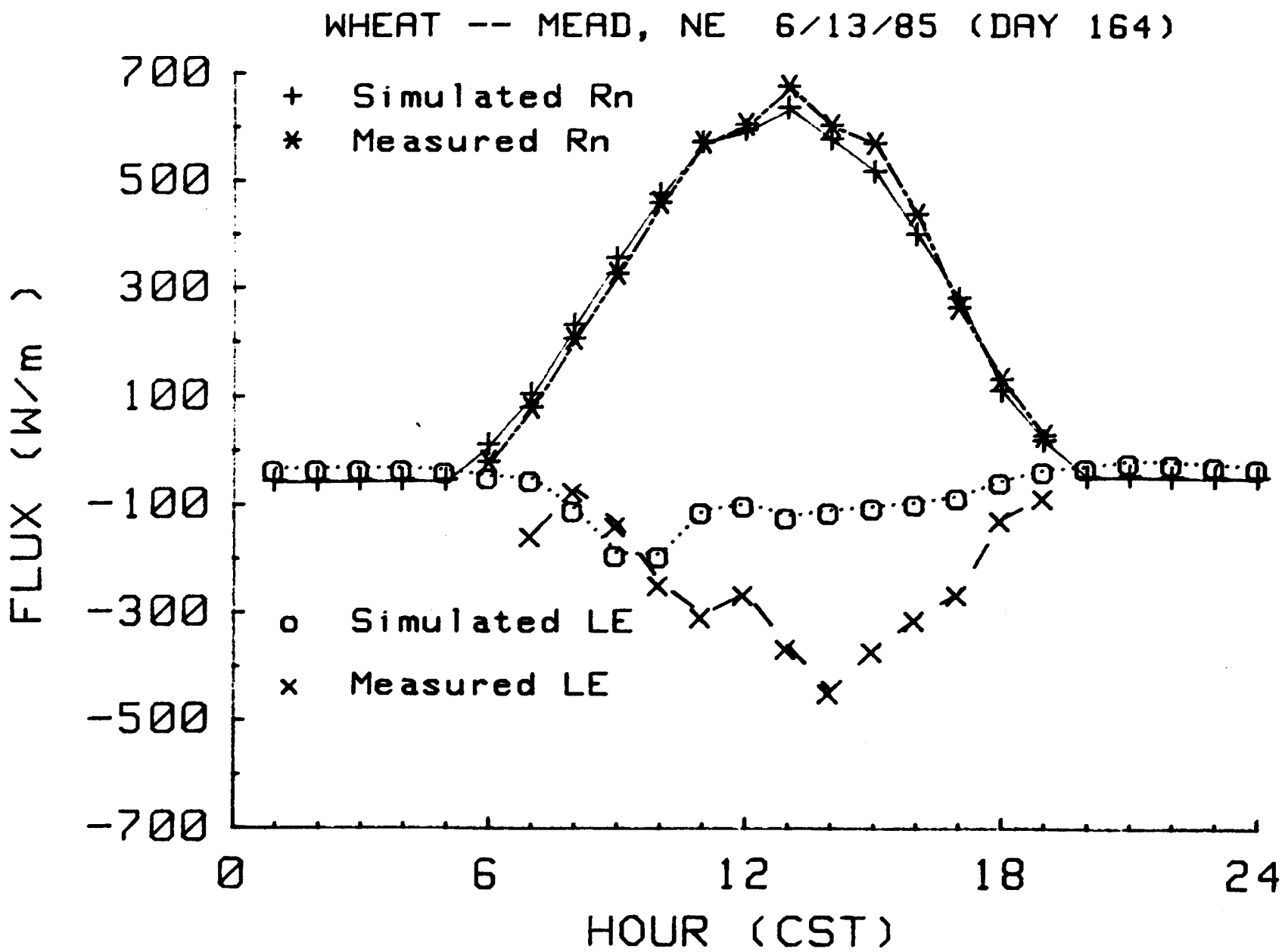

Figure 46. Comparison of measured and simulated Rn and LE fluxes on June 13, 1985 (Day 164).

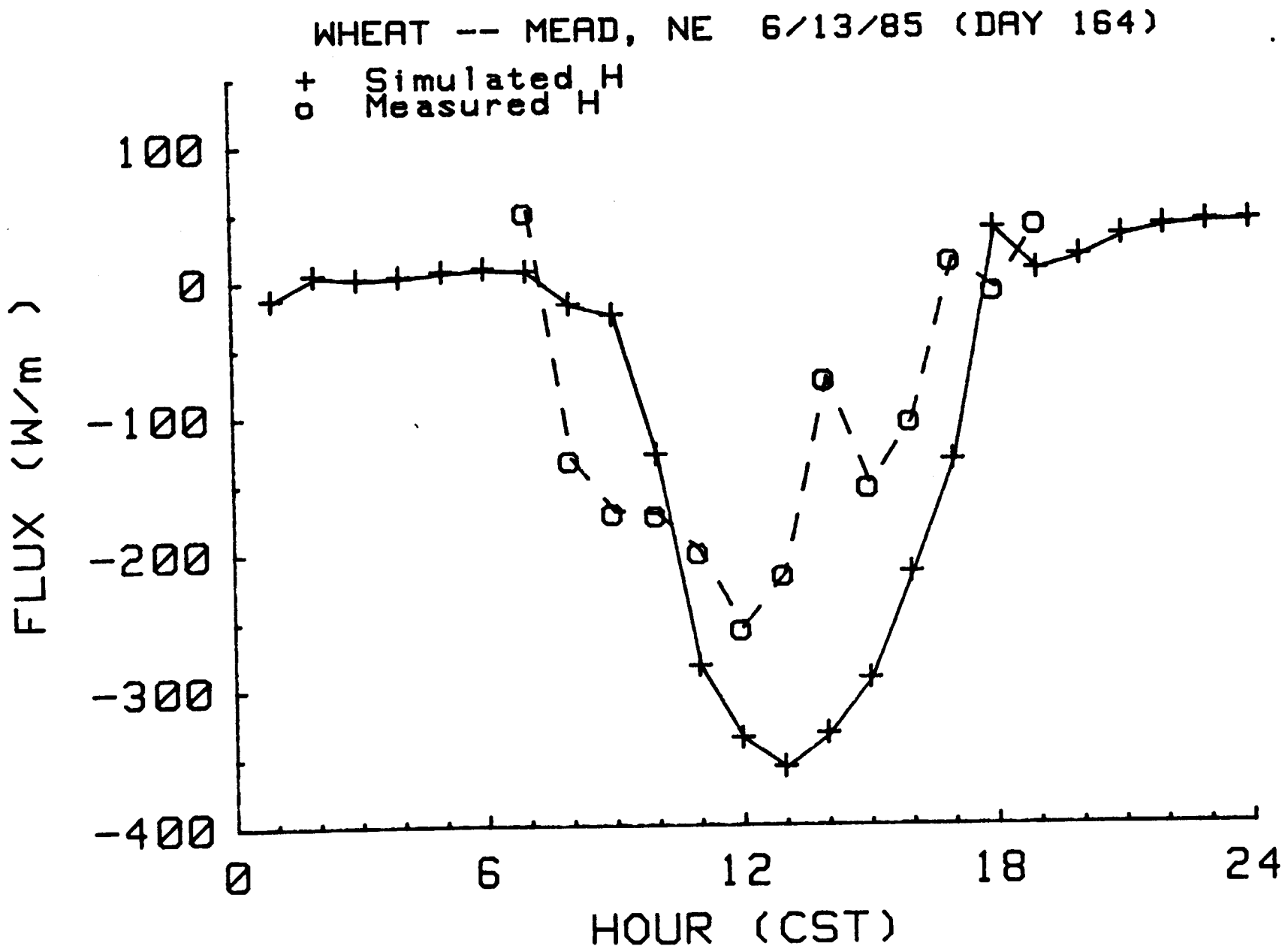

Figure 47. Comparison of measured and simulated H fluxes on June 13, 1985 (Day 164).

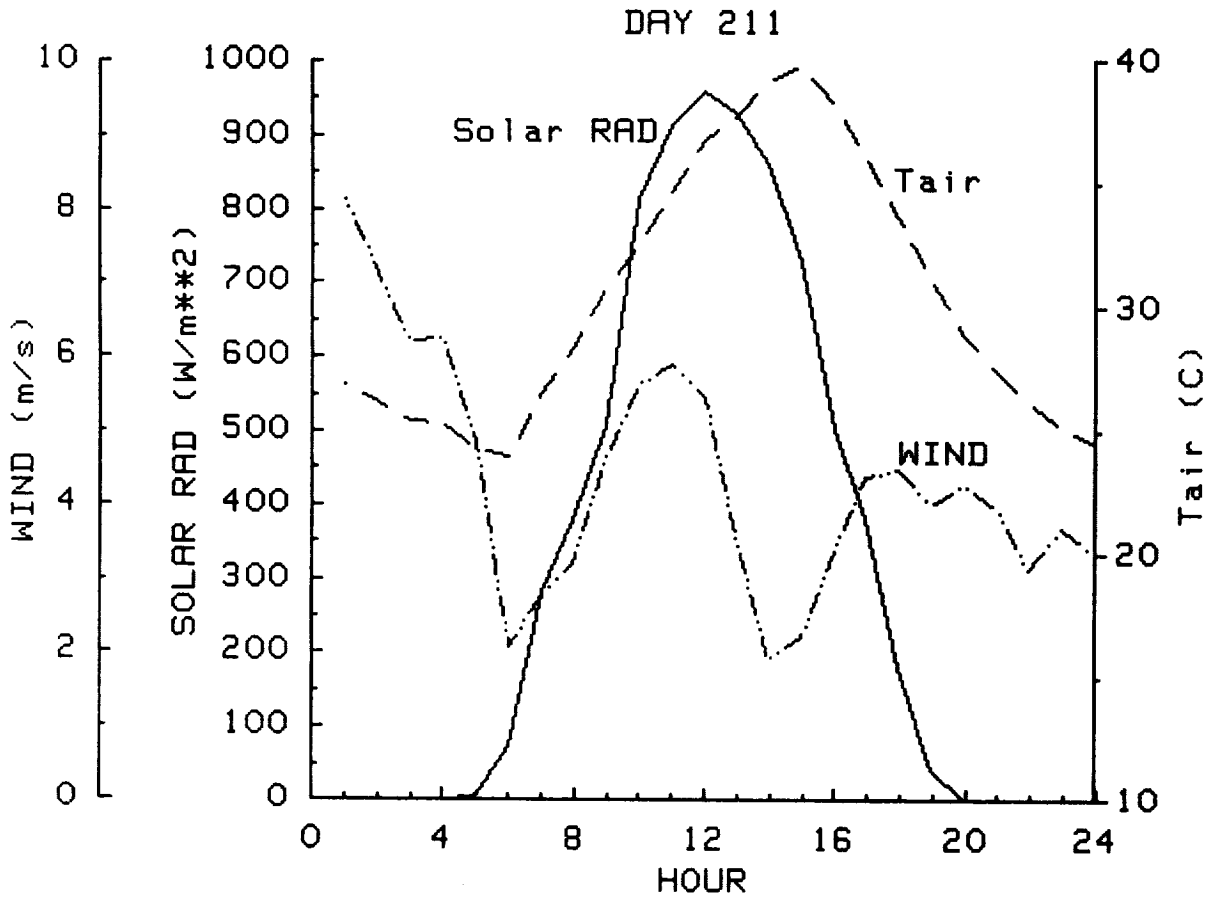

Figure 48. Hourly values of solar radiation, wind speed and air temperature on July 30, 1986 (Day 211).

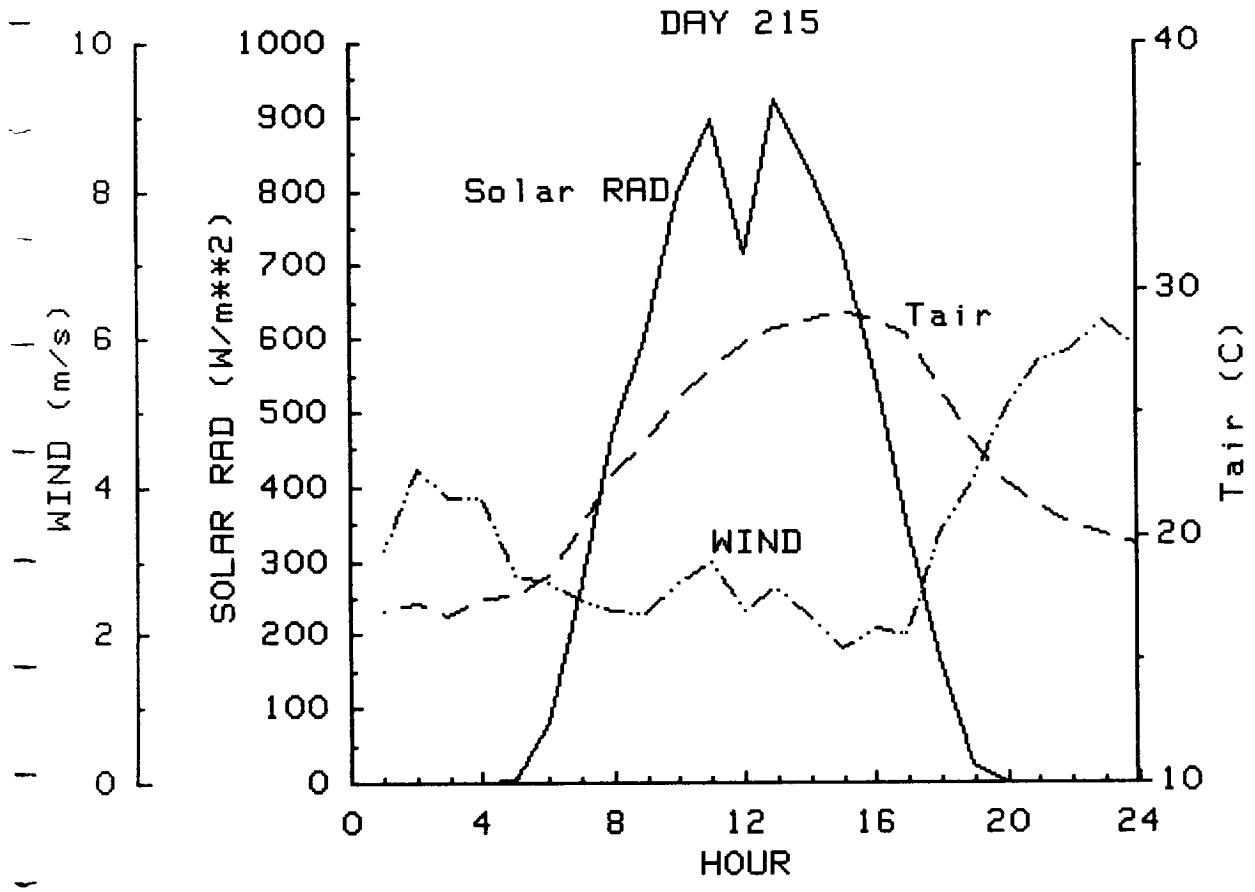

Figure 49. Hourly values of solar radiation, wind speed and air temperature on August 3, 1986 (Day 215).

Simulations of Rn were in good agreement with measured values for all days (Figs. 50 and 51). LE was overestimated for each case, although trends between measured and simulated were similar although differing in magnitude. H was consistently underestimated and was in poor agreement on August 3 (Figs. 52 and 53). Simulated values of S were in good agreement (Figs. 54 and 55).

CONCLUSIONS

Estimates of Rn, LE and H made in 1985 with the model Cupid agreed well with the estimates of these fluxes made with micrometeorological techniques over wheat, especially in May before plant senescence had begun. The agreement was less good in June as LAI values decreased significantly. The performance of the Cupid model for estimating LE, Rn and H fluxes in 1986 from prairie vegetation was poorer than that for the more homogeneous wheat canopy in 1985 even at comparable LAI values. Modifications to Cupid are needed to account for the nonhomogeneous, randomly-spaced clumps of prairie vegetation as well as a need to incorporate the influence of leaf litter on the fluxes of LE, H and S.

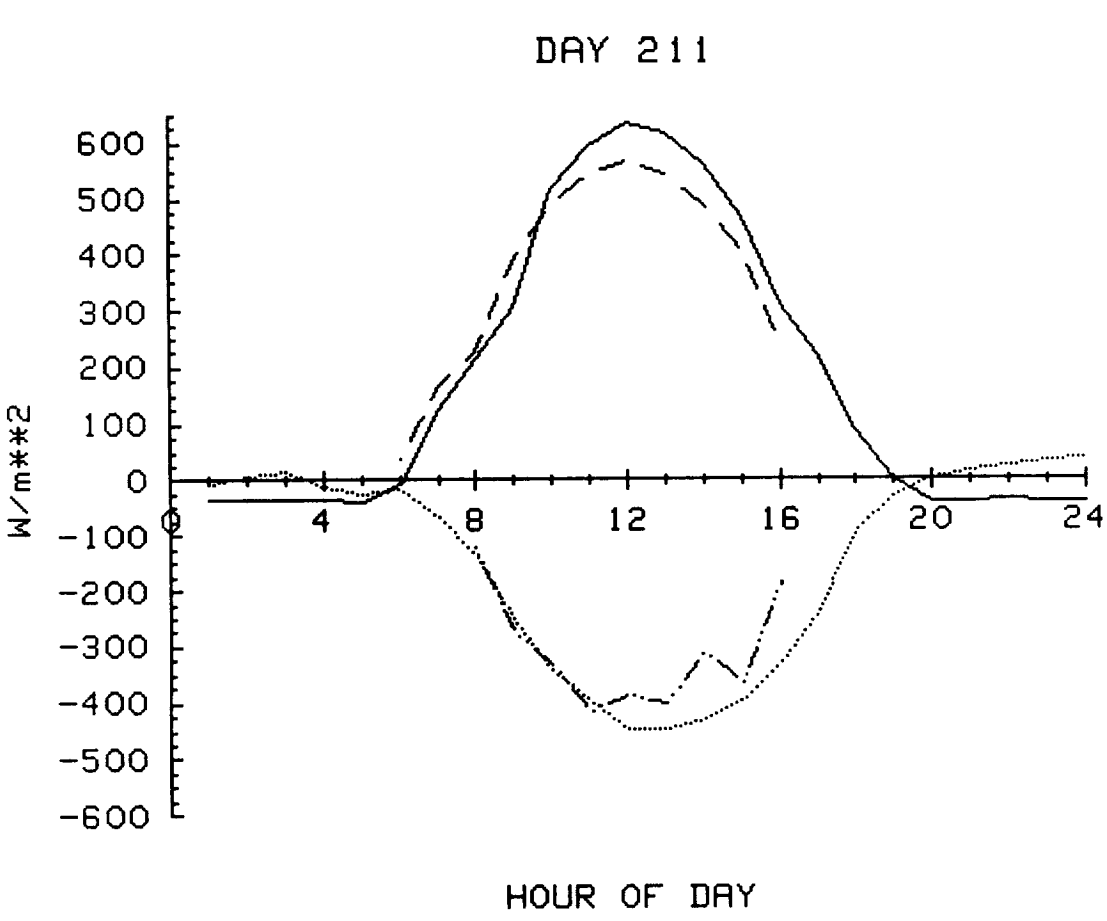

Figure 50. Measured and simulated values of net radiation (Rn) and latent heat flux (LE) for July 30, 1986 (Day 211).

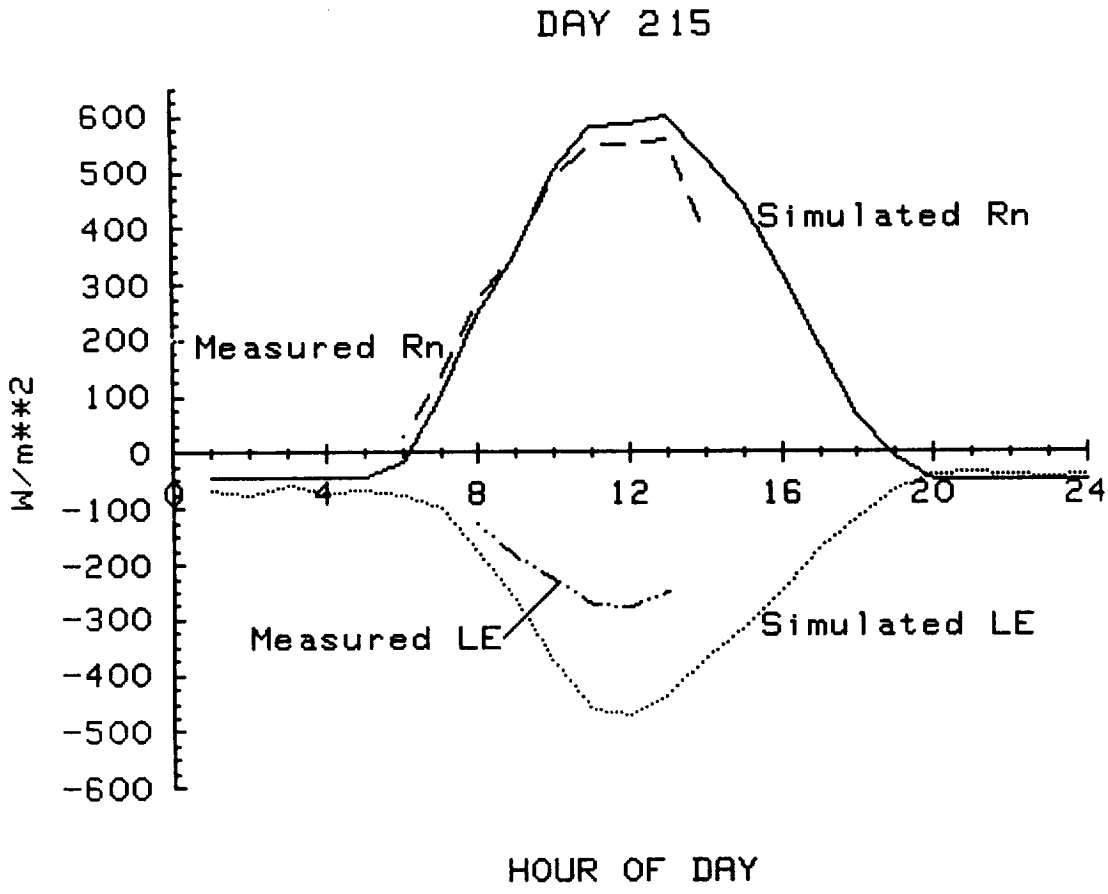

Figure 51. Measured and simulated values of net radiation (Rn) and latent heat flux (LE) for August 3, 1986 (Day 215).

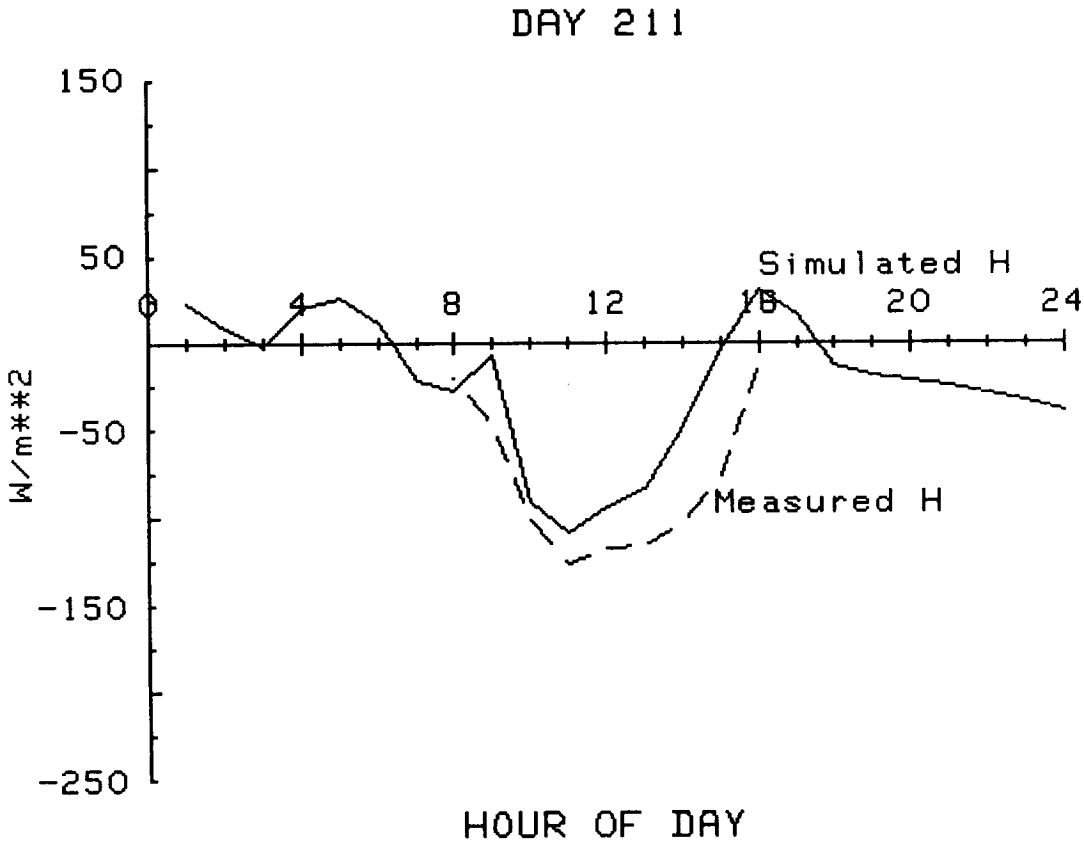

Figure 52. Measured and simulated values of sensible heat flux (H) for July 30, 1986 (Day 211).

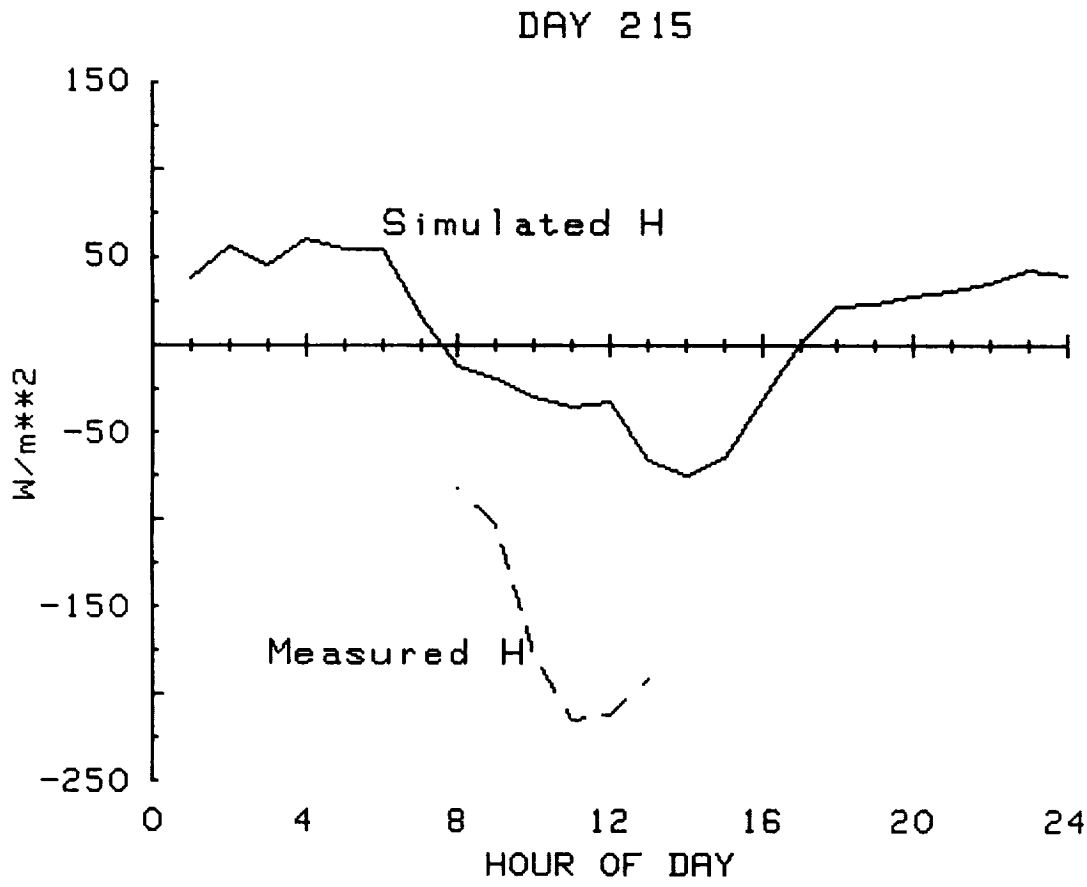

Figure 53. Measured and simulated values of sensible heat flux (H) for August 3, 1986 (Day 215).

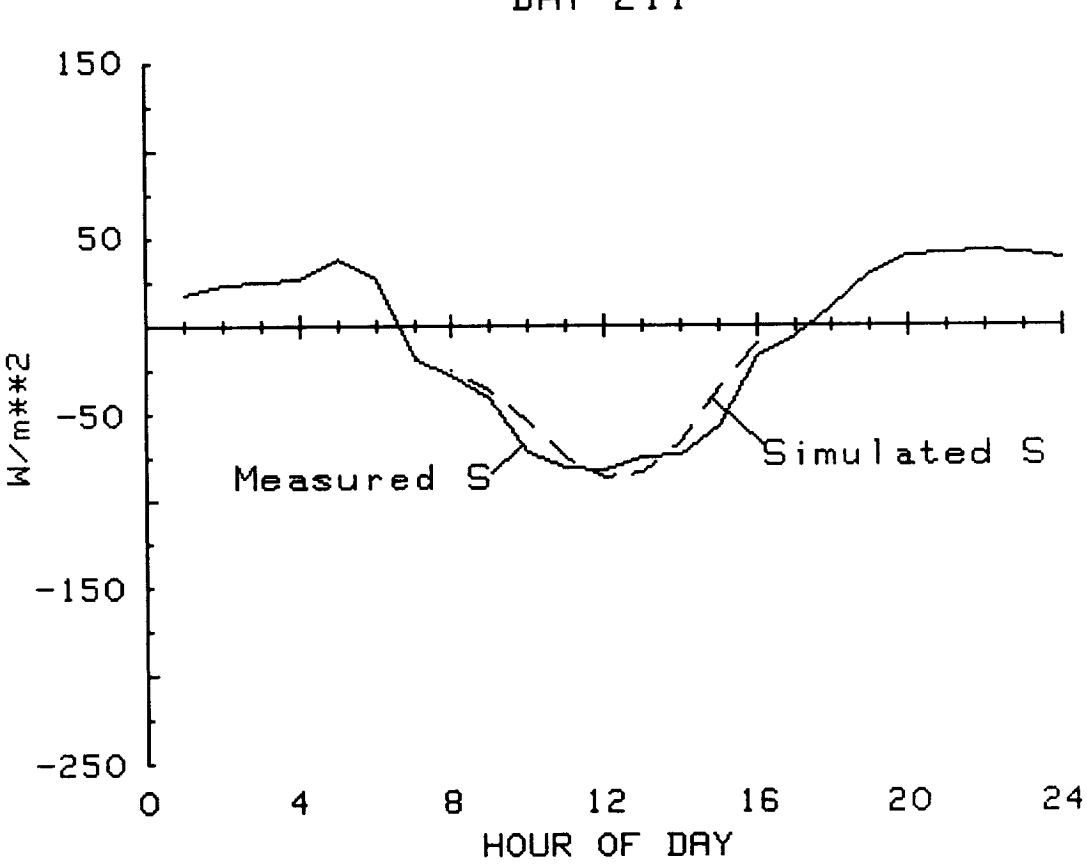

Figure 54. Measured and simulated values of soil heat flux (S) for July 30, 1986 (Day 211).

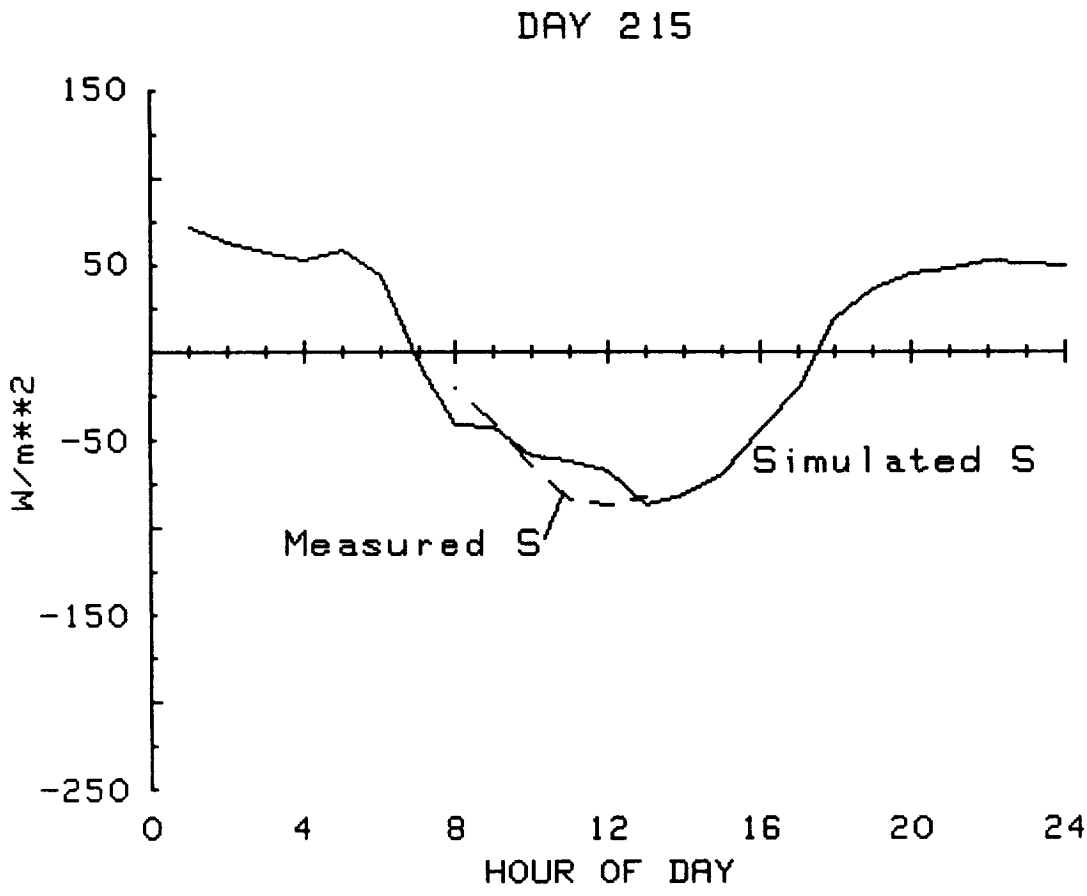

Figure 55. Measured and simulated values of soil heat flux (S) for August 3, 1986 (Day 215).

REFERENCES CITED

Bauer, M., B. F. Robinson, C. Daughtry, and L. L. Biehl. 1981. Field measurement workshop. October 14-16. Laboratory for Applications of Remote Sensing, Purdue University, Lafayette, IN.

Denmead, O. T. and B. D. Millar. 1976. Field studies of the conductance of wheat leaves and transpiration. Agron. J. 68:307-311.

Eaton, F. D., and I. Dirmhirn. 1979. Reflected irradiance indicatrices of natural surfaces and their effect on albedo. Appl. Optics 18:994-1008.

Gardner, Bronson, R. 1983. Techniques for Remotely Monitoring Canopy Development and Estimating Grain Yield of Moisture Stressed Corn. Ph.D. Dissertation. University of Nebraska-Lincoln.

Jackson, R. D. and P. J. Pinter, Jr. 1986. Spectral response of architecturally different wheat canopies. Remote Sensing Environ. 20:43-56.

Kalma, J. D., and R. Badham. 1972. The radiation balance of a tropical pasture. I. The reflection of short wave radiation. Agric. Meteorol. 10:251-259.

Kopeck, D. M., J. M. Norman, R. C. Shearman and M. J. Peterson. 1987. An indirect method for estimating leaf area of turf. Agron. J. (submitted).

Kriebel, K. T. 1979. Albedo of vegetated surfaces: Its variability with differing irradiances. Remote Sensing Environ. 8:283-290.

Lang, A. R. G, X. Yueqin and J. M. Norman. 1985. Crop structure and the penetration of direct sunlight. Agric. For. Meteorol. 35:83-101.

Landsberg, J. J. 1977. Some useful equations for biological studies. Expl. Agric. 13:272-286.

Lougeay, R. 1978. Ground level observations of signal contrast from various electromagnetic spectra. pp. 89-100. In: B. F. Richason, Jr. (ed.),

Introduction to Remote Sensing of the Environment. Kendall/Hunt Publ. Co., Dubuque, IA.

Moon, Parry. 1940. Proposed standard solar-radiation curves for engineering use. J. of The Franklin Institute 230:583-617.

Norman, J. M. and G. S. Campbell. 1987. Canopy structure, Chapter 14 In: Physiological Plant Ecology, R. W. Pearcy, J. R. Ehlringer, H. A. Mooney, P. Rundell (eds.), Chapman and Hall, New York. (in press).

Norman, J. M., S. G. Perry, A. B. Fraser and W. Mach. 1979. Remote sensing of canopy structure. Amer. Meteorol. Soc. Proc. 14th Conf. on Agricultural Forest Meteorology and 4th Conf. on Biometeorology, April 2-6, 1979, Minneapolis, MN, pp. 184-185. Amer. Meteorol. Soc., Boston.

Norman, J. M. 1982. Simulation of microclimates. In: Biometeorology in Integrated Pest Management, J. L. Hatfield and I. J. Thomason (eds.), Academic Press.

Norman, J. J., J. M. Welles, and J. T. Tolle. 1983. Rapid nondestructive field measurements of LAI. Agron. Abstracts, p. 14.

Perry, S. G. 1985. Remote sensing of plant canopy structure with simple radiation measurements. Ph.D. dissertation, Pennsylvania State Univ.

Pinter, P. J., Jr., R. D. Jackson, C. E. Ezra, and H. W. Gausman. 1985. Sun angle and canopy architecture effects on the spectral reflectance of six wheat cultivars. Itern. J. Remote Sens. 6:1813-1825.

Rosenberg, N. J., B. L. Blad, and S. B. Verma. 1983. Microclimate: The Biological Environment, 2nd Ed. John Wiley and Sons, New York. 495 pp.

Walthall, C. L., J. M. Norman, J. M. Welles, G. Campbell, and B. L. Blad. 1985. Simple equation to approximate the bidirectional reflectance from vegetative canopies and bare soil surfaces. Appl. Optics 24:383-387.